LOSS OF BOND IN

THE REINFORCED CONCRETE BEAM

THE INFLUENCE OF LOSS OF BOND ON THE MECHANICS OF FAILURE OF REINFORCED CONCRETE BEAMS

by

ANDREW C. C. WONG, B.Sc.

A Thesis

Submitted to the Faculty of Graduate Studies

in Partial Fulfilment of the Requirements

for the Degree

Master of Engineering

McMaster University

October 1964

MASTER OF ENGINEERING
(Civil Engineering)

McMASTER UNIVERSITY
Hamilton, Ontario.

TITLE: The Influence of Loss of Bond on the Mechanics of Failure of Reinforced Concrete Beams

AUTHOR: Andrew C. C. Wong, B.Sc. (Queen's University)

SUPERVISOR: Dr. H. Robinson

NUMBER OF PAGES; vii, 107

SCOPE AND CONTENTS:

This thesis involves the consideration of the reinforced concrete beam as a composite beam with incomplete interaction. The influence of bond slip and loading condition on the formation of cracks is studied analytically.

ACKNOWLEDGEMENTS

I wish to express my gratitude to Dr. H. Robinson for his advice and guidance during the course of this study.

My gratitude is also extended to the members of the computer center of McMaster University for their cooperation and assistance.

I wish to acknowledge the financial support of the project by the National Research Council.

TABLE OF CONTENTS

LIST OF ILLUSTRATIONS

CHAPTER I

INTRODUCTION

1.1 Introduction

Composite members are members consisting of two or more elements of the same or different materials connected by some means to form a single structural unit. In general, analytical solutions of composite beams have been developed for members having a reinforced concrete slab connected to the flange of a steel I beam, by means of shear connectors. This thesis involves the consideration of a reinforced concrete beam as a composite member with incomplete interaction. In particular, it entails a study of the influence of bond slip and loading condition on the nature of cracking phenomena observed frequently in tests of simply supported reinforced concrete beam. That is, a reinforced concrete beam is considered to be a composite member with incomplete interaction, which is a deviation from the conventional concept of the reinforced concrete beam.

A preliminary analytical study by Robinson[1] illustrated that the inclusion of loss of interaction or slip accounted for a reduction in the average steel stresses observed experimentally by Plowman[2]. The further possibility arose that such an analysis would account for the variation in the crack profile observed in a region of constant bending

moment for beams with a two point loading system, and that a rational explanation of the nature of the so-called 'diagonal cracking' in the shear span might be formulated. The need for further investigation of the cause of diagonal cracking is urged by the ACI-ASCE Committee 326[3][4] which has made intensive studies on the problem of shear and diagonal tension in a reinforced concrete beam.

1.2 Historical review

As early as the beginning of the 19th century, diagonal tension had been considered to be the basic cause of shear failures, and the widely accepted equation,

$$v = \frac{V}{bjd}$$

for shear calculation was developed. This equation together with some specified maximum shearing stresses which were based on the concrete cylinder strength(f'_c), had been adopted by most design codes in North America. In the year 1955, the nature of the well known failure at Wilkings Air Force Depot in Shelby, Ohio, intensified the doubt as to the validity of these design procedures and specifications for the calculation of shearing stress, currently used at that time. Hundreds of tests have been performed by investigators regarding this aspect. The ACI-ASCE Committee 326[3][4] has masterfully summarized the major contributions on shear studies carried out for the last 10 to 15 years, and explained the principles of shear. The inadequacy of the classical diagonal tension design equation and the adopted specifications was indicated. During the period of investigation, a new and an empirical design procedure was

developed and proposed by the ACI-ASCE Committee 326[3][4].

Many discussions regarding this particular problem appeared after the report of Committee 326[3][4], on shear and diagonal tension. Some have attempted to relate their own test results to the new empirical design procedures, or to evaluate the accuracy of different empirical formulae for shear stress calculations. Other investigators have attempted to explain the mechanism of shear failure and to differentiate between the general modes of failure[5][6][7][8][9] caused by some secondary causes brought about by the diagonal tension cracks, through their test observations and experiences.

In his paper "The Mechanism of so-called Shear Failure", Kani[10] used the 'teeth' concept and the 'comb-like' structure formed by the cracking process to explain the mechanism of shear and diagonal failure. Kani also suggested that, due to redistribution of stress caused by cracking, a reinforced concrete beam was transformed into a beam without bond or an arch with the reinforcement as a tie. The process of this transformation, analysis of diagonal failure, etc., was further detailed in Kani's recently presented paper "The Riddle of Shear Failure and its Solution"[11].

Generally speaking, experimental tests have been performed with such variables as concrete quality, percentage of longitudinal tensile reinforcement, shear span to effective depth ratio, shape of cross section, size of aggregate etc. being considered. Little or no attention has been given to the influence of bond slip on the mechanism of shear and diagonal failure of reinforced concrete beams.

1.3

Moe[12] indicated that the width of cracks, which depend on the bond characteristics of the steel, the percentage of reinforcement, the quality of the concrete etc. had detrimental effects on the failure mechanism of a reinforced concrete beam. His proposed equations, for shearing force which is transmitted across the cracks, and for the nominal shearing stress at the inclined crack, suggest that a theory could be developed by taking into account such factors as the bond quality of the reinforcing steel, the spacing between the flexural cracks, width of crack, etc.

It has long been considered by European investigators[13] that the width of cracks appearing on reinforced concrete structures at a given working stress depends primarily on the degree of bond between the steel and the concrete. That good bond between steel and concrete is the essential requirement for the safety of reinforced concrete structures has already been recognized.

Robinson[1][14] in his investigation of a composite beam consisting of a steel I-beam with a ribbed concrete slab formed by cellular steel decking, discovered that in spite of the fact that there was no distinct interfacial plane between the concrete slab and the steel beam, the strain distribution at any section had been observed to be essentially linear in the elastic range. He further suggested that the total slip between the concrete slab and the steel beam might be considered to consist of an interfacial slip and a larger slip, particularly after cracking, due to rotation of the concrete ribs formed by the cell. This can be considered to be analagous to the total slip of a reinforced

concrete beam, which would be expected to consist of the relative translational movement between the reinforcing steel and concrete, and the rotation of the 'teeth' referred to by Moe[12] and Kani[10][11]. It was considered that the reinforced concrete beam might well be considered to be a composite structure with incomplete interaction.

1.4

In spite of extensive tests made in the attempt to solve this existing problem of shear and diagonal tension in reinforced concrete structures, it is still conceded that a complete understanding and a fully rational solution to the problem have not been attained. In another word, practice is ahead of theory in the field of concrete engineering, this is unsatisfactory both for the scientist and the designer. This state of things ought really to be reversed, so that theory could lead the progress of practical development. However, a satisfactory design procedure and explanation of the inclined cracking may be developed through continuing experimental and analytical studies.

1.5

The main interest of the writer is to study analytically, the influence of bond slip and loading conditions on the formation of cracks of a simply supported reinforced concrete beam which is considered to be a composite structure with incomplete interaction. During the period of preliminary investigation the Newmark[15] solution for the conventional composite beam was slightly modified, and was used to estimate

the crack profiles of a reinforced concrete beam and an Araldite BRS model beam which was developed and tested by Bignell, Smalley and Roberts[16] in an attempt to simulate the behaviour of a reinforced concrete beam under load. In order that the field of investigation might be enlarged upon, the general analytical solutions were developed on the basis of non-linear stress-strain relationship for the concrete. The numerical solutions, unfortunately had to be obtained by a trial and error method, as outlined in Appendix B. However, the complications in the processes of evaluation were simplified by the aid of the IBM 7040 computer. The results have been found to be very significant and encouraging, though this is still at a very primitive stage of investigation. It is expected that further studies will provide a rational explanation of the nature of diagonal cracking. At least it is hoped that the importance of bond slip will be demonstrated through this investigation.

Chapter II

RÉSUMÉ

The Newmark[15] solutions for the conventional composite beam were slightly modified and were used to determine the variations of degree of interaction (F/F') along length of beam for various types of loading systems. The characteristics of these variations were studied. The crack profiles of a simply supported reinforced concrete beam and the Araldite BRS beam were determined by treating them as composite members, subjected to different types of loadings. The results obtained were found to be significant and encouraging. However, it was found that the analysis was limited to the application of a very small degree of break down of interaction between the composite elements, and required a relatively large tensile cracking strain for the concrete.

The analysis was extended to the consideration of an assumed parabolic stress-strain relationship of concrete under compression. Equations for this analysis were derived upon the requirements of satisfying conditions of equilibrium and compatibility. The validity and applicability of these equations were verified by the comparisons of results obtained with those for the linear analysis at low strain level.

Through investigations, it was found that as far as the consideration of a larger degree of break down of interaction was concerned, the curvilinear development did not overcome the difficulty encountered previously. Therefore, a new approach to the analysis of this problem was adopted.

In this approach, a certain degree of break down of interaction was assumed for the beam concerned. For a given applied load, the force parameters, such as the flexural moment of the concrete and horizontal forces, which fulfilled the equilibrium condition, were assumed to be those associated with a hypothetical total moment which the beam could carry when there was no break down of interaction between the composite elements.

The equilibrium relationship could be written as

$$F = \beta F'$$

$$M_t = M_{c+} + \beta F'_t \cdot z$$

The hypothetical moment at complete interaction was therefore,

$$M_{t+} = M_{c+} + F'_t \cdot z$$

In adopting this new approach, it was found that the problem could be extended to the analysis of any degrees of break down of interaction between the composite elements and a large applied load, with a more realistic tensile cracking strain of the concrete. With this approach, the crack profiles of the simply supported reinforced concrete beam were estimated with the interaction coefficient, 1/C, constant, and with 1/C varying along the beam, for the linear and curvilinear cases.

The equilibrium relationships of the first approach could be written as:

for complete interaction

$$M_t = M_c + F' z$$

$$F = F'$$

for incomplete interaction

$$F = \beta F'$$

then,

$$M_t = M_{cr} + \beta F' z$$

It may be seen that, if an assumed degree of break-down of interaction was given to the beam, the flexural moment of the concrete would have to be readjusted to restore the capacity of the beam to the required moment, M_t. Owing to the decrease of $\beta(F/F')$, the flexural moment of the concrete (M_c) increased rapidly which caused the cracking process to continue. The analysis was thus limited.

CHAPTER III

METHOD OF ANALYSIS

3.1

The theoretical developments for the analysis of the nature of the cracking patterns of the simply supported reinforced concrete beams, subjected to various types of loading, are based on the solution for the analysis of a composite T-beam (conventional composite beam), with incomplete interaction, by Newmark[15]. In this case, the analysis is based on the assumption of linear stress-strain relations for the materials.

3.2 Notation

The subscripts used with the notation of this thesis have the following meanings:

A_c	-	Effective cross-sectional area of the concrete.
A_s	-	Cross-sectional area of the steel.
b	-	width of the concrete beam.
C_c, C_s	-	Distances between the respective centroidal axes of the concrete and steel and their contact surfaces.

d - Diameter of the reinforcing steel.

D - Effective depth of the reinforced concrete beam.

E_c, E_s - Moduli of elasticity of the concrete and steel, respectively.

$F, F_c, F_s, F', F_L, F_R$ - Horizontal direct forces acting at the centroids of the cross-sectional areas of the concrete and steel.

$2H$ - Total depth of the concrete beam.

$2H'$ - Depth of the concrete beam after cracking.

I_c, I_s - Second moments of area of the concrete and steel, respectively.

k - modulus of the shear connection ($9.5/s$).

K_c, K_s - curvatures of the concrete beam and the steel, respectively.

L - Span length of the beam.

M_t - External moment applied to the beam.

$M_c, M_{c+}, M_{c++}, M_s$ - Flexural moment in concrete and steel, respectively.

P - Concentrated load applied to the beam.

q - Load transmitted from reinforcing steel to the concrete per unit length.

s - Spacing of discrete connection

u - Distance of the concentrated load P from the left support.

w - Uniformily distributed load (lb/in).

v - Unit shear stress

x - Distance of a cross-section from the left support.

y_c, y_s - Vertical distances from the centroidal axis of the concrete and the steel, respectively.

z - Distance between the centroidal axes of the concrete cross-section and the steel.

σ_c, σ_s - Stress in concrete and steel, respectively.

$\varepsilon_{ct}, \varepsilon_{cb}$ - Strains at top and bottom fibre of concrete.

$\varepsilon_{st}, \varepsilon_{sb}$ - Strains at top and bottom fibre of the steel.

α - Ratio of strains at bottom and top fibres of the concrete = $\varepsilon_{cb}/\varepsilon_{ct}$.

β - Degree of interaction = F/F'.

γ - Slip between the concrete and steel.

3.3 Basic Assumptions

Consider a T-beam as shown in Figure(3.1a) and Figure (3.1b) consisting of an I-beam and a slab tied together by a continuous shear connection which tends to prevent slip between the two elements and in so doing transfers horizontal force from one element to the other. Under loading, the strain distribution for complete and incomplete interaction for this section are shown in Figure (3.1c).

Now we consider that a reinforced concrete beam, as shown in Figure (3.2a) and Figure (3.2b) consists of a rectangular concrete section and the reinforcing steel, acting together through the connection of bond, between the two elements. The strain distribution in this section can therefore be shown in a similar manner, as in Figure (3.2c).

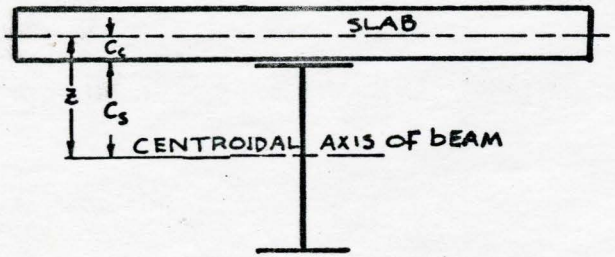

FIG. 3·1a CROSS SECTION

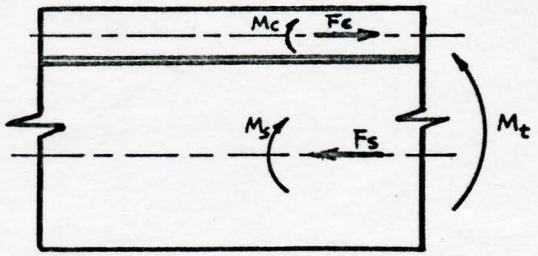

FIG. 3·1b FORCES

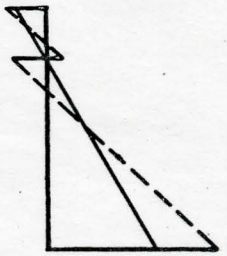

FIG·3·1c STRAIN DISTRIBUTION

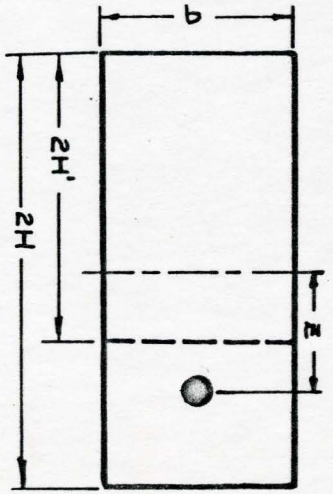

FIG: 3·2a CROSS SECTION

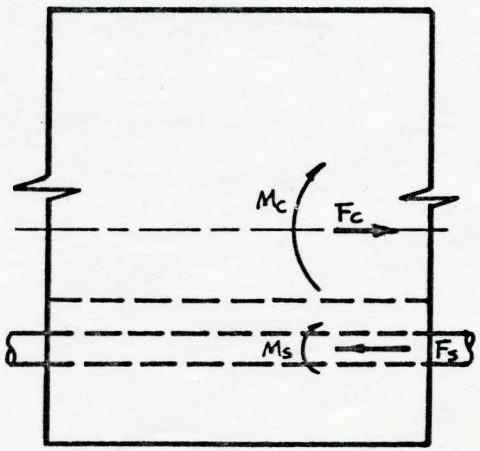

FIG. 3·2b FORCES

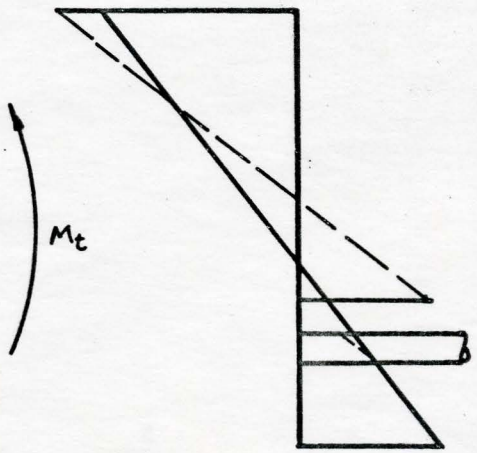

FIG. 3·2c STRAIN DISTRIBUTION

The principal assumptions made for this analysis are as follows:

1) The two components have equal curvatures at any section. That is, upon loading, it is assumed that two materials deflect equally at all points along their lengths.
2) The distribution of strains throughout the depth of the concrete and the steel is linear.
3) The amount of slip permitted by the shear connection (bond slip) is directly proportional to the load per unit length transmitted, before cracking occurs.

$$\gamma = \frac{q \cdot s}{k} \qquad \text{- - - - - - - - - - - - (3.1)}$$

s is unit length in this case

4) Concrete resists a certain amount of tension.
5) The stress-strain relationship for concrete is assumed to have the form of a parabolic curve, as shown in Figure (3.3), in the case of non-linear deformation analysis.

3.4 Method of Analysis: General

In this section, the analysis of the cracked and uncracked sections of the composite beam, for the elastic case is presented.

a) The equilibrium and compatibility conditions:

A free body diagram of an uncracked section is shown in Figure (3.4).

From statics, at any section of the beam, the following condition must be satisfied,

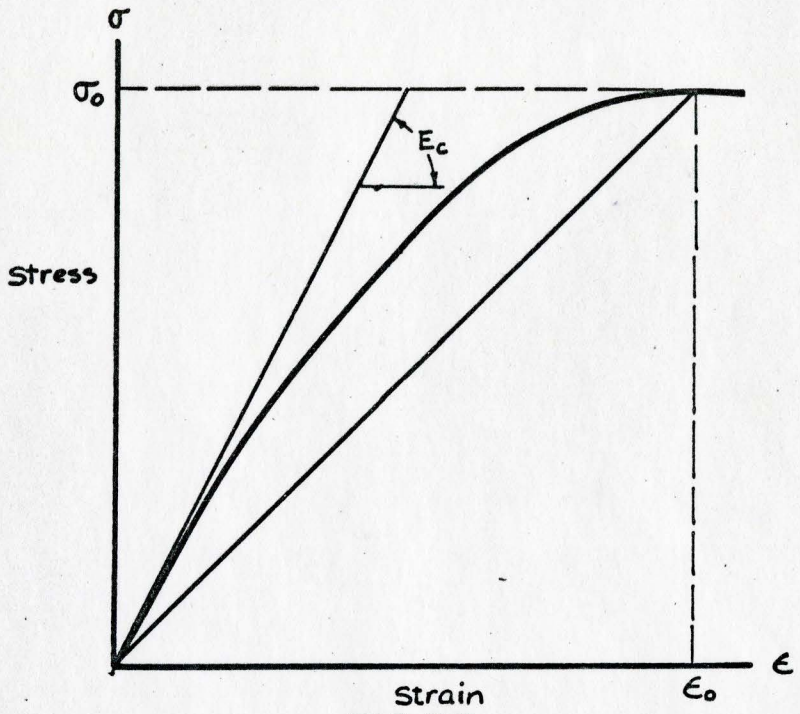

$$E_c = \frac{\sigma}{\epsilon}$$

$$E_{cs} = \frac{\sigma_o}{\epsilon_o}$$

$$\sigma = \sigma_o \left[2\frac{\epsilon}{\epsilon_o} - \left(\frac{\epsilon}{\epsilon_o}\right)^2 \right]$$

FIG. 3·3

STRESS-STRAIN CURVE OF CONCRETE

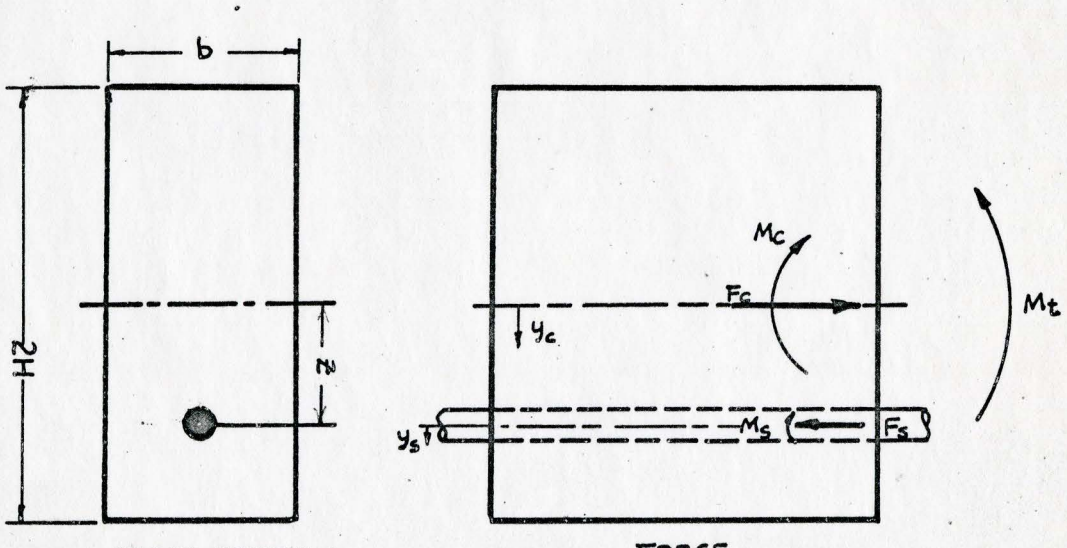

FIG. 3·4

$$\Sigma M = 0$$

The following equation is obtained,

$$M_t = M_c + M_s + F \cdot z \qquad \text{- - - - - - - - - - - - (3.2)}$$

where $F = F_c = F_s$

b) In order that the compatibility condition of the composite beam may be illustrated effectively, the deformation diagram of a section containing the i^{th} and $i + 1^{th}$ discrete shear connectors of a composite beam is shown in Figure (3.5).

ε_s - Strain at bottom fibre of concrete slab.

ε_b - Strain at top fibre of steel beam.

S_i - Spacing between the i^{th} and $i + 1^{th}$ discrete connections

γ_i - The slip at the i^{th} connection.

γ_{i+1} - The slip at the $i + 1^{th}$ connection.

The relation for the deformation at the horizontal section through the shear connection can be written as:

$$S_i + \int_{S_i} \epsilon_s \, dx + \gamma_{i+1} = \gamma_i + S_i + \int_{S_i} \epsilon_b \, dx$$

$$\gamma_{i+1} - \gamma_i = \int_{S_i} (\epsilon_b - \epsilon_s) \, dx$$

$$(\text{Slip}) \quad \gamma = \int_{S_i} (\epsilon_b - \epsilon_s) \, dx$$

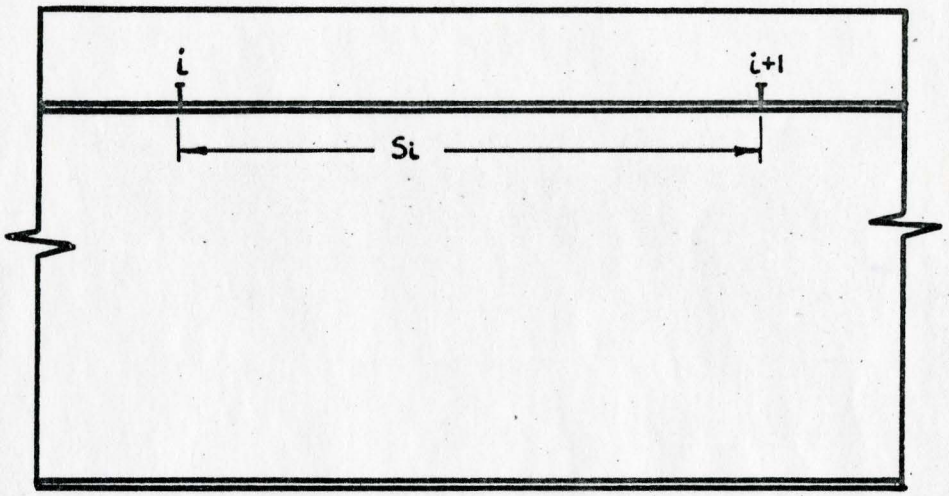

UNDEFORMED STATE

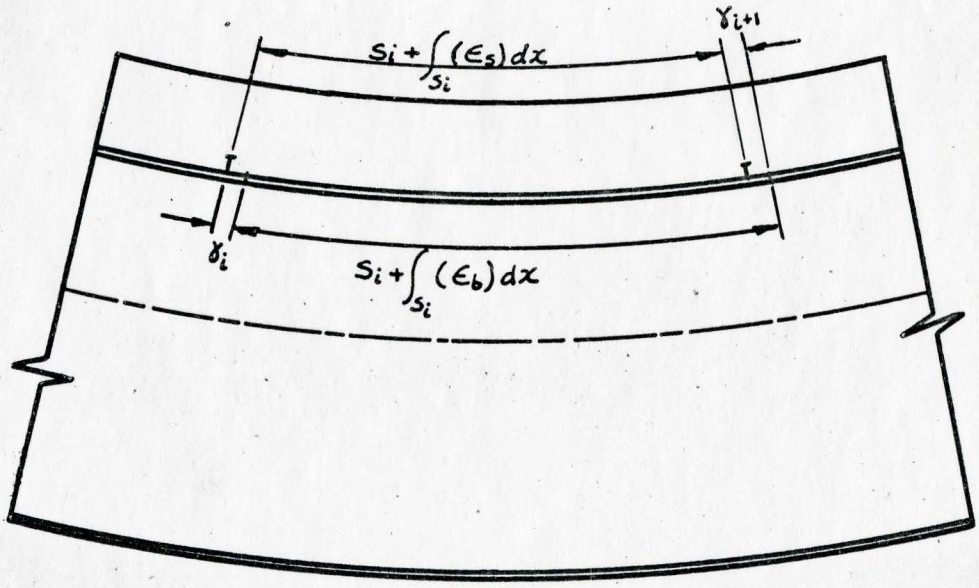

DEFORMATION DIAGRAM

FIG. 3·5

$$\frac{d\gamma}{dx} = \epsilon_b - \epsilon_s \qquad \text{----------(3.3a)}$$

or

$$\frac{d\gamma}{dx} = \epsilon_{st} - \epsilon_{cb} \qquad \text{----------(3.3b)}$$

i.e. the rate of change of slip along the length of the beam is equal to the difference in strain in the two components at the level at which slip occurs. In the case of a discrete connection with uniform spacings the horizontal force transmitted by the connector is equal to the sum of the unit horizontal shear over the intervals, i.e. $Q = q.s$ where q is the load, per unit of length, transmitted between the two components.

$$q = \frac{dF}{dx} \qquad \text{----------(3.4a)}$$

$$Q = \frac{dF}{dx} \cdot s \qquad \text{----------(3.4b)}$$

In the case of the reinforced concrete beam s can be considered to be unity.

3.5 Method of Analysis - elastic case

The entire beam is assumed to be elastic. From the strain distribution diagram, as shown in Figure (3.6), of the cracked and

uncracked sections of a reinforced concrete beam, the compatibility equation can be written as:

$$\frac{d\gamma}{dx} = \epsilon_{st} - \epsilon_{cb} + \epsilon_r \qquad \text{- - - - - - - - - - - - - - - - - - (3.5)}$$

in which dx is measured along the length of the beam and (ε_r) is defined as additional strain due to the formation of the "concrete teeth", created by the cracking process, on what may be called the "pseudo interface" of the concrete and the steel, viz. the bottom fibre of the remaining uncracked concrete section.

By geometry

$$\epsilon_r = \frac{(-\epsilon_{sb} + \epsilon_{st}) \cdot (D - d/2 - 2H')}{d}$$

Note: the negative sign is introduced to make the development analagous to that of Newmark[15].

From the assumption that the distribution of strain throughout the depth of the beam is linear, it follows that:

$$-\epsilon_{sb} = -\left(\frac{F_s}{E_s A_s} + \frac{M_s C_s}{E_s I_s}\right) \qquad \text{- - - - - - - - (3.6a)}$$

$$\epsilon_{st} = \frac{F_s}{E_s A_s} - \frac{M_s C_s}{E_s I_s} \qquad \text{- - - - - - - - (3.6b)}$$

$$\epsilon_{cb} = \frac{-F_c}{E_c A_c} + \frac{M_c C_c}{E_c I_c} \qquad \text{- - - - - - - - (3.6c)}$$

$$\epsilon_r = \frac{-2 M_s C_s}{E_s I_s} \cdot \frac{(D - d/2 - 2H')}{d} \qquad \text{- - - - - - - - (3.6d)}$$

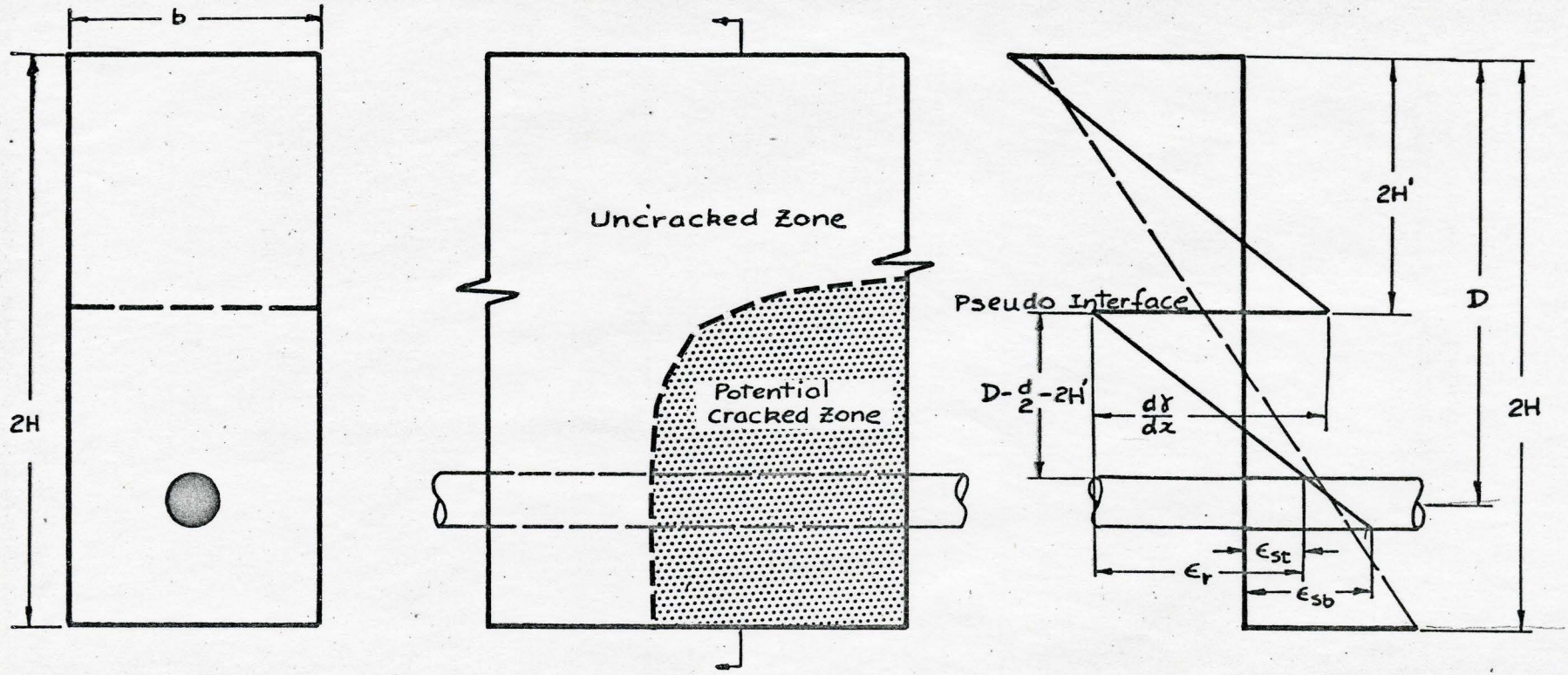

STRAIN DISTRIBUTION IN CRACKED AND UNCRACKED SECTIONS

FIG.3·6

The rate of change of slip can be written as

$$\frac{d\gamma}{dx} = \epsilon_{st} - \epsilon_{cb} - \frac{2M_s y_s}{E_s I_s d}\cdot(D - d/2 - 2H') \qquad ---(3.7)$$

from equation (3.1) and (3.4)

$$\frac{d\gamma}{dx} = \frac{1}{k}\frac{dq}{dx} = \frac{1}{k}\frac{d^2F}{dx^2} \qquad ---(3.8)$$

substituting equation (3.6), (3.7) and (3.8) in equation (3.5)

$$\frac{1}{k}\frac{d^2F}{dx^2} = F\left(\frac{1}{E_s A_s} + \frac{1}{E_c A_c}\right) - \left[\frac{M_s C_s}{E_s I_s} + \frac{M_c C_c}{E_c I_c} + \frac{2M_s C_s}{E_s I_s d}\cdot(D - d/2 - 2H')\right] \qquad (3.9)$$

Since it is assumed that the concrete and steel deflect equally at all points, that is, they have equal curvatures, the moments M_s and M_c are related as follows:

$$\frac{M_s}{E_s I_s} = \frac{M_c}{E_c I_c}$$

Further, from equation (3.2)

$$\frac{M_c}{E_c I_c} = \frac{M_s}{E_s I_s} = \frac{M_t - F\cdot z}{\Sigma EI} \qquad ------(3.10)$$

where

$$\Sigma EI = E_s I_s + E_c I_c$$

By definition

$$C_c = H'$$

$$C_s = d/2$$

$$\frac{1}{k}\frac{d^2F}{dx^2} = F\left(\frac{1}{E_sA_s} + \frac{1}{E_cA_c}\right) - \frac{M_t - F\cdot z}{\Sigma EI}\left[C_s + C_c + \frac{2C_s}{d}\cdot\left(D - \frac{d}{2} - 2H'\right)\right]$$

in which $C_s + C_c + \frac{2C_s}{d}\left(D - \frac{d}{2} - 2H'\right)$ can be reduced to D - H'

and is equal to Z.

Therefore,

$$\frac{1}{k}\frac{d^2F}{dx^2} = F\left[\frac{1}{E_sA_s} + \frac{1}{E_cA_c} + \frac{z^2}{\Sigma EI}\right] - \frac{M_t\cdot z}{\Sigma EI}$$

or $$\frac{d^2F}{dx^2} - Fk\frac{\bar{EI}}{\bar{EA}\Sigma EI} = -k\frac{M_t\cdot z}{\Sigma EI} \qquad -- (3.11)$$

where the following expressions are introduced for convenience

$$\bar{EI} = \Sigma EI + \bar{EA}\cdot z^2$$

$$\frac{1}{\bar{EA}} = \frac{1}{E_sA_s} + \frac{1}{E_cA_c}$$

For the uncracked section

$$D - \frac{d}{2} - 2H' = 0$$

$$\therefore \quad \epsilon_r = 0$$

then

$$\frac{d\gamma}{dx} = \epsilon_{st} - \epsilon_{cb}.$$

An identical result to equation (3.11) will be obtained for this case[15]. Therefore equation (3.11) is applicable to both cracked and uncracked sections.

If the external moment M_t is expressed as a function of x solutions of the differential equation (3.11) may be obtained for different loading conditions.

3.6 Variation of degree of interaction for different loading conditions

The following solutions have been obtained for three loading conditions: a concentrated load P, two concentrated loads, and a uniformly distributed load (ω), acting on a simply-supported beam.

1) A single concentrated load P.

When $x < u$, the moment is

$$M_t = \frac{P \cdot x}{L}(L - u)$$

Equation (3.11) will have the form

$$\frac{d^2 F_L}{dx^2} - F_L k \frac{\bar{E}I}{\bar{E}A\Sigma EI} = -k \frac{P \cdot (L-u) \cdot z}{L \cdot \Sigma EI} \cdot x \qquad \text{- - - (3.12a)}$$

When $x > u$, the moment is

$$M_t = \frac{P \cdot u}{L}(L - x)$$

and equation (3.11) will have the form

$$\frac{d^2 F_R}{dx^2} - F_R k \frac{\bar{E}I}{\bar{E}A\Sigma EI} = k \frac{P \cdot u \cdot z}{L \cdot \Sigma EI} \cdot (L - x) \qquad \text{- - - (3.12b)}$$

The differential equations (3.12) can be solved for known end conditions.

For this case the end conditions are:

at x = 0 $\quad F_L = 0$

at x = L $\quad F_R = 0$

at x = u $\quad \frac{dF_L}{dx} = \frac{dF_R}{dx}$, $F_L = F_R$

The solutions for the force F are

for x < u

$$F_L = \frac{\bar{E}A \cdot z}{\bar{E}I} PL \left\{ \left(1 - \frac{u}{L}\right) \frac{x}{L} - \frac{\sqrt{C}}{\pi} \frac{\sinh\left[\frac{\pi}{\sqrt{C}}\left(1 - \frac{u}{L}\right)\right]}{\sinh \frac{\pi}{\sqrt{C}}} \sinh\left(\frac{\pi}{\sqrt{C}} \frac{x}{L}\right) \right\} \quad -- (3.13a)$$

and for x > u

$$F_R = \frac{\bar{E}A\, z}{\bar{E}I} PL \left\{ \frac{u}{L}\left(1 - \frac{x}{L}\right) - \frac{\sqrt{C}}{\pi} \frac{\sinh\left(\frac{\pi}{\sqrt{C}} \cdot \frac{u}{L}\right)}{\sinh \frac{\pi}{\sqrt{C}}} \sinh\left[\frac{\pi}{\sqrt{C}}\left(1 - \frac{x}{L}\right)\right] \right\} \quad -- (3.13b)$$

where

$$C = \frac{1}{k} \frac{\pi^2 \bar{E}A\, z\, EI}{L^2\, \bar{E}I} \quad -- (3.14)$$

is a dimensionless expression introduced for convenience.

If the modulus of the bond is infinitely large, the slip will be zero and there will be complete interaction between the concrete and the steel. The force (F') for complete interaction can be obtained by setting C = 0

$$F' = \frac{\bar{E}\bar{A}\,\bar{z}}{\bar{E}\bar{I}} M_t \quad * \qquad \text{- - - - - - - - - - (3.13c)}$$

The ratio of the horizontal force (F) for incomplete interaction to horizontal force (F') for complete interaction is:

for $x < u$

$$\frac{F_L}{F'} = 1 - \frac{\sqrt{C}}{\pi} \frac{1}{(1-\frac{u}{L})\frac{x}{L}} \frac{\sinh\left[\frac{\pi}{\sqrt{C}}(1-\frac{u}{L})\right]}{\sinh\frac{\pi}{\sqrt{C}}} \sinh\left(\frac{\pi}{\sqrt{C}}\frac{x}{L}\right) \qquad \text{- - (3.15a)}$$

for $x > u$

$$\frac{F_R}{F'} = 1 - \frac{\sqrt{C}}{\pi} \frac{1}{(1-\frac{x}{L})\frac{u}{L}} \frac{\sinh\left(\frac{\pi}{\sqrt{C}}\frac{u}{L}\right)}{\sinh\frac{\pi}{\sqrt{C}}} \sinh\left[\frac{\pi}{\sqrt{C}}(1-\frac{x}{L})\right] \qquad \text{- - (3.15b)}$$

'Bond slip' is an inherent characteristic of the reinforced concrete beam. Slip between the reinforcing steel and the concrete may be considered to be the most obvious manifestation of loss of interaction; or alternatively loss of interaction occurs because of 'bond slip'. The ratio (F/F') for any section depends on the coefficient C and on the location of the section and load. Coefficient C can be said to depend upon the 'bond modulus' of a reinforced concrete beam with given span length and cross sectional shape.** This in

---

* $\frac{dF'}{dx} = \frac{\bar{E}\bar{A}\,\bar{z}}{\bar{E}\bar{I}} \frac{dM_t}{dx} = \frac{\bar{E}\bar{A}}{\bar{E}\bar{I}} \bar{z} \cdot V = q'$ which is equivalent to Zhurawski formula

**(17)

$$\frac{1}{C} = \frac{I}{\frac{1}{n}I_c + I_s} \frac{1}{E_s} \frac{\bar{z}}{\bar{y}} \frac{L^2}{A_c} \frac{k}{S}$$

turn influences the ratio (F/F'), equation (15). Thus the ratio (F/F') furnishes a convenient measure of the degree of interaction at any section.

F/F' is equal to unity for complete interaction, and to zero for no interaction.

The horizontal shear per unit length of the beam may be obtained from equation (3.4a) and (3.13)

for $x < u$

$$q_L = \frac{\bar{E}A}{\bar{E}I} z P \left\{ \left(1 - \frac{u}{L}\right) - \frac{\sinh\left[\frac{\pi}{\sqrt{C}}\left(1 - \frac{u}{L}\right)\right]}{\sinh \frac{\pi}{\sqrt{C}}} \cosh\left(\frac{\pi}{\sqrt{C}} \frac{x}{L}\right) \right. \tag{3.16a}$$

for $x > u$

$$q_R = \frac{\bar{E}A}{\bar{E}I} z P \left\{ - \frac{u}{L} - \frac{\sinh\left(\frac{\pi}{\sqrt{C}} \frac{u}{L}\right)}{\sinh \frac{\pi}{\sqrt{C}}} \cosh\left[\frac{\pi}{\sqrt{C}}\left(1 - \frac{x}{L}\right)\right] \right\} \tag{3.16b}$$

The horizontal unit shear for complete interaction is given by the equation

$$q' = \frac{\bar{E}A}{\bar{E}I} z V \tag{3.16c}$$

Equations (3.16) may then be written in the form of a ratio.

For $x < u$

---

where, I - second moment of area of the composite section

$n = \frac{E_s}{E_c}$

$\bar{y}$ - distance between the centroidal axis of the concrete section and the neutral axis of the composite section.

$$\frac{q_L}{q'} = 1 - \frac{1}{(1-\frac{u}{L})} \frac{\sinh\left[\frac{\pi}{\sqrt{c}}(1-\frac{u}{L})\right]}{\sinh\frac{\pi}{\sqrt{c}}} \cosh\left(\frac{\pi}{\sqrt{c}}\frac{x}{L}\right) \qquad (3.17a)$$

and for x > u

$$\frac{q_R}{q'} = 1 - \frac{L}{u} \frac{\sinh\left(\frac{\pi}{\sqrt{c}}\frac{u}{L}\right)}{\sinh\frac{\pi}{\sqrt{c}}} \cosh\left[\frac{\pi}{\sqrt{c}}(1-\frac{x}{L})\right] \qquad (3.17b)$$

2) Two symmetrical point loads on simply supported beam

when x < u

$$M_t = P \cdot x$$

The expression for the differential equation may be written as,

$$\frac{d^2F_L}{dx^2} - k\left(\frac{\bar{E}\bar{I}}{\bar{E}\bar{A}\Sigma EI}\right)F_L = -k\,\frac{P\Sigma}{\Sigma EI}\,x$$

The boundary conditions are the same as in Case (1), similar solutions for F/F' are obtained as follows

$$\frac{F_L}{F'} = 1 - \frac{\sqrt{c}}{\pi}\frac{L}{x} \frac{\cosh\left[\frac{\pi}{\sqrt{c}}\left(\frac{1}{2}-\frac{u}{L}\right)\right]}{\cosh\left(\frac{\pi}{\sqrt{c}}\frac{1}{2}\right)} \sinh\left(\frac{\pi}{\sqrt{c}}\frac{x}{L}\right) \qquad (3.18a)$$

when $u < x < \frac{1}{2}L$

$$M_t = Pu$$

$$\frac{d^2F_R}{dx^2} - k\left(\frac{\bar{E}\bar{I}}{\bar{E}\bar{A}\Sigma EI}\right)F_R = -k\,\frac{P\Sigma}{\Sigma EI}\,u$$

and

$$\frac{F_R}{F'} = 1 - \frac{\sqrt{C}}{\pi}\frac{L}{u}\,\frac{\sinh\left(\frac{\pi}{\sqrt{C}}\frac{u}{L}\right)}{\cosh\left(\frac{\pi}{\sqrt{C}}\frac{1}{2}\right)}\,\cosh\left[\frac{\pi}{\sqrt{C}}\left(\frac{1}{2} - \frac{x}{L}\right)\right] \qquad (3.18b)$$

The ratio of the unit horizontal shears are

for $x < u$

$$\frac{q_L}{q'} = 1 - \frac{\cosh\left[\frac{\pi}{\sqrt{C}}\left(\frac{1}{2} - \frac{u}{L}\right)\right]}{\cosh\left(\frac{\pi}{\sqrt{C}}\frac{1}{2}\right)}\cosh\left(\frac{\pi}{\sqrt{C}}\frac{x}{L}\right) \qquad (3.19a)$$

for $u < x < \frac{1}{2}L$

$$\frac{q_R}{q'} = \frac{\sinh\left(\frac{\pi}{\sqrt{C}}\frac{u}{L}\right)}{\cosh\left(\frac{\pi}{\sqrt{C}}\frac{1}{2}\right)}\,\sinh\left[\frac{\pi}{\sqrt{C}}\left(\frac{1}{2} - \frac{x}{L}\right)\right] \qquad (3.19b)$$

3) Uniformly distributed load on a simply supported beam

$$M_t = \frac{\omega x}{2}(L - x)$$

The expression for the differential equation is

$$\frac{dF^2}{dx^2} - k\left(\frac{\bar{E}\bar{I}}{\bar{E}\bar{A}\Sigma EI}\right)F = -k\,\frac{z}{\Sigma EI}\left(\frac{\omega x L}{2} - \frac{\omega x^2}{2}\right)$$

The boundary conditions are:

when $x = 0 \quad F = 0$

$$x = \frac{L}{2}, \quad \frac{dF}{dx} = 0$$

The expression for F/F' is therefore,

$$\frac{F}{F'} = 1 - \frac{2}{x(L-x)} \left(\frac{\sqrt{C}L}{\pi}\right)^2 \left\{1 - \frac{\cosh\left[\frac{\pi}{\sqrt{C}} \frac{1}{L} \left(\frac{1}{2} - x\right)\right]}{\cosh\left(\frac{1}{2} \frac{\pi}{\sqrt{C}}\right)}\right\} \qquad - (3.20)$$

The expression for q/q' is

$$\frac{q}{q'} = 1 - \frac{2\sqrt{C}L}{\pi(L-2x)} \frac{\sinh\left[\frac{\pi}{L} \frac{1}{\sqrt{C}} \left(\frac{L}{2} - x\right)\right]}{\cosh\left(\frac{1}{2} \frac{\pi}{\sqrt{C}}\right)} \qquad - (3.21)$$

The manner in which F/F' varies along the length of the beam, for the above three cases with various 1/C values is shown in Figures (3.7), (3.8) and (3.9). From these curves, it is important to note that the reduction in the interaction is a somewhat localized effect, and is increased by decreasing the values of 1/C.

It can be seen that the major loss of interaction occurs at the location under the load point but not necessarily at the location where the bending moment is maximum. In particular for the case of the beam with the uniformly distributed load, the degree of interaction is a minimum towards the support or position of zero moment. A consistent effect might be observed if the beam with uniformly distributed load is inverted and the support reaction force is considered to be an applied point load.

CASE I UNSYMMETRICAL SINGLE POINT LOAD.

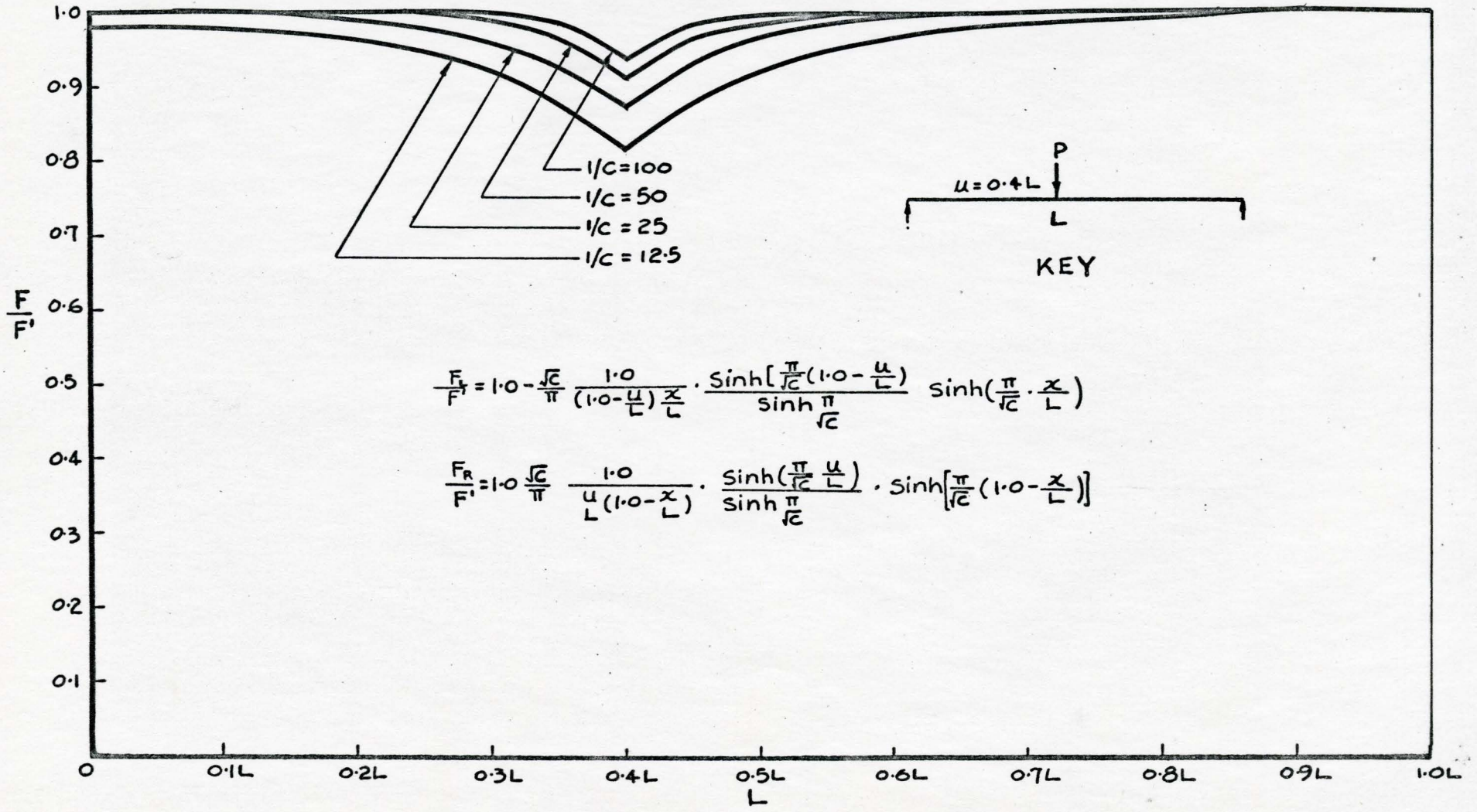

DEGREE OF INTERACTION (F/F') VS. LENGTH OF BEAM

FIG. 3·7

CASE II SYMMETRICALLY SITUATED TWO-POINT LOADS

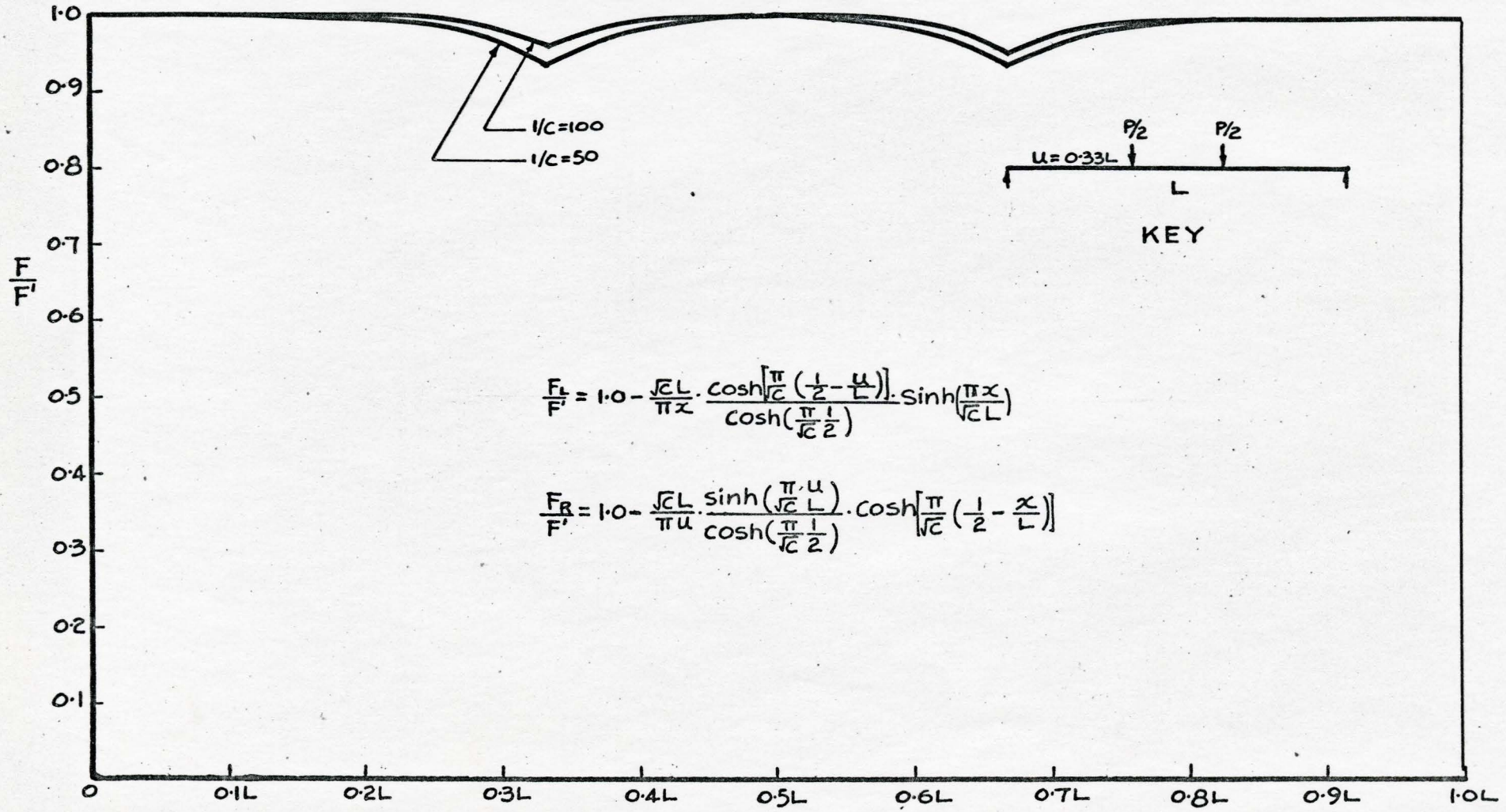

DEGREE OF INTERACTION (F/F') VS. LENGTH OF BEAM

FIG. 3·8

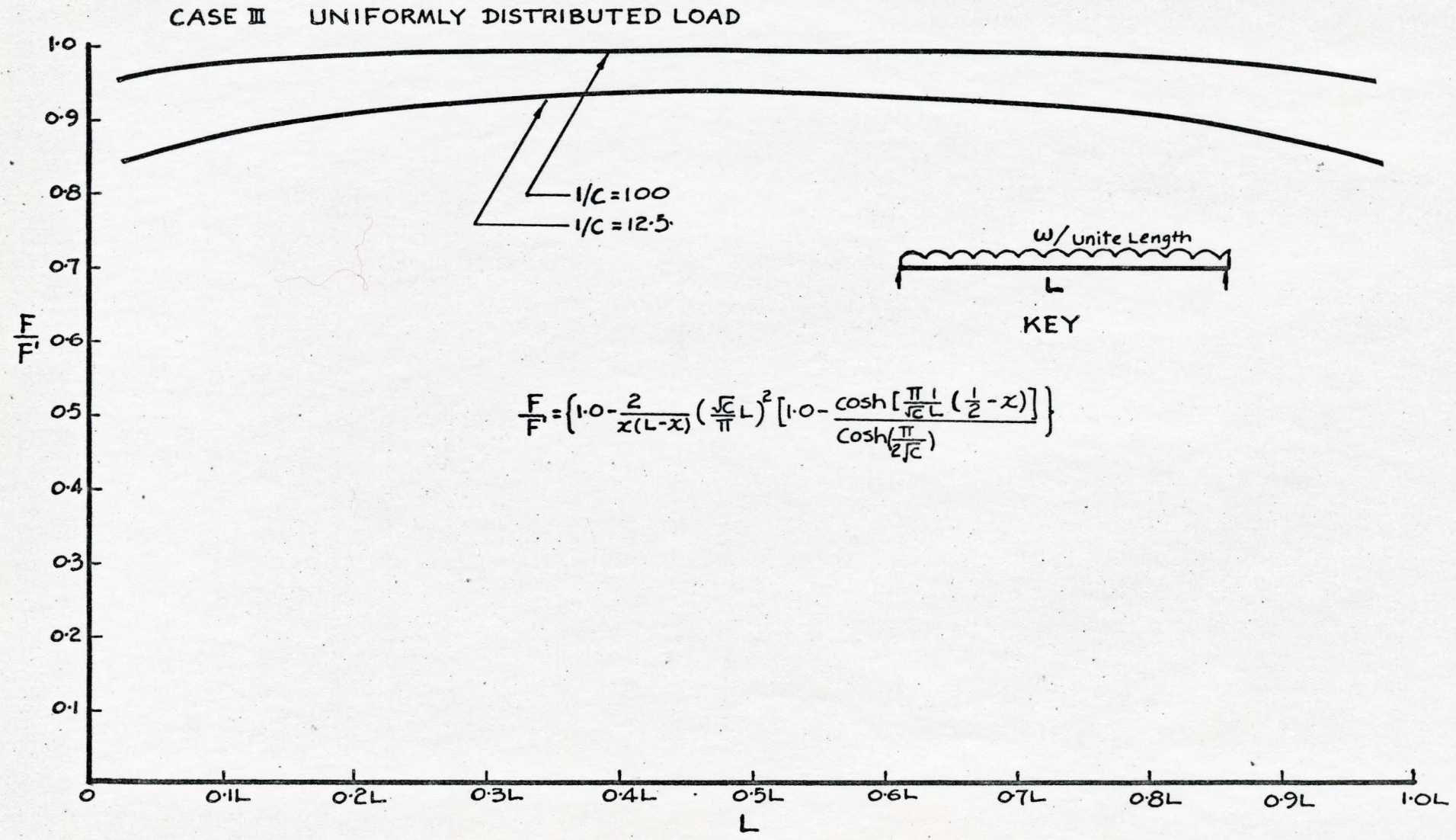

DEGREE OF INTERACTION (F/F') VS. LENGTH OF BEAM

FIG. 3·9

3.7 Strains

Strains in the simply supported reinforced concrete beam may be determined for any degree of interaction, for various type of loading systems from equations:

$$\epsilon_c = \frac{-F}{E_c A_c} + \frac{M_c y_c}{E_c I_c} \qquad \text{-----(3.22a)}$$

and

$$\epsilon_s = \frac{F}{E_s A_s} + \frac{M_s y_s}{E_s I_s} \qquad \text{-----(3.22b)}$$

where ϵ_c and ϵ_s are concrete and steel strains and y_c, y_s are the distances from the centroid of the concrete portion or of the reinforcement to the point at which the strain is desired. In both cases y is positive when measured downward. The force F in these equations may be computed from equation (3.12) or (3.13), and the moments M_c and M_s may be obtained from equation (3.10) as follows:

$$M_c = \frac{E_c I_c}{\Sigma EI} \left(M_t - Fz \right) \qquad \text{-----(3.23a)}$$

$$M_s = \frac{E_s I_s}{\Sigma EI} \left(M_t - Fz \right) \qquad \text{-----(3.23b)}$$

The equations for the strains may be obtained from equations (3.13a), (3.15), (3.22) and (3.23).

$$\epsilon_c = \left[S_c - \frac{F}{F'} \frac{\bar{E}\bar{A}\bar{z}}{\bar{E}\bar{I}} \left(S_c \bar{z} + \frac{1}{E_c A_c} \right) \right] M_t \qquad \text{- - (3.24a)}$$

$$\epsilon_s = \left[S_s - \frac{F}{F'} \frac{\bar{E}\bar{A}\bar{z}}{\bar{E}\bar{I}} \left(S_s \bar{z} - \frac{1}{E_s A_s} \right) \right] M_t \qquad \text{- - (3.24b)}$$

where

$$S_c = \frac{y_c}{\Sigma EI} \qquad \text{- - (3.25a)}$$

$$S_s = \frac{y_s}{\Sigma EI} \qquad \text{- - (3.25b)}$$

Equations (3.24) show that strains depend on the moment, the properties of the reinforced concrete beam section, and the degree of interaction (F/F') at the particular section at which strains are desired. (F/F') depends on the bond modulus (k), and on the properties of the beam section, all these are contained in the coefficient C given by equation (3.14).

3.8 Crack height

From equation (2.19a) strains for the top and bottom fibres of the concrete, (ϵ_{ct}) & (ϵ_{cb}), may be obtained for any section and

any type of loading condition by letting

$$S_c = \pm \frac{C_e}{\Sigma EI} \qquad \text{- - (3.26)}$$

in equation (3.25a) for given properties of concrete, shape of the section and the degree of interaction.

From geometry, as shown in Figure (3.10), the extent of cracking of the concrete at any section due to the application of a given moment at that section can be written as:

$$C.H. = \frac{(\epsilon_{cb} - \epsilon_p)\ 2H}{\epsilon_{cb} + \epsilon_{ct}} \qquad \text{- - (3.27)}$$

where C.H. = height of crack

ε_p = the tensile cracking strain of concrete

The new section of the beam is therefore,

$$2H' = 2H - C.H.$$

It may be noted from equation (3.27) that a stable section of the concrete will remain in an equilibrium condition only when the strain at the bottom fibre of the concrete at that section is equal to or less than the tensile cracking strain of the concrete.

That is, if $\varepsilon_p < \varepsilon_{cb}$, a new uncracked section is formed, in accordance with equation (3.27). The strain at bottom fibre of the concrete, for the new section is again computed by equation (3.24).

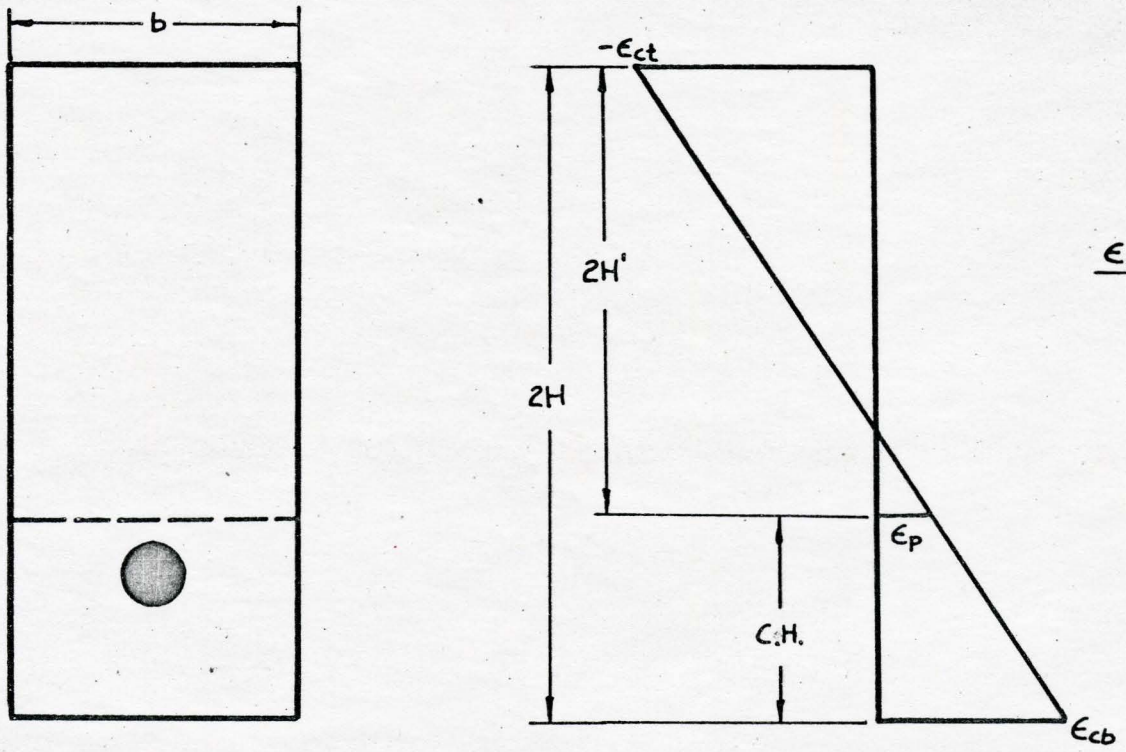

$$\frac{\epsilon_{ct} + \epsilon_{cb}}{2H} = \frac{\epsilon_{cb} - \epsilon_p}{C.H.}$$

$$2H' = 2H - C.H.$$

CRACKED SECTION

FIG. 3·10

This process is repeated until at a certain cracked level $\epsilon_p \geq \epsilon_{cb}$. A stable section is thus attained, otherwise the cracking process will continue.

Chapter IV

Preliminary Investigations

4.1

Robinson[14] in a preliminary study of this aspect speculated that consideration of the reinforced concrete beamas a composite beam with incomplete interaction might lead to a rational explanation of the nature of the inclined cracking which occurs in many reinforced concrete beams.

Computations of strain-distribution along the reinforcing rod of a reinforced concrete beam, in which the effect of loss of interaction was included, showed a reduction of the mid-height strain of the rod, compared to that computed by the conventional straight-line theory, and which was in general agreement with experimental observations made by Plowman[2].

It became evident from the computations that the locus of the upper extremity of the potential crack in the concrete at any section also differed from that for the straight-line case. (The potential cracked height is equivalent to saying that the concrete below the neutral axis or below the level of a given tensile strain in the concrete is ineffective: one of the assumptions made in the conventional theory).

Further it was evident that the extent of cracking was greatest

under the load point in a beam subjected to say a two-point loading system, causing the locus of the extremities of the flexural cracks or the crack profile to be displaced upwards and towards the load, this effect being most pronounced locally in the region of the point load.

Such an effect can be inferred by looking at the visible flexural cracks observed on the surface of test beams, see Figure (4.1).

It could be further reasoned that such a displacement of the crack profile due to loss of interaction is the cause of the extremity of the diagonal crack being so close to the load point after it appears and as is frequently observed experimentally.

A reinforced concrete beam and an Araldite BRS beam were investigated on the basis of this analysis.

4.2 A simply supported reinforced concrete beam subjected to one and two point loading systems.

According to the Newmark[15] solution for a composite beam, the value of 1/C less than infinity (i.e. $F/F' < 1.0$), indicates that there is a loss of interaction between the two elements of a composite beam. Without the support of experimental data, it is impossible to predict a reasonable value of 1/C for a particular reinforced concrete beam (or for the beam made from Araldite BRS). Thus, an assumption must be made as to the value of 1/C for the purpose of this investigation.

A simply supported reinforced concrete beam, with the same cross-sectional properties as Plowman's[2] beams, was treated as a

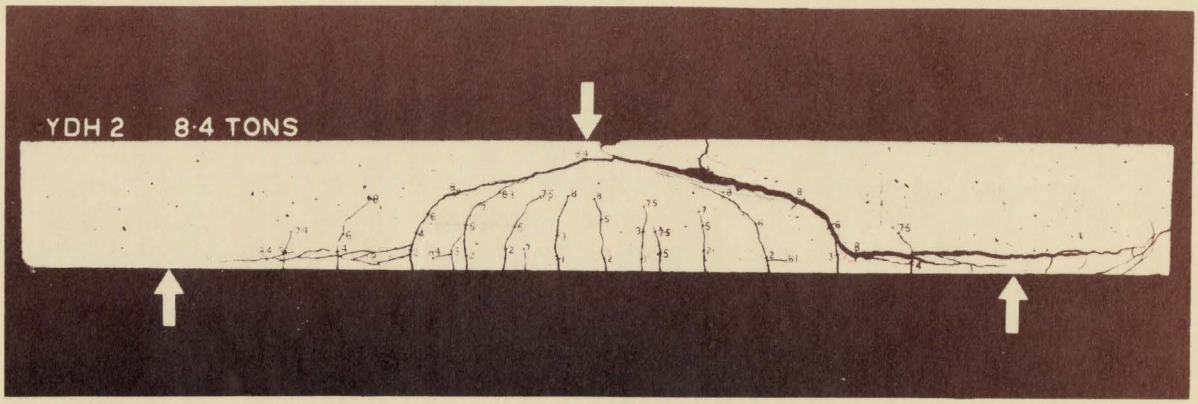

DUE TO TAYLOR & BREWER

Typical crack patterns on beams.

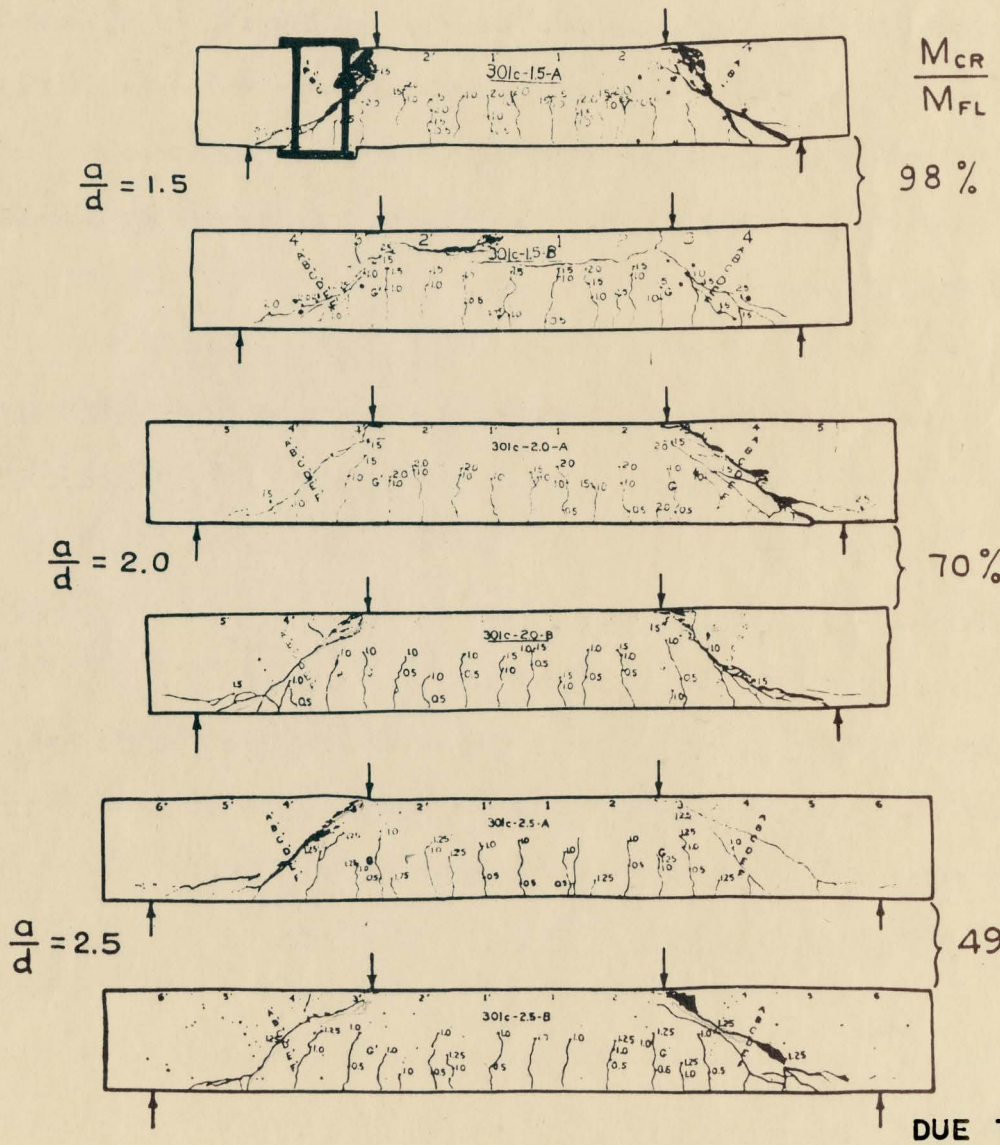

DUE TO KANI

-Beams of Toronto Test Series C

FIG. 4·1

composite beam with incomplete interaction. This beam was analysed in accordance with the Newmark[15] solution for a composite beam as presented in Chapter III. Fig. (4.2) shows a family of curves of the uncracked section of the beam, with different values of 1/C, for a section subjected to the maximum design moment and at the load point. From this curve, a value of 1/C and the tensile cracking strain of the concrete, equal to 100 and 171.0 micro in/in, respectively, were chosen for the purpose of estimating the crack profile along the reinforced concrete beam. From the curves in Figure (4.2) it may be seen that the tensile cracking strain of the concrete must be less than 189 micro in/in, in order that a crack can begin to propagate at the design moment chosen for the example. If there is complete interaction, then for $\varepsilon_p < 189$ micro in/in the crack will propagate until the strain at the bottom fibre of the uncracked section reaches whatever value selected for this particular computation, viz. $\varepsilon_p = 100$ m.in/in, see Figure (4.2). Note that, if $\varepsilon_p = 0$ the curve for complete interaction would continue until it intersected the ordinate axis and the uncracked depth would be the same as the depth of the neutral axis, according to the straight-line theory.

If, however, there is a loss of interaction, represented by 1/C = 100, say, it may be seen that for the purpose of this computation ε_p must not be less than 171 micro in/in, otherwise, the cracking will continue to the top of the beam. Thus, for the purpose of computation, the allowable limits of ε_p must be $171 \leq \varepsilon_p < 189$ micro in/in.

It may be further seen, however, that if 1/C = 50, no sensible solution can be obtained, because as the curve shows, either the beam

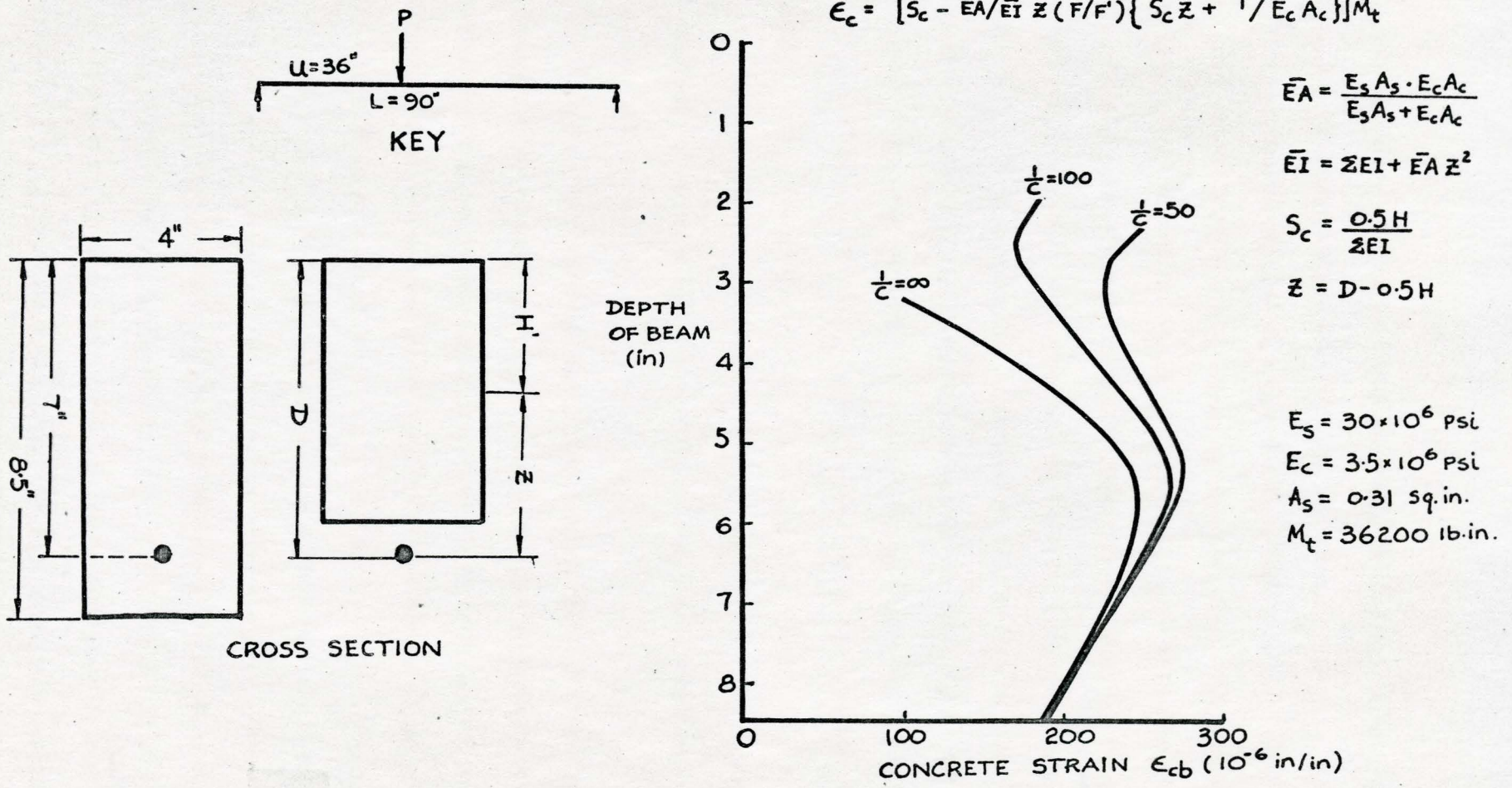

ESTIMATED CONCRETE STRAIN UNDER LOAD POINT WITH VARIATION OF DEGREE OF INTERACTION

FIG. 4-2

will not crack ($\varepsilon_p > 189$), or that if cracking begins at the design moment, it will continue to the top of the beam.

A sample calculation is shown in Appendix A.

Crack profiles of the simply supported reinforced concrete beam with complete and incomplete interactions, for an unsymmetrical single point load and symmetrically situated two point loads, were estimated by equations outlined in Chapter III, and are shown in Figure (4.3) and Figure (4.4). A comparison between the crack profiles with complete interaction and that of the incomplete interaction, shows that there are up-shooting portions of the crack profiles close to the locations of the point loads, in the case of incomplete interaction.

This phenomenon, could in fact be predicted by the strain distribution of concrete at the bottom fibres, due to the effect of incomplete interaction.

This inclined part of the crack profile may be considered as the incipient path of the inclined crack observed by many investigators, in tests on simply supported reinforced concrete beams. It is the boundary between the uncracked and potentially micro-cracked zones or regions of the concrete. The forms or curvatures of this incipient path of the inclined crack depend upon the degree of interaction between the composite elements, and the nature of the external loading system, which in their turn govern, the distribution and magnitudes of (F/F') along the beam as shown previously.

One must also bear in mind that these estimated cracks are micro-cracks. They may not be observed by the naked eye before mature

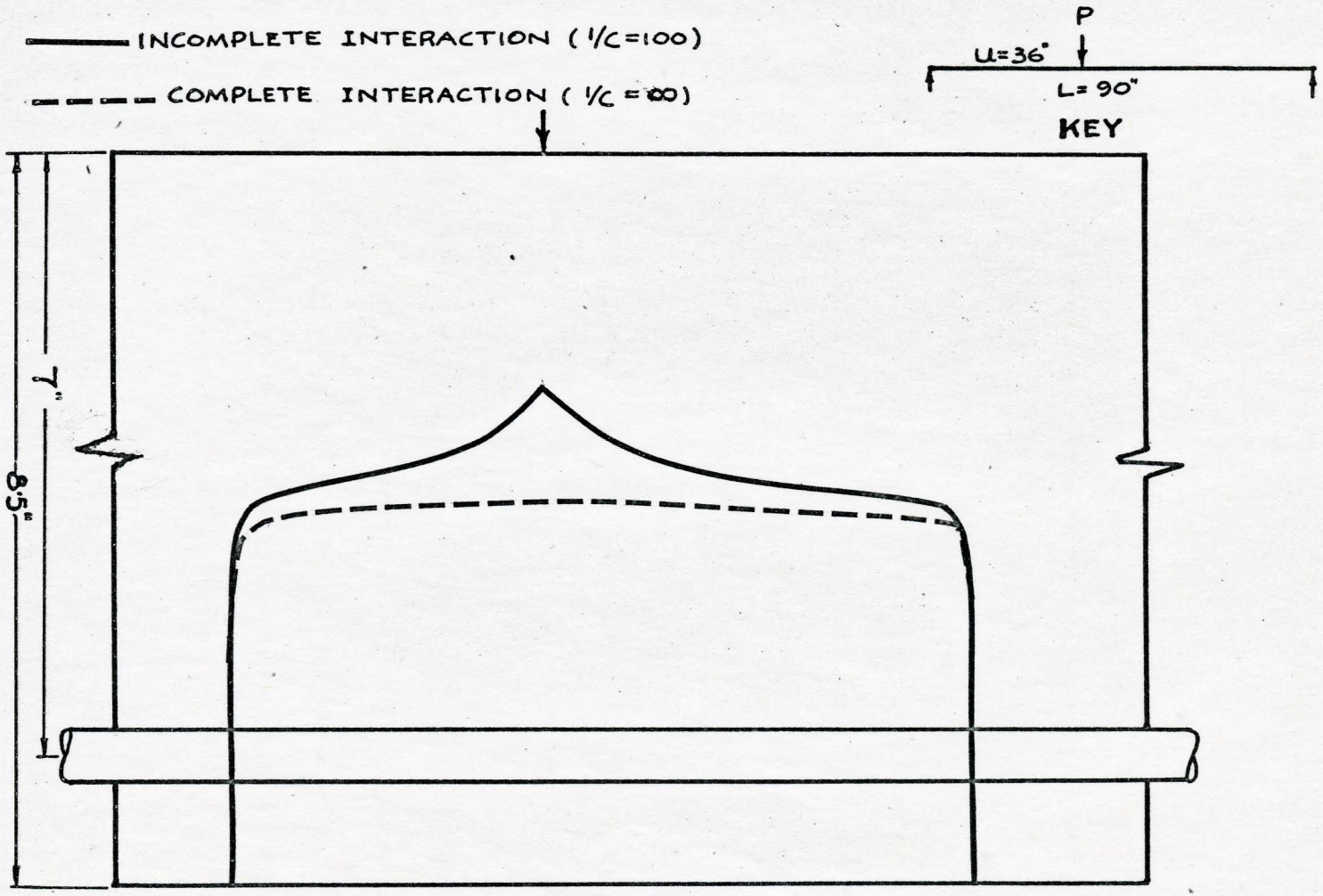

ESTIMATED EXTREMITIES OF FLEXURAL CRACKS OF A REINFORCED CONCRETE BEAM

FIG. 4·3

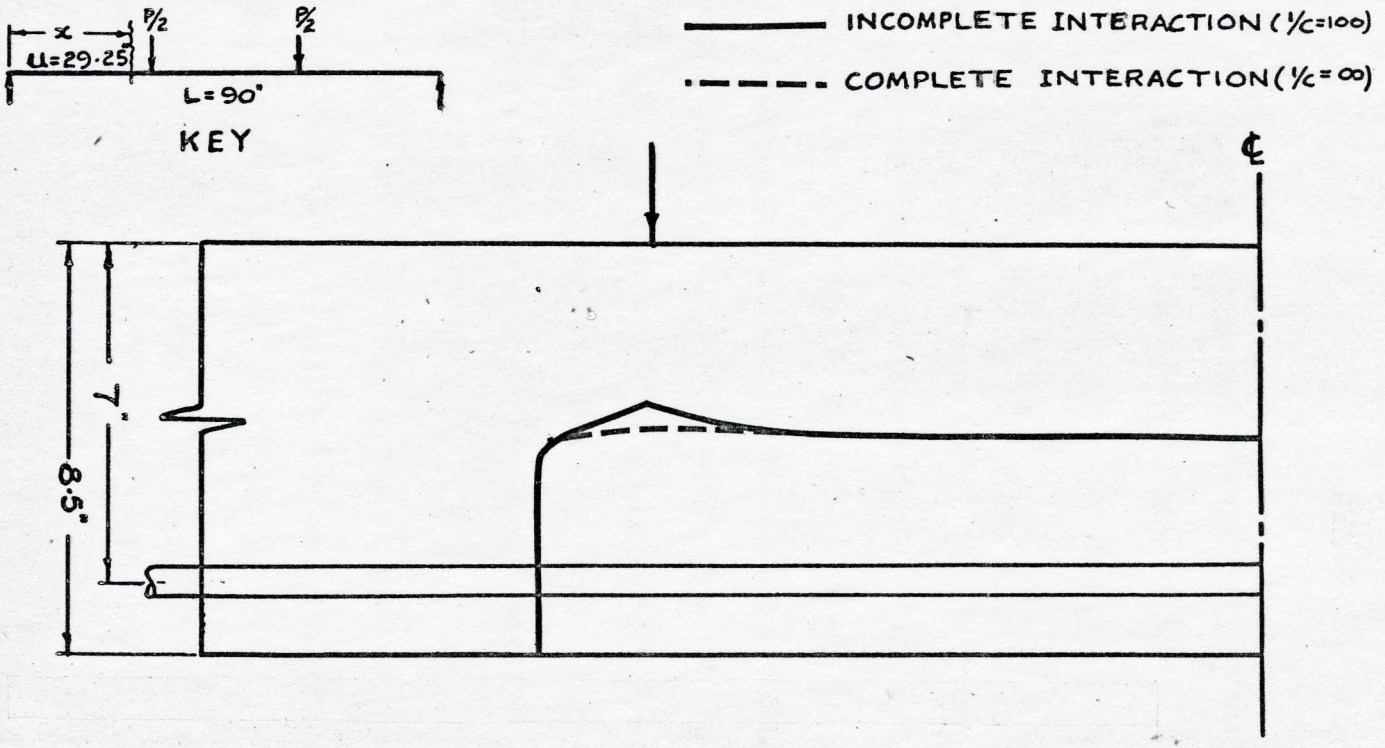

ESTIMATED EXTREMITIES OF FLEXURAL CRACKS OF A REINFORCED CONCRETE BEAM

FIG. 4·4

cracks are formed at a later stage.

4.3 An Araldite BRS beam, reinforced with an extruded magnesium rod subjected to a two point load system.

An Araldite BRS model beam which has been reported to possess brittle properties, was developed and tested by Bignell, Smalley & Roberts[16] in an attempt to simulate the behaviour of a reinforced concrete beam under load. A section of the Araldite BRS beam located under maximum moment was analysed in accordance with the Newmark[15] solution presented in Chapter III. From the family of curves for the Araldite beam strains at the bottom fibre of the uncracked section versus the depth of the beam, as shown in Figure (4.5), the value of 1/C and tensile cracking strain for the Araldite beam equal to 100 and 600 micro in/in, respectively, were chosen for the purpose of estimating the crack profiles.

The crack profiles of the simply supported Araldite beam with complete and incomplete interactions, for an unsymmetrical concentrated load, symmetrical two point load and uniformly distributed load, were estimated by procedures outlined in Chapter III, and are shown in Figure (4.6), (4.7) and (4.8). The effects of break down of interaction on inclined cracking could be seen distinctly by comparing these crack profiles for complete and incomplete interactions. The comparison between the estimated crack profile for incomplete interaction, in the case of two point loading with 1/C equal to 100, and that of the test Araldite BRS beam, as shown in Figure (4.9) of identical

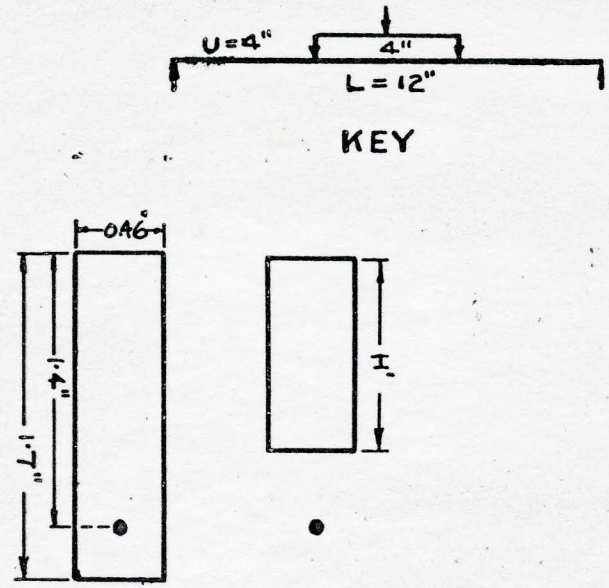

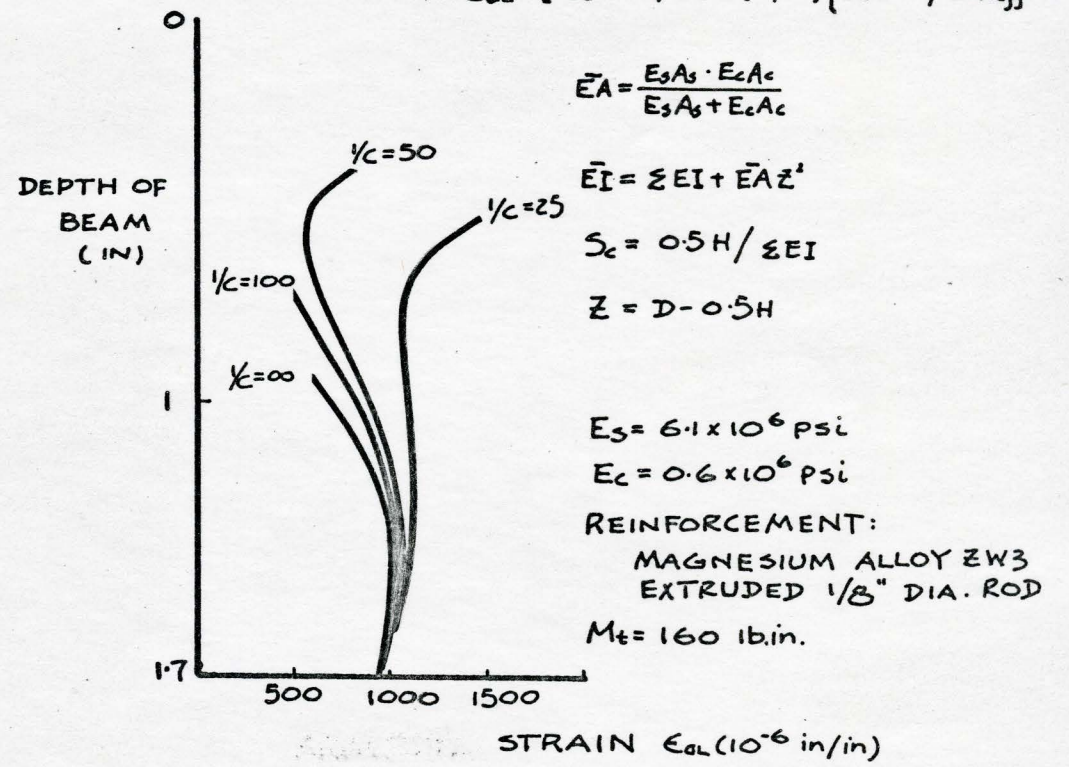

ESTIMATED STRAIN UNDER LOAD POINT WITH VARIATION OF DEGREE OF INTERACTION FOR AN ARALDITE BEAM

FIG. 4·5

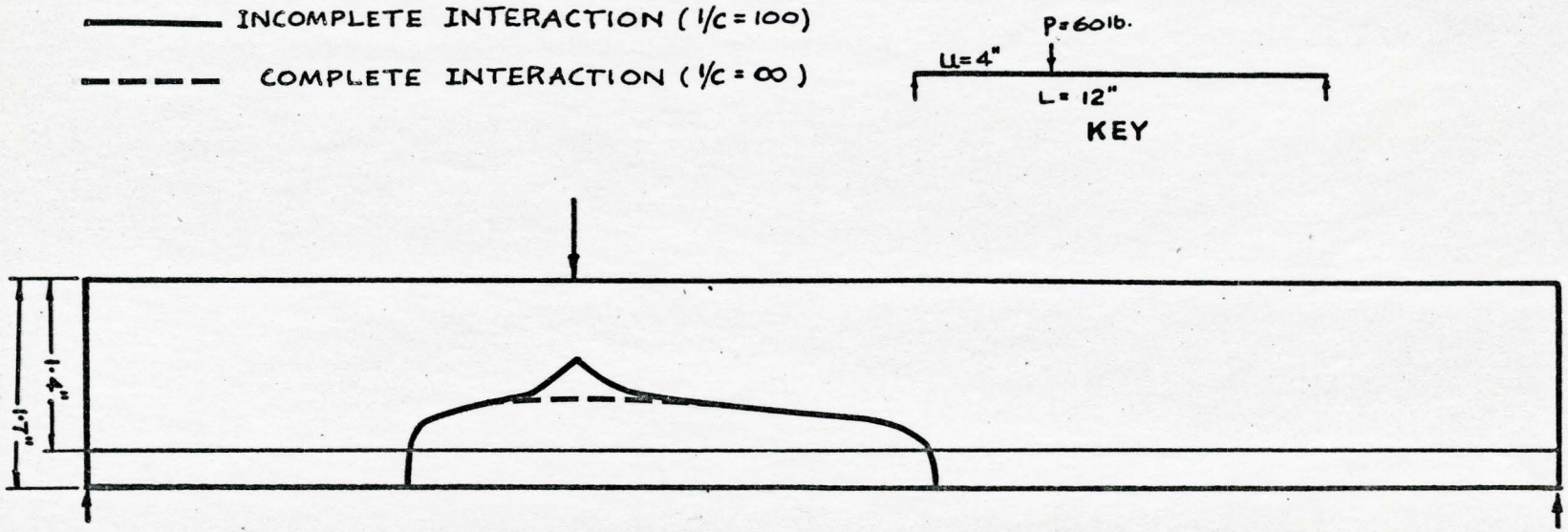

ESTIMATED EXTREMITIES OF FLEXURAL CRACKS OF AN ARALDITE BEAM
(ONE POINT LOAD)

FIG. 4·6

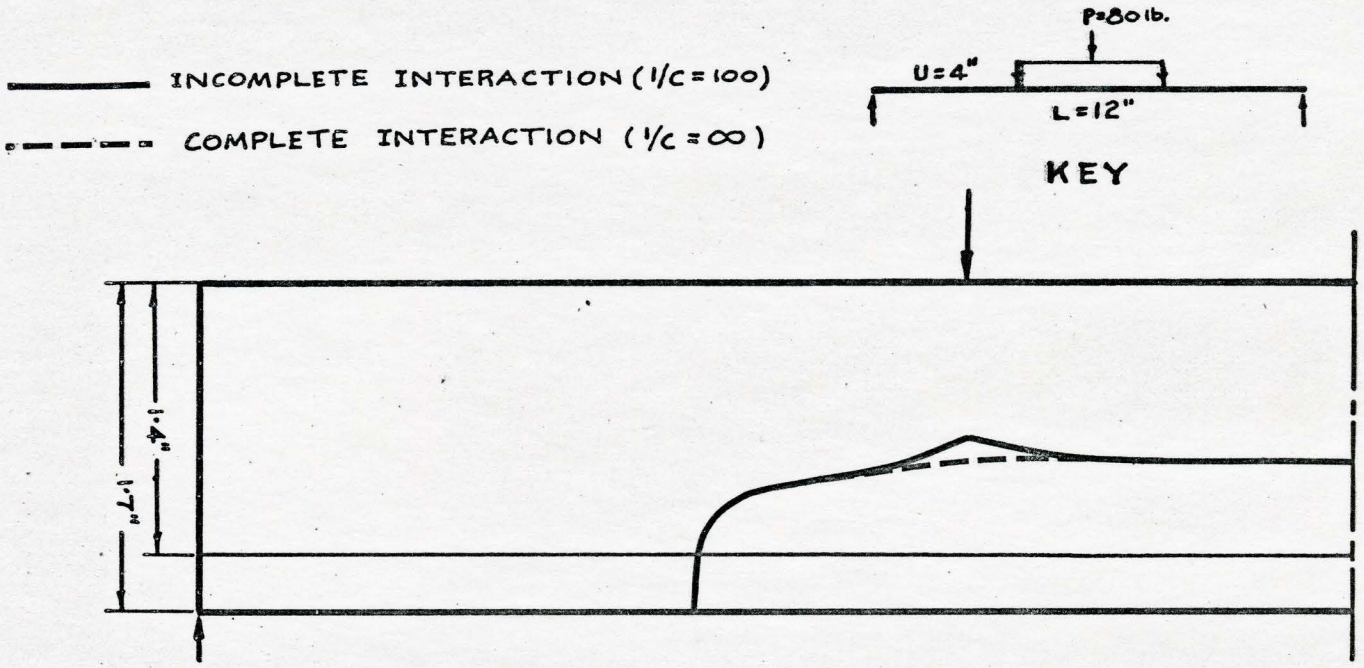

ESTIMATED EXTREMITIES OF FLEXURAL CRACKS OF AN ARALDITE BEAM

(TWO POINT LOAD)

FIG. 4·7

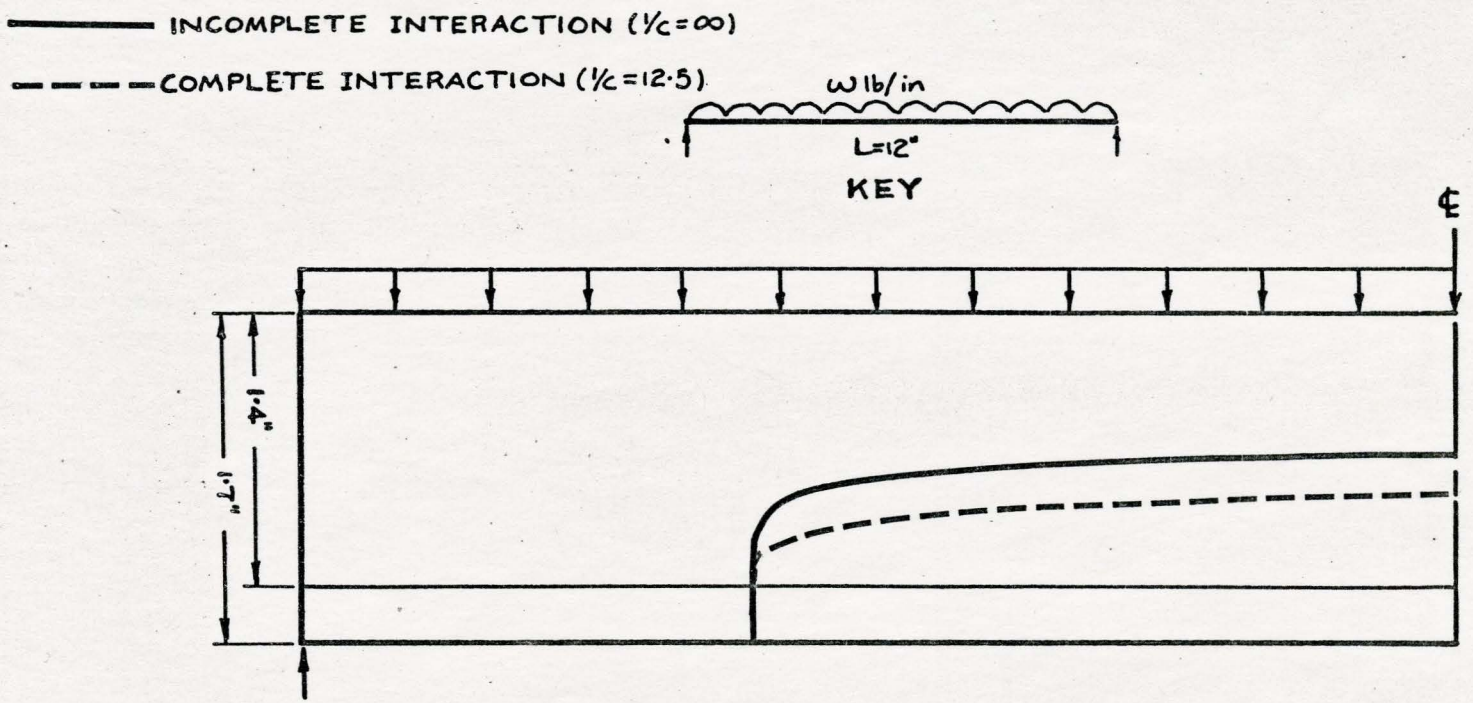

ESTIMATED EXTREMITIES OF FLEXURAL CRACKS OF AN ARALDITE BEAM
(UNIFORMLY DISTRIBUTED LOAD)

FIG. 4·8

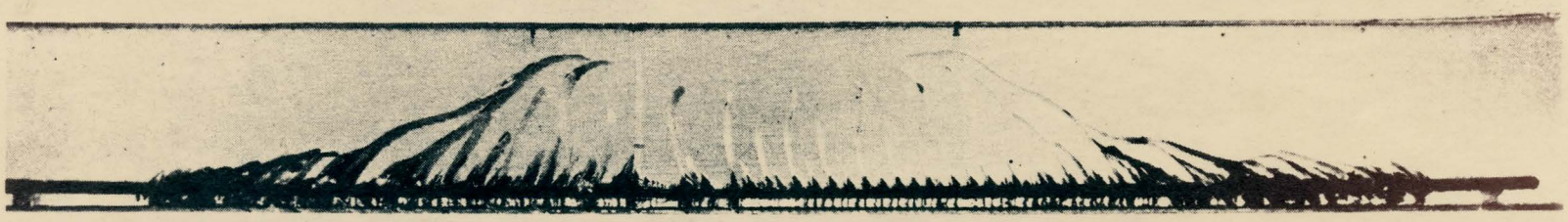

Cracked Araldite BRS beam, 15 × 1·7 × 0·46 in., reinforced with $\frac{1}{8}$ in. diameter " plain bar " magnesium alloy ZW3. The load points are marked.

DUE TO BIGNELL, SMALLEY & ROBERTS

FIG. 4·9

dimensions and properties, were noted to have close similarities. It was also observed that these estimated crack profiles have a form somewhat similar to the cracking phenomena observed in many tests of reinforced concrete beam as shown in Figure (4.1). It might be noted, in particular, that the Araldite BRS beam shows the inclined crack in the region of the point load to have a reverse curvature which is similar in nature to that predicted by this analysis.

It might be said, at this stage, that the effects of break down of interaction on a beam are more vividly shown in the investigation of the Araldite BRS beam than in the case of the reinforced concrete beam. It could be reasoned that the Araldite BRS is a homogeneous material which might eliminate factors, such as inter-locking of aggregate, bond conditions, etc., which affect the mechanism of inclined cracking in reinforced concrete. Thus, the purpose of using the Araldite BRS beam to simulate the behaviour of a reinforced concrete beam under load, may be considered to be rather impressive.

4.4

In the analysis of the Plowman[2] reinforced concrete beam, the use of 171.0 micro in/in, though arbitrary is not entirely unreasonable. Many reports pertaining to tensile strength of concrete have suggested that the tensile strain of concrete varies in a wide range, depending on the volume of coarse aggregate, etc. A more likely value for the tensile cracking strain is, however, in the range 85 - 160 micro in/in[17].

The value of 1/C = 100 has been recognized as an indication of a very small degree of break down of interaction, through the investigation of the conventional composite beam[15][18].

It was thought that the necessity of using a relatively large value for the tensile cracking strain of the concrete and a small degree of break down of interaction, (represented by 1/C = 100), in this analysis, was due to the effect of the assumed linear stress-strain relationship for the concrete, which prevented the attainment of an equilibrium condition after first cracking, particularly as the degree of interaction diminished. This led to the consideration of a curvilinear stress-strain relationship for the concrete, which is outlined in the next Chapter. However, it was found that the hypothetical statement of the problem required modification.

Chapter V

Method of Analysis - inelastic case

5.1

The applicability of the equations of Chapter III requires that materials be linearly elastic. This limitation greatly restricts the use of the equations for investigation of behaviour of composite beams where the materials may have non-linear stress-strain characteristics. In this Chapter, the analysis has been extended to include a non-linear stress-strain characteristic of the concrete. This consideration was originally based on the hope that the increase of lever arm together with the development of a curvilinear stress distribution would give an equilibrium condition of the concrete beam with a more realistic tensile cracking strain of the concrete and a larger degree of break down of interaction. In such a way, it was hoped that a smaller degree of interaction could be considered with a state of equilibrium at a certain cracked level being attained. Hence the scope of the investigation could be enlarged. In addition, analytical solutions presented in this Chapter may serve as the general solutions, for this sort of problem where the composite members consist of materials having non-linear stress-strain characteristics.

In this case, the quantities, strain of concrete and steel (ε_c) and (ε_s), can no longer be expressed uniquely, in terms of F/F' and moment for the beam, as in section (3.7). Different expressions

are required to satisfy the conditions of equilibrium and compatibility for the strain distribution in a composite section. A general solution was not obtained but a trial and error method has been used to solve the equations in this investigation.

5.2 Method of analysis.

For the sake of simplicity, the ultimate strength behaviour of concrete based on the Madrid[19] equation (5.1), as shown in Figure (3.3)

$$\sigma = \sigma_o\left[2\frac{\epsilon}{\epsilon_o} - \left(\frac{\epsilon}{\epsilon_o}\right)^2\right] \qquad (5.1)$$

is used in the analysis.

Where, σ_o - maximum stress which defines the quality and strength of concrete.

ϵ_o - the corresponding strain at σ_o

Note: A solution was obtained, see Appendix C, using the Stress-strain relationship due to Desayi and Krishnan[20]

$$\sigma = \frac{E_c \epsilon}{1+\left(\frac{\epsilon}{\epsilon_o}\right)^2}$$

but some complications in numerical solution were encountered at low strain level.

An enlarged view of an element of length dx on the centroidal axis of a beam is shown in Figure (5.1). From similar triangles it is

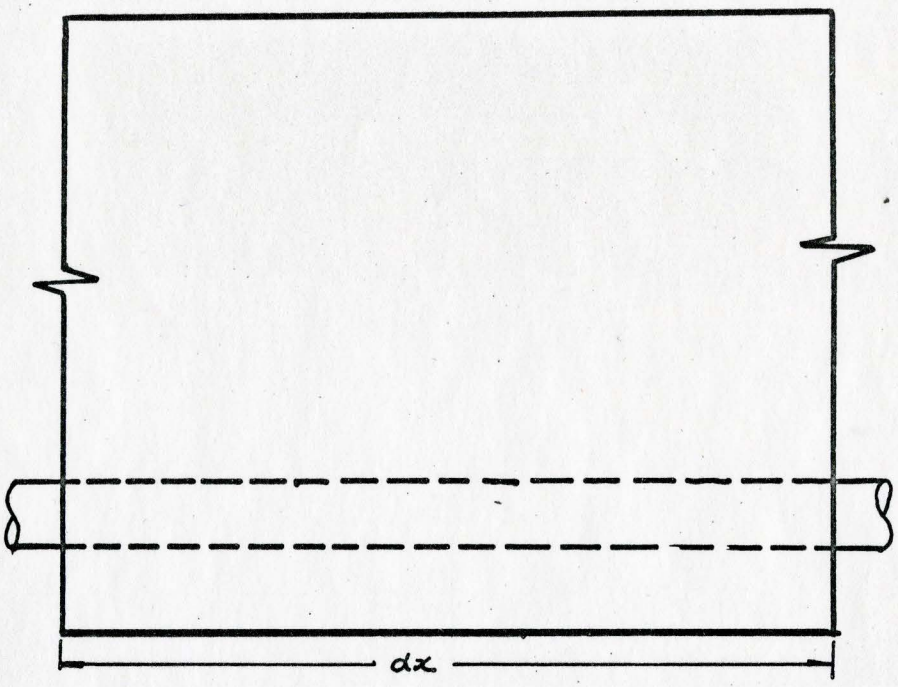

UNDEFORMED STATE

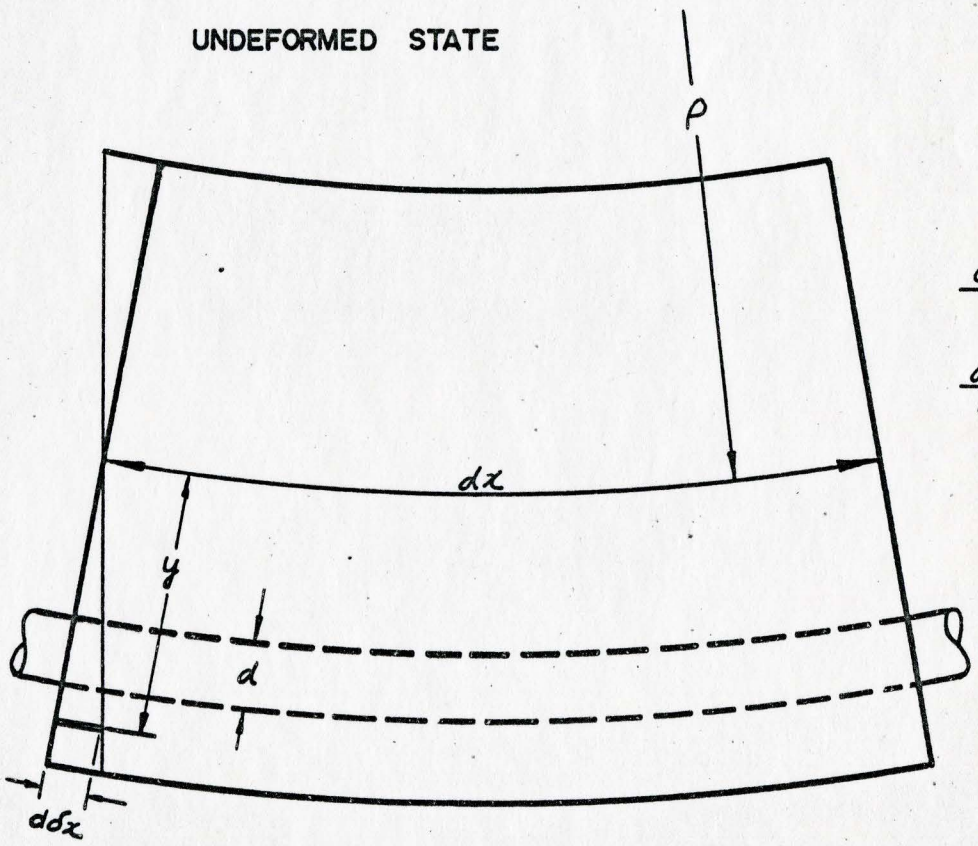

$$\frac{dx}{\rho} = \frac{d\delta x}{y}$$

$$\frac{d\delta x}{dx} = \epsilon$$

$$= Ky$$

DEFORMED DIAGRAM

FIG. 5·1

seen that

$$\frac{d\delta x}{dx} = \frac{y}{\rho} \tag{5.2}$$

where ρ - radius of curvature is equal to $\frac{1}{K}$

K - curvature

y - distance below the neutral surface.

by definition

$$\frac{d\delta x}{dx} \text{ - strain}$$

Equation (5.2) may be written as

$$K = \frac{\epsilon}{y} \tag{5.3}$$

Therefore, the curvature of the concrete section is

$$K_c = \frac{\epsilon_{ct} + \epsilon_{cb}}{2H} \tag{5.4a}$$

and the curvature of the steel is

$$K_s = \frac{\epsilon_{sb} - \epsilon_{st}}{d} \tag{5.4b}$$

If the ratio of the strain at the bottom fibre of the concrete to the strain at the top fibre of the concrete is α, i.e.

$$\alpha = \frac{\epsilon_{cb}}{-\epsilon_{ct}} \tag{5.5}$$

Equation (5.4a) becomes

$$K_c = \frac{1}{2H} \epsilon_{cb} \left(\frac{\alpha - 1}{\alpha} \right) \qquad (5.4c)$$

According to the assumption(1) made in section (3.3) that the concrete and the steel have equal curvatures at any section

$$K_c = K_s \qquad (5.6)$$

5.3

In the equilibrium condition, it is desirable to express each component in terms of strains at the bottom fibre of the concrete (ϵ_{cb}), and the ratio (α).

a) Expression for the flexural moment in the concrete - M_c

Figure (5.2) shows an idealized cross section, a strain distribtuion, and the corresponding stress distribution. If K is the curvature, ρ is the radius of curvature, y is the distance from the neutral axis of the fibre with the strain ϵ, and

$$\sigma = f(\epsilon)$$

is the stress-strain formula, then

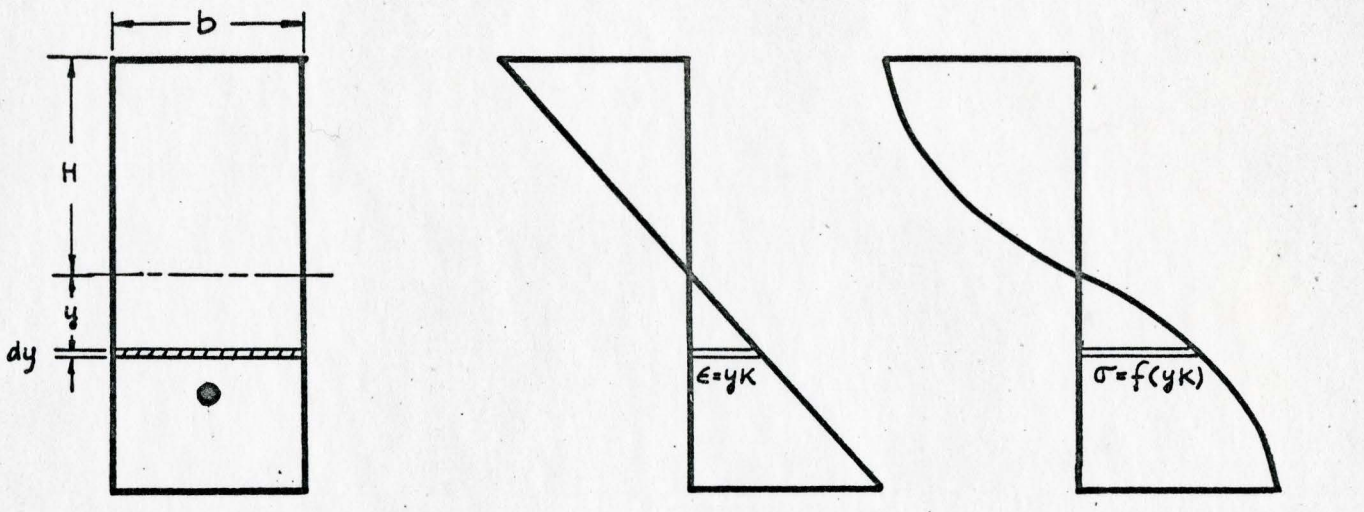
b
H
y
dy
ϵ=yK
σ=f(yK)
CROSS SECTION
STRAIN DISTRIBUTION
STRESS DISTRIBUTION

FIG. 5·2

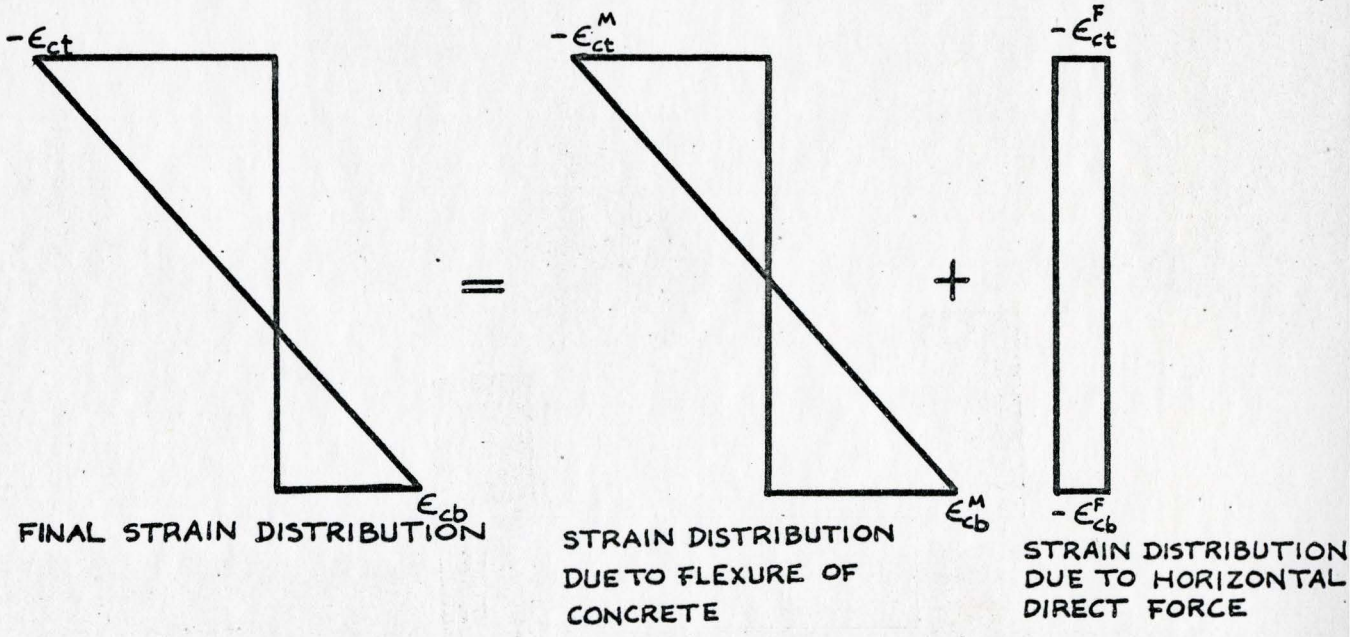
-ϵct
ϵcb
FINAL STRAIN DISTRIBUTION
=
-ϵct M
ϵcb M
STRAIN DISTRIBUTION DUE TO FLEXURE OF CONCRETE
+
-ϵct F
-ϵcb F
STRAIN DISTRIBUTION DUE TO HORIZONTAL DIRECT FORCE

FIG. 5·3

$$\epsilon = yK$$

$$\sigma = f(yK) \tag{5.7}$$

From equation (5.3) and (5.7), the force acting on the area b dy will be

$$f(yK_c)b\,dy \tag{5.8}$$

The statical moment of this force with respect to the neutral axis is

$$\int_{y=0}^{y=H} f(yK_c)\,y\,b\,dy \tag{5.9}$$

Because of the symmetry, the statical moment of the stresses acting on the upper and lower half of the cross section will be the same, therefore the flexural stress resultant in the concrete section can be expressed as[21]

$$M_c = 2\int_{y=0}^{y=H} f(yK_c)\,by\,dy \tag{5.10}$$

From equation (5.1) and (5.3)

$$M_c = 2b\sigma_o \int_{y=0}^{y=H} \left(\frac{2K_c y}{\epsilon_o} - \frac{K_c^2 y^2}{\epsilon_o^2}\right) y\,dy \tag{5.11}$$

$$= 2b\sigma_o \left(\frac{2K_c H^3}{3\epsilon_o} - \frac{K_c^2 H^4}{4\epsilon_o^2}\right)$$

Substituting equation (5.4c) to equation (5.11)

$$M_c = 2b\sigma_o \left[\frac{\epsilon_{cb} H^2}{3\epsilon_o} \left(\frac{\alpha-1}{\alpha}\right) - \frac{\epsilon_{cb}^2 H^2}{16\epsilon_o^2} \left(\frac{\alpha-1}{\alpha}\right)^2 \right] \qquad (5.12)$$

The flexural moment of concrete is expressed in terms of strain at the bottom fibre of concrete (ϵ_{cb}), and the ratio (α).

b) Expressions for the direct forces acting at the centroids of the concrete and the steel

From Figure (5.3), showing the strain distribution of the concrete for incomplete interaction at the equilibrium condition, the following relationships can be obtained,

$$-\epsilon_{ct} = -\epsilon_{ct}^M - \epsilon_{ct}^F$$

$$\epsilon_{cb} = \epsilon_{cb}^M - \epsilon_{cb}^F$$

$$-\epsilon_{ct} + \epsilon_{cb} = -2\epsilon_{cb}^F$$

Since, $\epsilon_{ct}^M = \epsilon_{cb}^M$

and $\epsilon_{ct}^F = \epsilon_{cb}^F$

The strain caused by the direct force (F) alone on the concrete will be

$$\epsilon_{cb}^F = \frac{\epsilon_{ct} - \epsilon_{cb}}{2} \qquad (5.13)$$

From equation (5.1) and (5.5), stress due to direct force alone (σ^F) can be obtained

$$\sigma^F = \sigma_o \left[\left(\frac{-1-\alpha}{\alpha}\right) \frac{\epsilon_{cb}}{\epsilon_o} - \left(\frac{-1-\alpha}{\alpha}\right)^2 \frac{\epsilon_{cb}^2}{4\epsilon_o^2} \right] \qquad (5.14)$$

The direct force (F_c) acting at the centroid of the cross section area of the concrete, may therefore be written as

$$F_c = \sigma_o A_c \left(\frac{-1-\alpha}{\alpha}\right) \frac{\epsilon_{cb}}{\epsilon_o} \left[1 - \left(\frac{-1-\alpha}{\alpha}\right) \frac{\epsilon_{cb}}{4\epsilon_o} \right] \qquad (5.15)$$

Similarly, the horizontal direct force acting at the centroid of the cross section area of the steel will be

$$F_s = E_s A_s \frac{\epsilon_{st} + \epsilon_{sb}}{2} \qquad (5.16)$$

c) Expression for the flexural moment in the steel - M_s

$$M_s = E_s I_s K_s$$

From equation (5.4) and (5.6)

$$M_s = E_s I_s \frac{\epsilon_{cb}}{2H} \left(\frac{\alpha-1}{\alpha}\right) \qquad (5.17)$$

However, it is assumed that the magnitude of the flexural moment in the steel is negligible when compared with M_c and

$F \cdot z$

Therefore, the condition of equilibrium as seen in equation (3.2) becomes

$$M_t = 2b\sigma_o\left[\frac{\epsilon_{cb}H^2}{3\epsilon_o}\left(\frac{\alpha-1}{\alpha}\right) - \frac{\epsilon_{cb}^2 H^2}{16\epsilon_o^2}\left(\frac{\alpha-1}{\alpha}\right)^2\right] + \sigma_o A_c z\left(\frac{-1-\alpha}{\alpha}\right)\frac{\epsilon_{cb}}{\epsilon_o} \quad (5.18)$$

$$\left[1-\left(\frac{-1-\alpha}{\alpha}\right)\frac{\epsilon_{cb}}{4\epsilon_o}\right] + E_s I_s \frac{\epsilon_{cb}}{2H}\left(\frac{\alpha-1}{\alpha}\right)$$

4.4 The condition of compatibility.

From the strain distribution diagram for a cracked and uncracked section of the reinforced concrete beam as shown in Figure (5.4), and from geometry, the following relationships are obtained

$$\epsilon_L = \epsilon_{sb} - \frac{B}{d}(\epsilon_{sb} - \epsilon_{st}) \quad (5.19)$$

in which B and ε_L are the geometric features as indicated in Figure (5.4).

$$B = 2H - 2H' - D_s + \frac{d}{2}$$

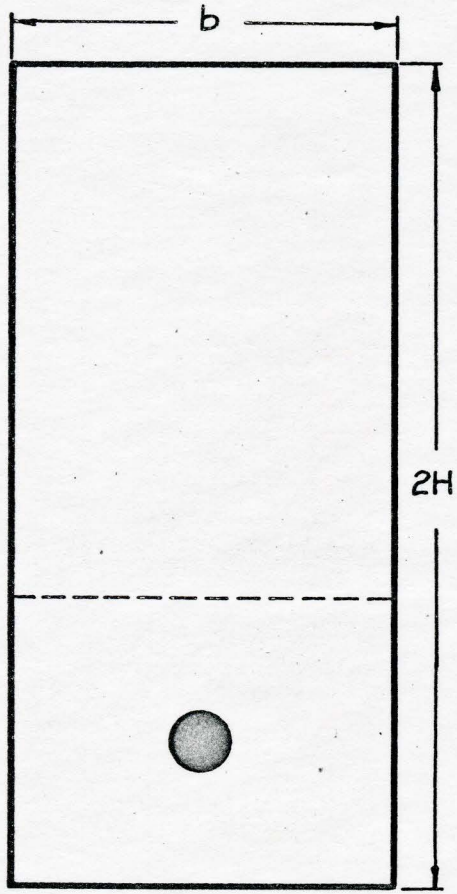

CROSS SECTION

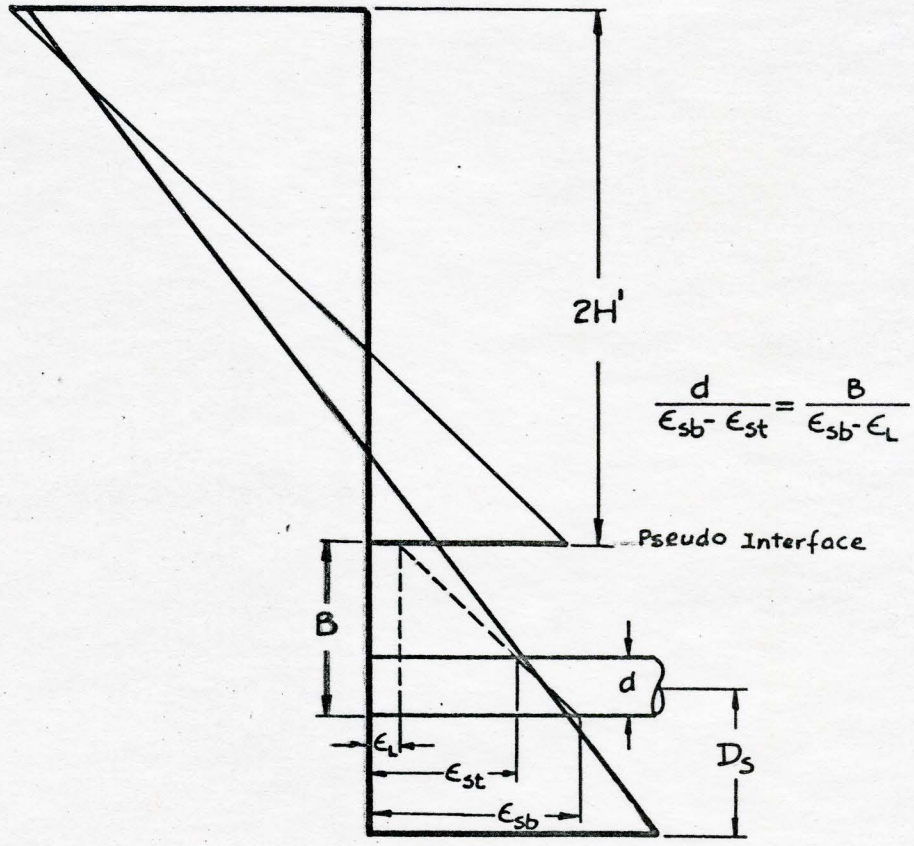

STRAIN DISTRIBUTION

FIG.5·4

From equation (5.4a), (5.4b) and (5.6)

$$\epsilon_{sb} - \epsilon_{st} = \frac{d}{2H} (\epsilon_{ct} + \epsilon_{cb})$$

therefore, equation (5.19) can be written as

$$\epsilon_L = \epsilon_{sb} - \frac{B}{2H} \left(\frac{\alpha - 1}{\alpha} \right) \epsilon_{cb} \qquad (5.20)$$

From equations (5.4a) and (5.4b)

$$\epsilon_{sb} - \epsilon_{st} = \frac{d}{2H} (\epsilon_{ct} + \epsilon_{cb})$$

and from equations (5.6) and (5.16)

$$\epsilon_{st} + \epsilon_{sb} = \frac{2F}{E_s A_s}$$

$$\epsilon_{sb} = \frac{d}{4H} \left(\frac{\alpha - 1}{\alpha} \right) \epsilon_{cb} - \frac{F}{E_s A_s}$$

Therefore equation (5.20) may be written as

$$\epsilon_L = \frac{F}{E_s A_s} + \frac{1}{2H} \epsilon_{cb} \left(\frac{\alpha - 1}{\alpha} \right) \left(\frac{d}{2} - B \right) \qquad (5.21)$$

From Figure (5.4), according to the compatibility condition, and equation (5.21), the equation of compatibility may be written as

$$\frac{d\gamma}{dx} = \epsilon_{cb} - \epsilon_L \qquad (5.22)$$

$$= \frac{F}{E_s A_s} + \frac{1}{2H}\left(\frac{\alpha-1}{\alpha}\right)\epsilon_{cb}\left(\frac{d}{2} - B\right) - \epsilon_{cb}$$

$$= \frac{F}{E_s A_s} - \epsilon_{cb}\left(\frac{\alpha-1}{\alpha}\right)\left[\left(\frac{\alpha}{\alpha-1}\right) - \frac{d}{4H} + \frac{B}{2H}\right]$$

Substituting equation (5.22) in equation (3.1) and (3.4)

$$\frac{1}{k}\frac{d^2F}{dx^2} = \frac{F}{E_s A_s} - \epsilon_{cb}\left(\frac{\alpha-1}{\alpha}\right)\left[\left(\frac{\alpha}{\alpha-1}\right) - \frac{d}{4H} + \frac{B}{2H}\right] \qquad (5.23)$$

For complete interaction, the rate of change of slip at this section is equal to zero, i.e.

$$\frac{d\gamma}{dx} = 0$$

The direct horizontal force F becomes F', and from equation (5.23) the expression for the direct horizontal force for complete interaction is obtained,

$$F' = E_s A_s \epsilon_{cb}\left(\frac{\alpha-1}{\alpha}\right)\left[\left(\frac{\alpha}{\alpha-1}\right) - \frac{d}{4H} + \frac{B}{2H}\right] \qquad (5.24)$$

4.5 Force per unit length transmitted by reinforcing steel to the concrete, (q).

from the chain-rule

$$\frac{dF}{dx} = \frac{dF}{d\epsilon_{cb}} \cdot \frac{d\epsilon_{cb}}{dx} \tag{5.25}$$

Taking the derivative of F in equation (5.15) with respect to (ε_{cb}) and writing the applied moment as a function of x along the beam in equation (5.18), the expression for $\frac{d\epsilon_{cb}}{dx}$ and $\frac{dF}{d\epsilon_{cb}}$ may be obtained, in a straight-forward manner.

Simply supported beam with an unsymmetrical point load

For a section to the left of the load P, that is, where $x < u$, the moment is

$$M_t = \frac{Px}{L}(L-u)$$

$$\frac{d\epsilon_{cb}}{dx} = \frac{P}{L}(L-u) \Big/ \left\{ 2b\sigma_o\left[\frac{H^2}{3\epsilon_o}\left(\frac{\alpha-1}{\alpha}\right) - \frac{\epsilon_{cb}H^2}{8\epsilon_o^2}\left(\frac{\alpha-1}{\alpha}\right)^2\right] + \right. \tag{5.26}$$

$$\left. \frac{\sigma_o A_c z}{\epsilon_o}\left(\frac{1-\alpha}{\alpha}\right)\left[1 - \left(\frac{1-\alpha}{\alpha}\right)\frac{\epsilon_{cb}}{2\epsilon_o}\right] + \frac{E_s I_s}{2H}\left(\frac{\alpha-1}{\alpha}\right)\right\}$$

From equation (5.15)

$$\frac{dF}{d\epsilon_{cb}} = \frac{\sigma_o A_c}{\epsilon_o}\left(\frac{1-\alpha}{\alpha}\right)\left[1 - \left(\frac{1-\alpha}{\alpha}\right)\frac{\epsilon_{cb}}{2\epsilon_o}\right] \tag{5.27}$$

From equations (5.25), (5.26) and (5.27)

$$q_L = \frac{dF}{dx}$$

$$= \left\{ \sigma_0 A_c \left(\frac{-1-\alpha}{\alpha}\right) \frac{1}{\epsilon_0} \left[1 - \left(\frac{-1-\alpha}{\alpha}\right) \frac{\epsilon_{cb}}{2\epsilon_0} \frac{P(L-u)}{L} \right] \right\} /$$

$$\left\{ 2b\sigma_0 \left[\frac{H^2}{3\epsilon_0} \left(\frac{\alpha-1}{\alpha}\right) - \frac{\epsilon_{cb} H^2}{8\epsilon_0^2} \left(\frac{\alpha-1}{\alpha}\right)^2 \right] + \sigma_0 A_c z \left(\frac{-1-\alpha}{\alpha}\right) \frac{1}{\epsilon_0} \right.$$

$$\left. \left[1 - \left(\frac{-1-\alpha}{\alpha}\right) \frac{\epsilon_{cb}}{2\epsilon_0} \right] + \frac{E_s I_s}{2H} \left(\frac{\alpha-1}{\alpha}\right) \right\}$$

for the single point loading system and q_L, q_R for the other loading systems may be obtained in a similar fashion.

4.6 Strains and height of crack.

Since it is difficult to express strains in terms of parameters of force uniquely, numerical solutions for strains will have to be solved by the approach of trial and error.

In order that both the requirements of equilibrium and compatibility be satisfied, equations (5.15), (5.18) and (5.24) should be used simultaneously in solving for the unknowns (ε_{cb}) and (α).

The height of crack is obtained in the same manner as seen in section 3.8.

Chapter VI

Investigations for the Curvilinear deformation Analysis

6.1

In order to demonstrate the validity and application of the equations developed for the curvilinear deformation analysis, it is desirable that the analytical procedures for some examples be presented. As stated previously, the developed equations in Chapter V have to be solved simultaneously by the approach of trial and error. The Newton-Raphson[22] method of solving simultaneous equations is used in this investigation as outlined in Appendix B. This method requires that only one point be known in the neighbourhood of the desired solution.

The remainder of this Chapter is devoted to the application of the equations developed for investigation of complete and incomplete interaction in a reinforced concrete beam.

6.2 For the case of complete interaction

Since it is important to satisfy the requirements of equilibrium and compatibility, equations (5.15), (5.18) and (5.24) must be solved simultaneously for the unknowns concrete strain (ε_{cb}) and strain ratio (α). From the relationships

$F = F'$ for complete interaction

and $M_t = M_c + F \cdot z + M_s$

the following equations are obtained:

$$\sigma_o A_c \left(\frac{-1-\alpha}{\alpha}\right) \frac{\epsilon_{cb}}{\epsilon_o} \left[1 - \left(\frac{-1-\alpha}{\alpha}\right) \frac{\epsilon_{cb}}{4\epsilon_o}\right] = E_s A_s \frac{\epsilon_{cb}}{\alpha} \left(\frac{\alpha-1}{\alpha}\right) \left[\left(\frac{\alpha}{\alpha-1}\right) + \frac{B}{2H} - \frac{d}{4H}\right] \quad (6.1)$$

and

$$M_t = 2b\sigma_o \left[\frac{\epsilon_{cb} H^2}{3\epsilon_o} \left(\frac{\alpha-1}{\alpha}\right) - \frac{\epsilon_{cb}^2 H^2}{16\epsilon_o^2} \left(\frac{\alpha-1}{\alpha}\right)^2\right] + \sigma_o A_c z \left(\frac{-1-\alpha}{\alpha}\right) \frac{\epsilon_{cb}}{\epsilon_o}$$
$$\left[1 - \left(\frac{-1-\alpha}{\alpha}\right) \frac{\epsilon_{cb}}{4\epsilon_o}\right] + E_s I_s \frac{\epsilon_{cb}}{2H} \left(\frac{\alpha-1}{\alpha}\right) \quad (6.2)$$

The Newton-Raphson[22] method of trial and error is used, with the aid of the IBM 7040 computer, to solve for the unknowns (ε_{cb}) and (α) which satisfy both equations (6.1) and (6.2), for a specified applied moment. A sample calculation is shown in Appendix B.

For a section having identical properties as those described previously located under the load point, subjected to design moment, strain at bottom fibre of concrete (ε_{cb}) and (α) are obtained from equations (6.1) and (6.2). The section is then allowed to crack with a tensile cracking strain equal to 100 micro in/in. A new section is formed in accordance with the method shown in section (3.8). This process is repeated until an equilibrium state is reached at a certain

cracked level. For the section located under the point load and subjected to design moment the concrete strain (ε_{cb}) and ratio (α) are plotted against the depth of the beam, as shown in Figure (6.1a) and (6.1b), respectively.

According to definition, the ratio (α) is equal to unity, if there is no interaction between the concrete and the steel. From Figure (6.1b), it is obvious that the paths of the curve for any degree of break down of interaction will lie in the region between these two curves of complete and no interaction, for specified section properties.

Compare Figure (6.1a) with Figure (4.2), which is obtained from the elastic analysis, it may be noted that both of the two analyses give similar results. Table (6.1) shows the results of the two analyses, for design moment, at the section under the load point, for complete interaction and identical conditions.

Case	x in	M_t lb-in	F/F'	2H' in	ε_{cb} m "/"	ε_{ct} m "/"	ε_{sb} m "/"	ε_{st} m "/"
linear (Newmark)	29.25	36200	1.0	3.268	100.0	-349.32	656.2	570.24
non-linear	29.25	36200	1.0	3.288	100.0	-357.12	659.4	572.52

Table (6.1)

The crack profiles for a reinforced concrete beam subjected to a two point loading system with complete interaction obtained for both the

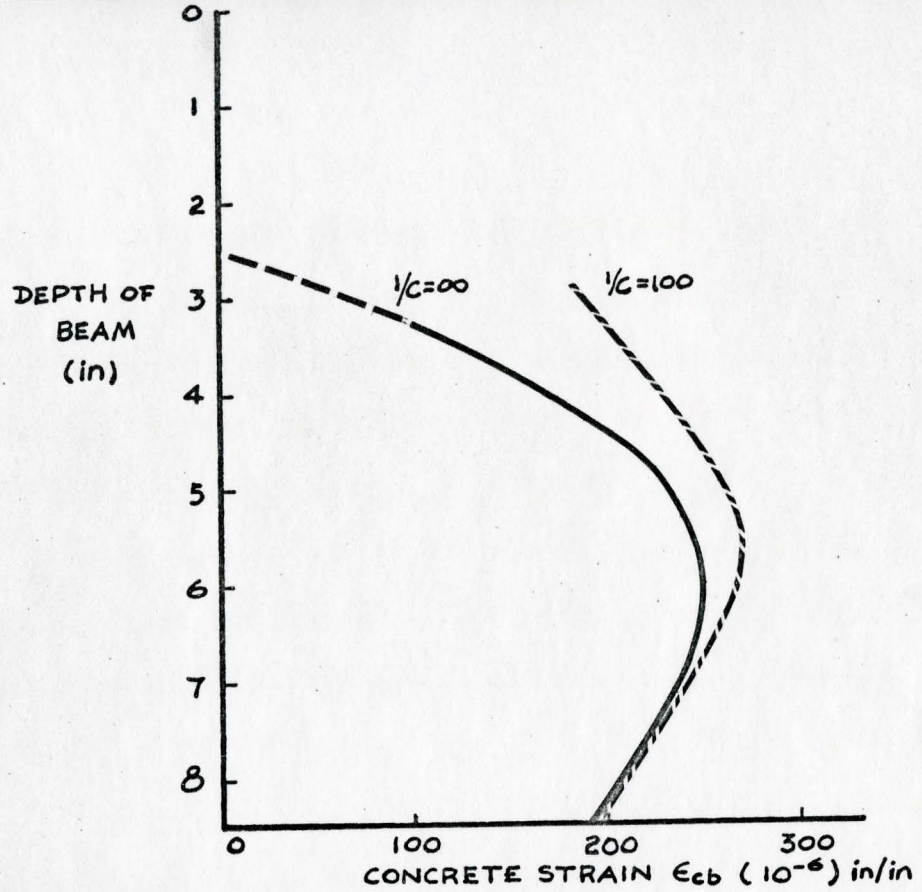

FIG. 6·1a STRAIN VS. DEPTH OF BEAM

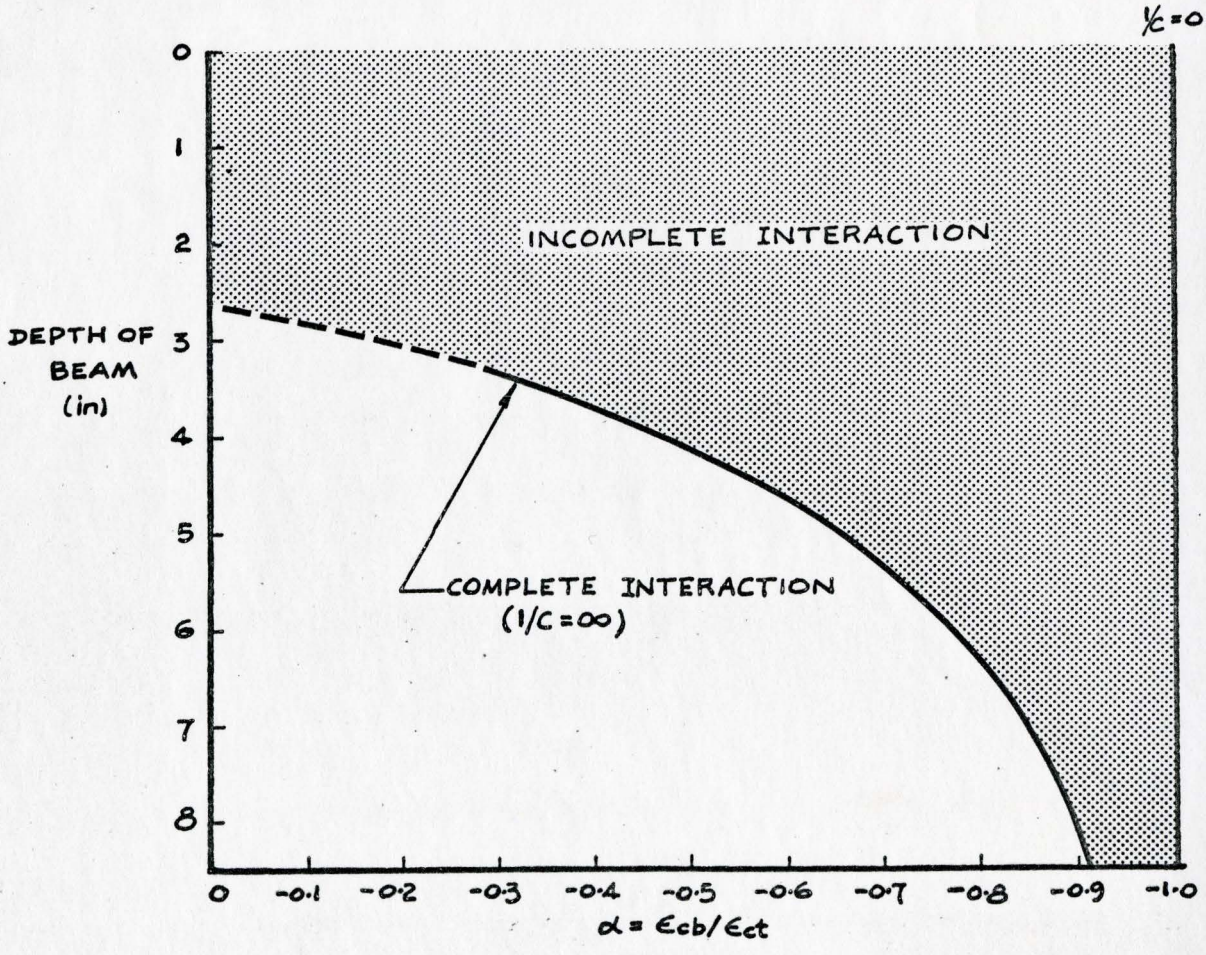

FIG. 6·1b RATIO (α) VS. DEPTH OF BEAM

linear and curvilinear cases are shown in Figure (6.2).

The close agreement between the results of these two analyses is due to the fact that the concrete strain at design moment is still very low, and at a magnitude at which the linear and curvilinear stress-strain curves are practically coincident.

The convergence of the two curves of Figure (6.1a) and (4.2) at the equilibrium configuration provides a check on the correctness of the solutions of the equations for the curvilinear case.

6.3 For the case of incomplete interaction

Value of horizontal direct force with complete interaction (F') for a particular section, was found by the same procedures as outlined in section 6.2.

When there is incomplete interaction

$$F(\epsilon_{cb}, \alpha) = \beta F'$$

For the purpose of determining the effect of loss of interaction, in this case, a value of $\beta = F/F'$ was taken as that under a single load point for a value of 1/C equal to 100, as derived by Newmark[15] solution.

The equilibrium condition may be written as

$$M_t = M_{c+t}(\epsilon_{cb}, \alpha) + F(\epsilon_{cb}, \alpha) z$$

The values of concrete strain at the bottom fibre (ε_{cb}), and the ratio (α) were obtained by the trail and error method. New sections

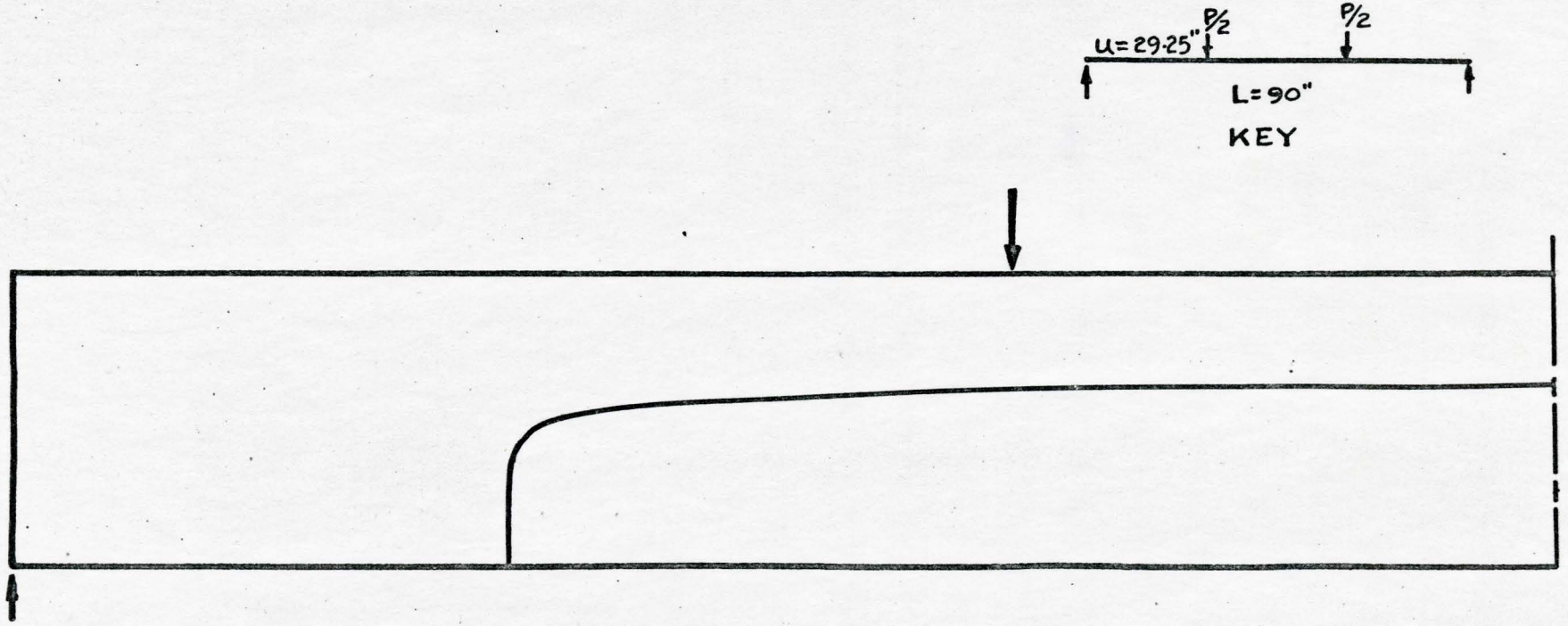

ESTIMATED EXTREMITIES OF POTENTIAL CRACKS OF A REINFORCED CONCRETE BEAM WITH COMPLETE INTERACTION (TWO POINT LOAD)

FIG. 6·2

were obtained. As the cracking procedure continued, it was found that no more solutions for (ε_{cb}) and (α) could be obtained for incomplete interaction after the height of crack for this case extended to, or above, the crack height at which the curve hits the ordinate in the case of complete interaction (C.H. $\doteq$ 6" in this case). This could be reasoned to mean that there are no more solutions for (ε_{cb}) and (α) above this crack height, which would satisfy both compatibility and equilibrium conditions. However, regarding the path of the curve for incomplete interaction, (1/C = 100), shown in Figure (6.1a), it can be seen that a convergent point at a tensile cracking strain (ε_p = 100 micro in/in) still cannot be attained. This is because no values of F' exist for crack heights in excess of that for the complete interaction case.

It is therefore concluded that, in order to further the analysis, a new approach to this problem must be adopted.

Chapter VII

Estimated Crack Profiles of a Reinforced Concrete Beam

7.1

Having discovered that the application of the non-linear strain-stress relationship for the concrete did not lead to an improvement in the solution of the problem, and analysis was then carried out by assuming that the actual beam is in a degenerate form as outlined in Chapter II. That is to say that the beam under load suffers a loss of interaction and has degenerated from a hypothetical state of complete interaction. In this hypothetical state the beam would be capable of supporting some higher load.

A section of the reinforced concrete beam subjected to the design moment and at the load point, was analysed by this approach for the linear and non-linear cases. Figure (7.1) shows the family of curves of the concrete strain at the bottom fibres of the uncracked section versus the depth of the beam for different values of 1/C (∞, 100, 25, 6.25, 3.125). It may be noted that all these curves intersect an ordinate passing through the specified tensile cracking strain (ε_p = 100 micro in/in.) of the concrete, at equilibrium condition. A similar effect could be attained, for the section subjected to moments other than the design moment, as shown in Figure (7.1).

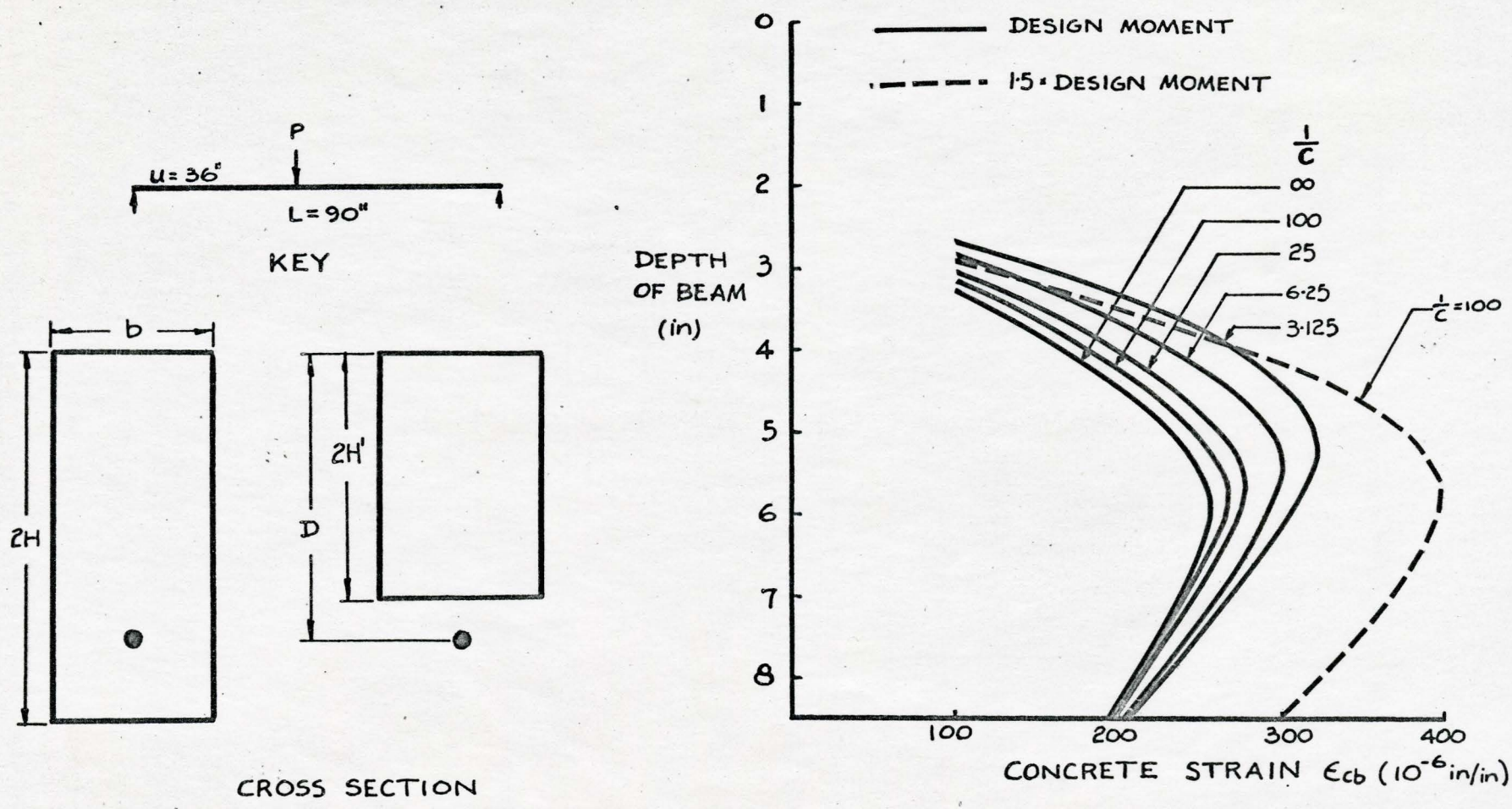

ESTIMATED CONCRETE STRAIN UNDER LOAD POINT WITH VARIATION OF DEGREE OF INTERACTION

FIG. 7·1

Thus it can be seen that a comprehensive analysis is attainable and the computation of crack profiles was then carried out for both linear and non-linear cases.

7.2

In this analysis, the variation of F/F' along the length of beam, due to Newmark[15] was used in both cases. The justification for using the Newmark solution in the case of non-linear deformation analysis was reasoned by assuming that the compressive strains of the concrete for the cracked beam at design moment are small enough to be close to those obtained for the straight line analysis. This assumption is also necessary to simplify the solution of the non-linear equations.

Figure (7.2) and (7.3) show the crack profiles of the reinforced concrete beam with incomplete interaction (1/C = 3.125), subjected to one and two point loading systems, for both the linear and non-linear cases. The results obtained by these two cases though not identical, illustrate that the difference is not big enough to be shown on the scale used in plotting the crack profiles.

7.3

From Figure (7.2) and Figure (7.3), it is seen that the upshooting part of the crack profiles near the load point are not very pronounced with respect to the crack profiles for the complete interaction

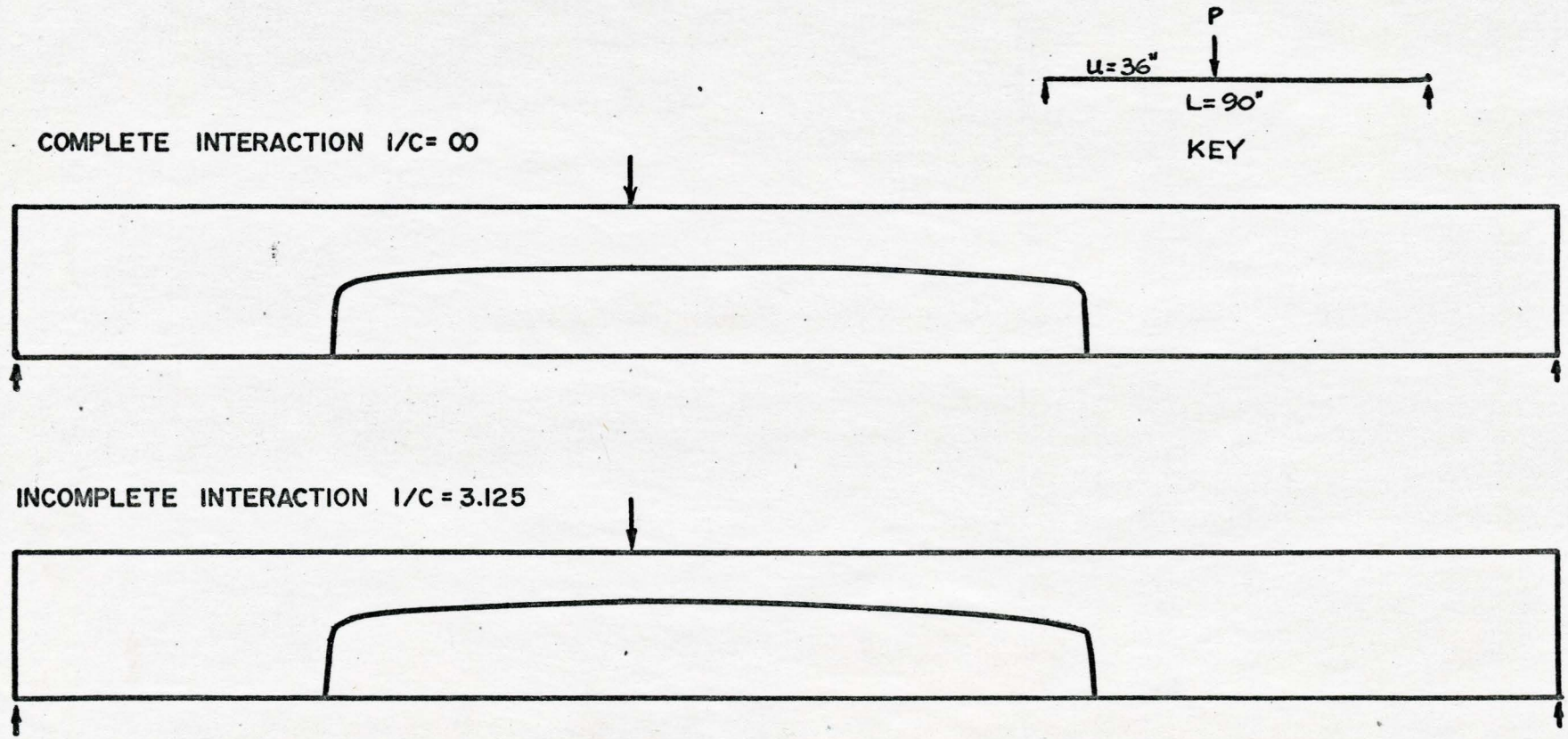

ESTIMATED EXTREMITIES OF POTENTIAL CRACKS OF A REINFORCED CONCRETE BEAM
(ONE POINT LOAD)

FIG. 7·2

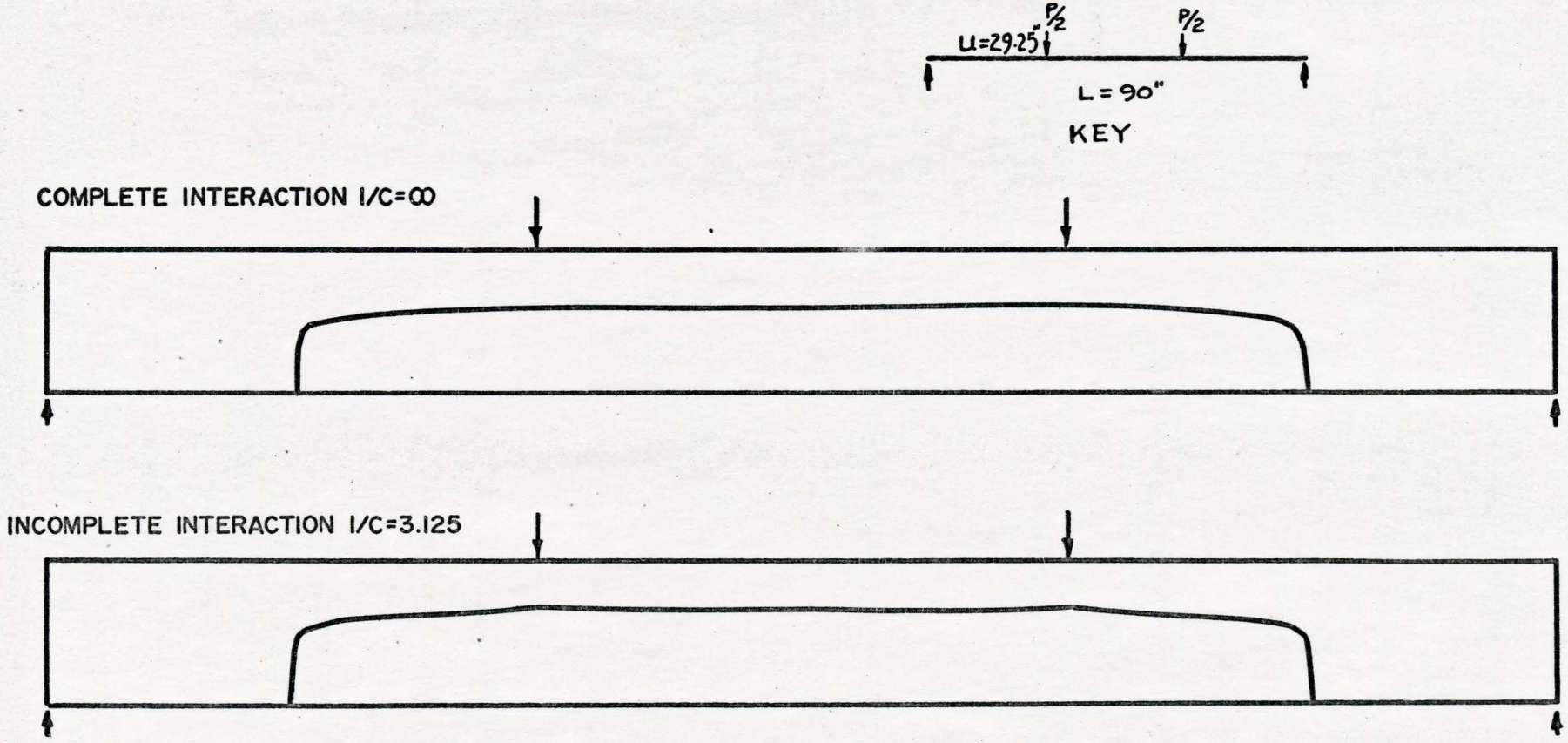

ESTIMATED EXTREMITIES OF POTENTIAL CRACKS OF A REINFORCED CONCRETE BEAM

(TWO POINT LOAD)

FIG. 7·3

case and the influence of other parameters must certainly be considered. However, particularly after cracking it may well be realized that further complications arise. The cracked beam is no longer a prismatic beam, since the cracking process causes a change of geometry of the cross-section along the beam. Thus it may be expected that the values of 1/C will vary along the length of the beam, and therefore the distribution of F/F' along the beam will be different from that of the uncracked beam. These variations may depend on the loading condition, geometry of the beam, percentage of steel, etc., but most importantly the bond slip conditions will be expected to have radically changed.

Robinson[14] pointed out in the light of observations of composite beams, that "even if bond strength was high, and there was no perceptible slip between the steel and the concrete at the ends of the beam (hooks), slip and associated loss of interaction could occur locally in the region of the load points".

Moe[12] suggested that the amount of vertical shear transmission across the bending cracks by friction decreases gradually as the width of the crack (slip) increases.

These speculations were, in fact, verified by slip (or crack width) measurements at the level of reinforcement, see Figure (7.4) and Figure (7.5), performed by Evans and Robinson[23] and Manning[24]. It was shown that the magnitude of slip was largest where the crack occured and diminished with distance away from the crack.

Based on these speculations and observations, a variation of the value of 1/C along the beam was assumed. 1/C is a measure of degree of interaction assumed to be constant in a prismatic or uncracked

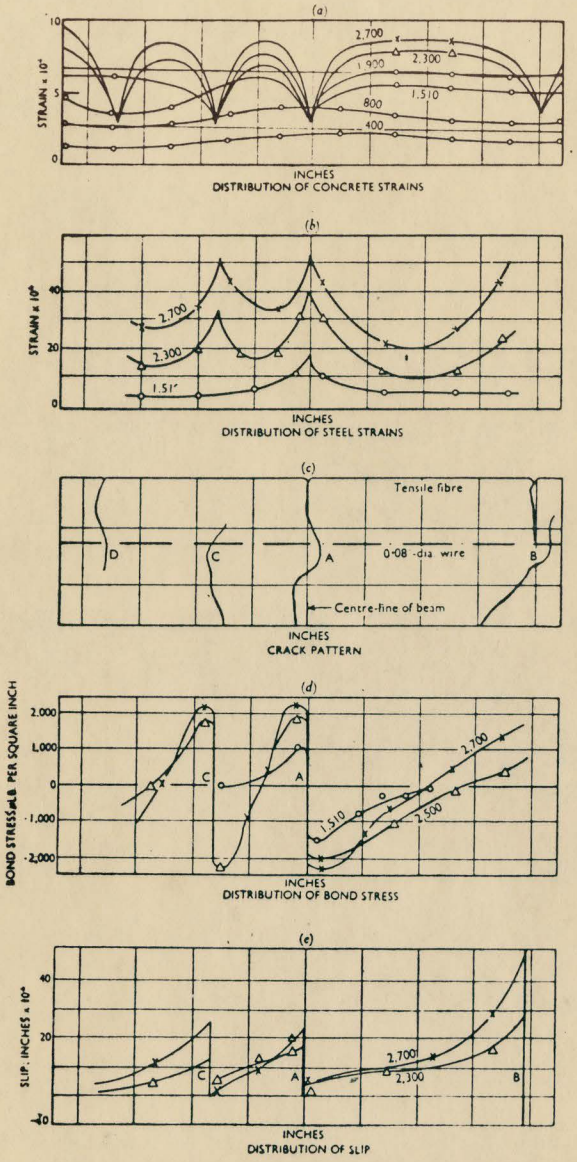

Beam A4. Slip, strains, and stresses
(Six 0·08″-dia wires)

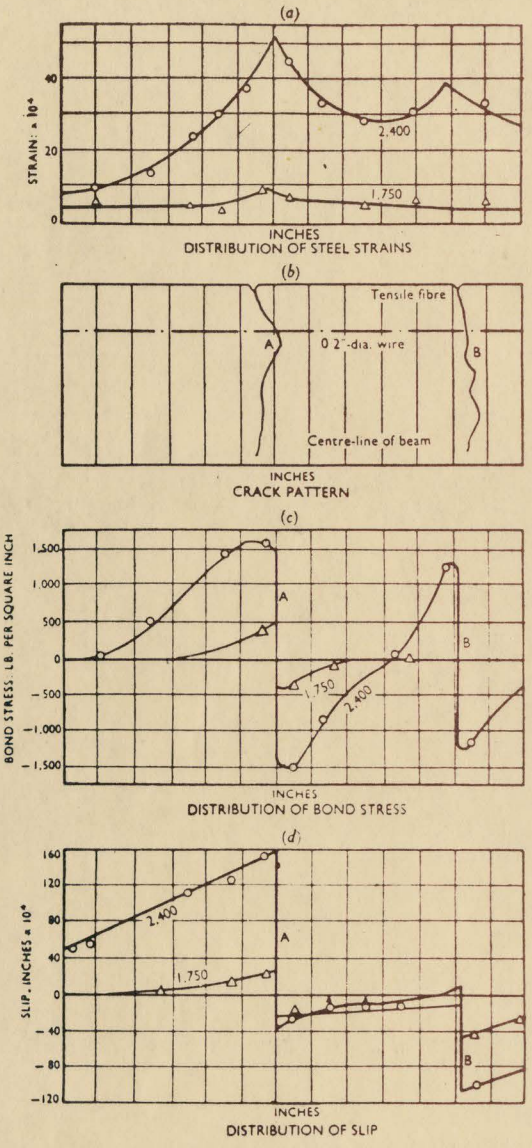

Beam A10
(One 0·2″-dia wire)

DUE TO EVANS & ROBINSON

FIG. 7·4

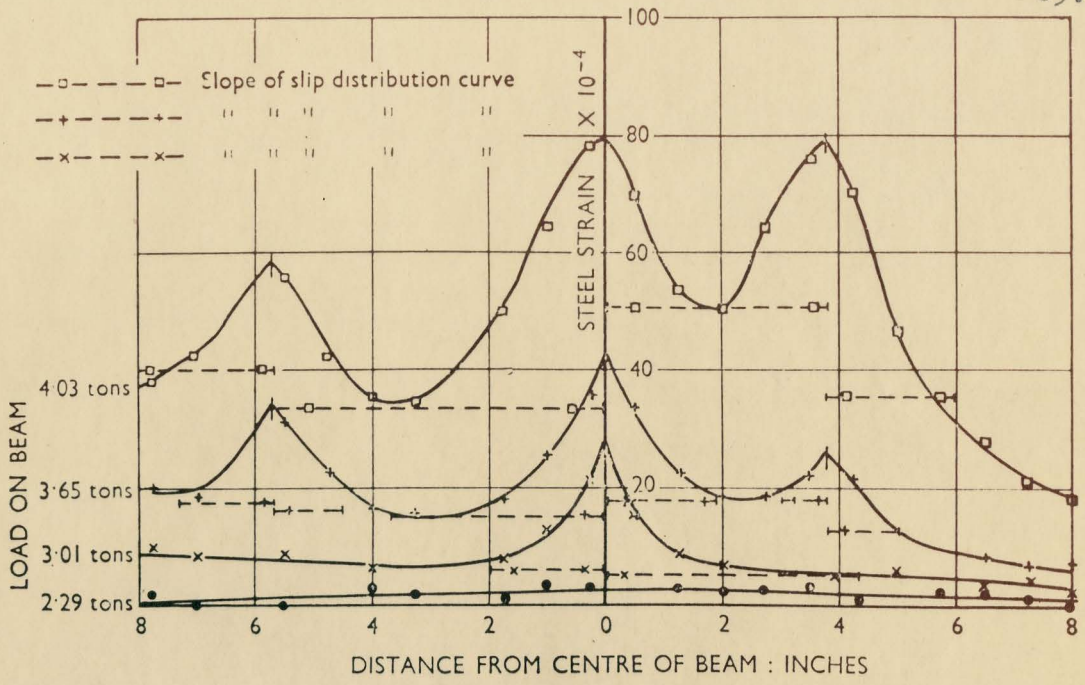

STEEL STRAIN DISTRIBUTION FOR BEAM X2

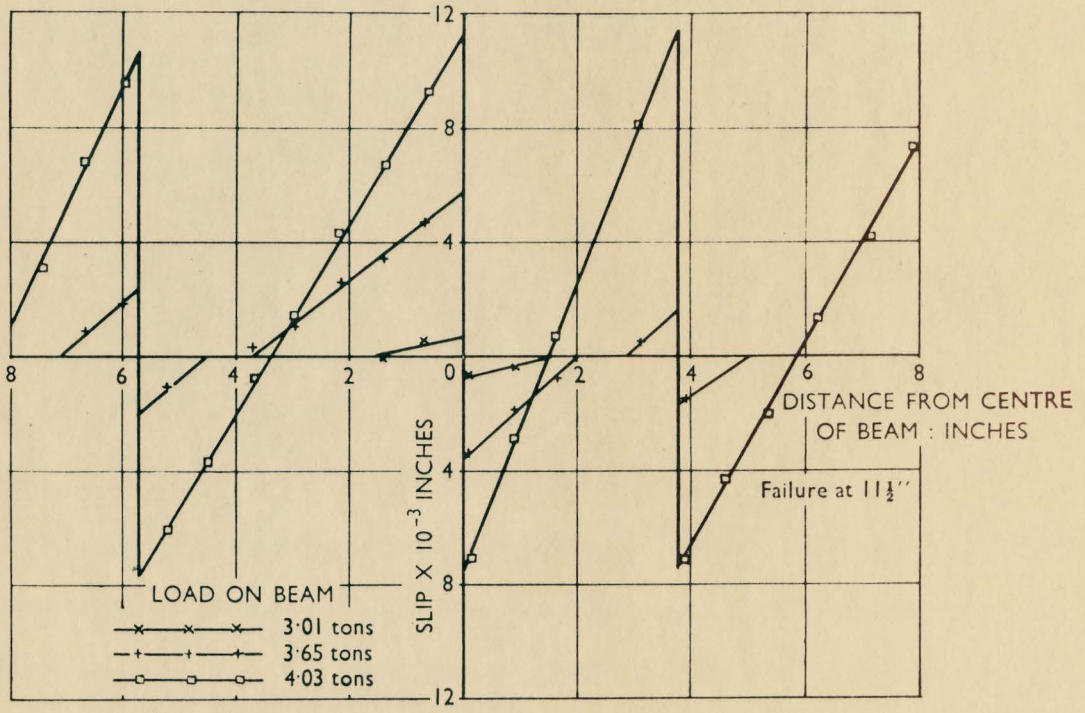

CRACK WIDTHS AT LEVEL OF REINFORCEMENT **DUE TO MANNING**

				0·0010				
0·0050	6·3''	0·0022	5·7''	0·0088	3·8''	0·0028	7·7''	0·012
0·0220		0·0172		0·0208		0·0134		0·0465

SLIP DISTRIBUTION FOR BEAM X2

FIG. 7·5

composite beam. However, in a cracked beam with varying section, it is reasonable to assume that 1/C will vary markedly along the beam. In particular at a probable crack, value of 1/C could be greatly diminished or even zero. For the sake of simplicity, it was assumed that the value of 1/C varied linearly in accordance with the assumption that a relatively large crack was formed under the load points, and that there was virtually no slip at the supports. In order to obtain a numerical solution, 1/C was assumed to vary from 200 at the supports to 0.4 at the load points where a crack is most likely to occur. For the sake of simplicity it was further assumed that 1/C would vary symmetrically with distance on either side of a probable crack, see Figure (7.6). The resulting crack profile of the reinforced concrete beam, subjected to symmetrical two point loading system, at design moment was then estimated and is shown in Figure (7.7).

7.4

Figure (7.8) shows the variation of upper, mid-height and lower strain along the reinforcement of a cracked and uncracked reinforced concrete beam with the above conditions of break down of interaction. It may be observed that in general the form of the variation of strain could provide an envelope for variations of strain along the reinforcement similar to those observed experimentally by Plowman[2], see Figure (7.9). Since stresses observed by Plowman[2] are intended to be those at the mid-height of the rod, it may now be seen that they might be expected to be lower in magnitude, while the lower steel fibre stresses

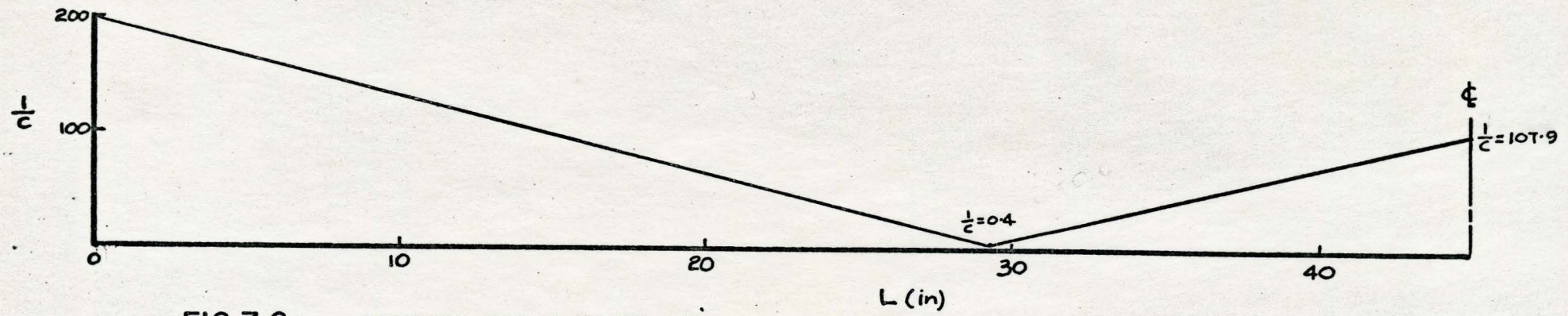

FIG. 7·6a ASSUMED VARIATION OF 1/C

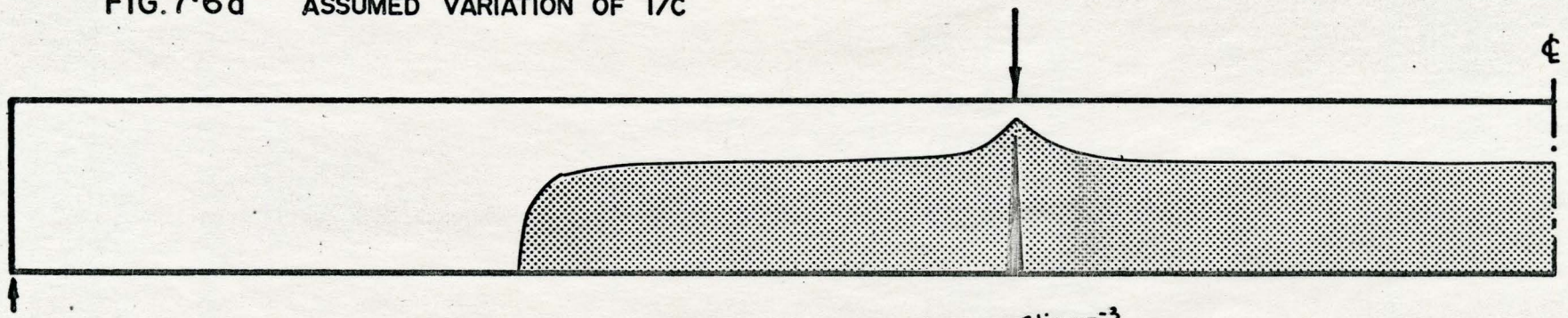

FIG. 7·6b CRACKED BEAM

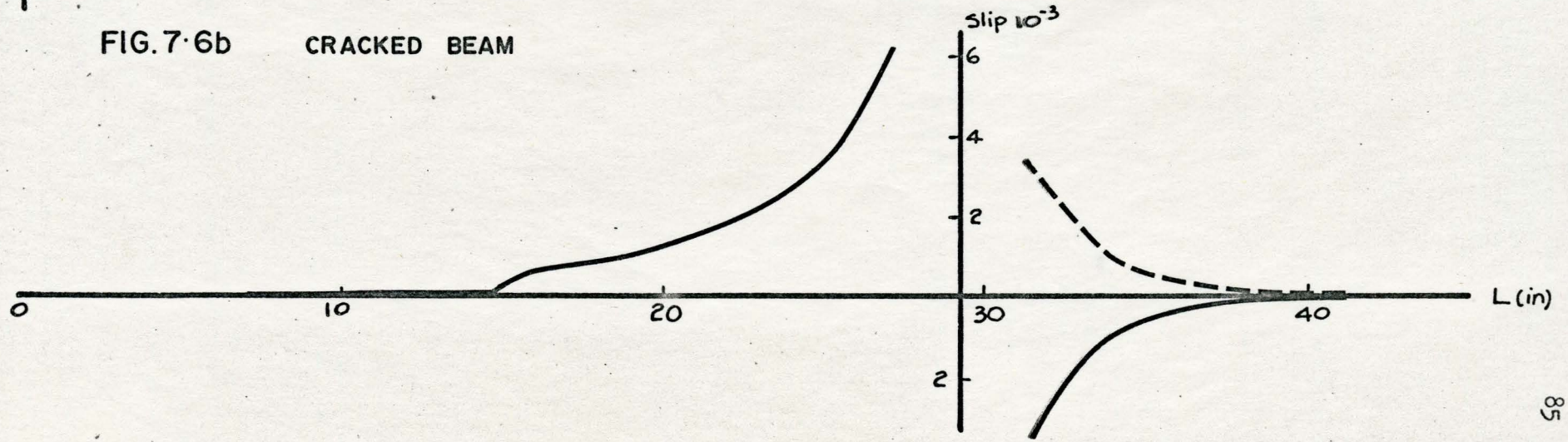

FIG. 7·6c ESTIMATED SLIP DISTRIBUTION

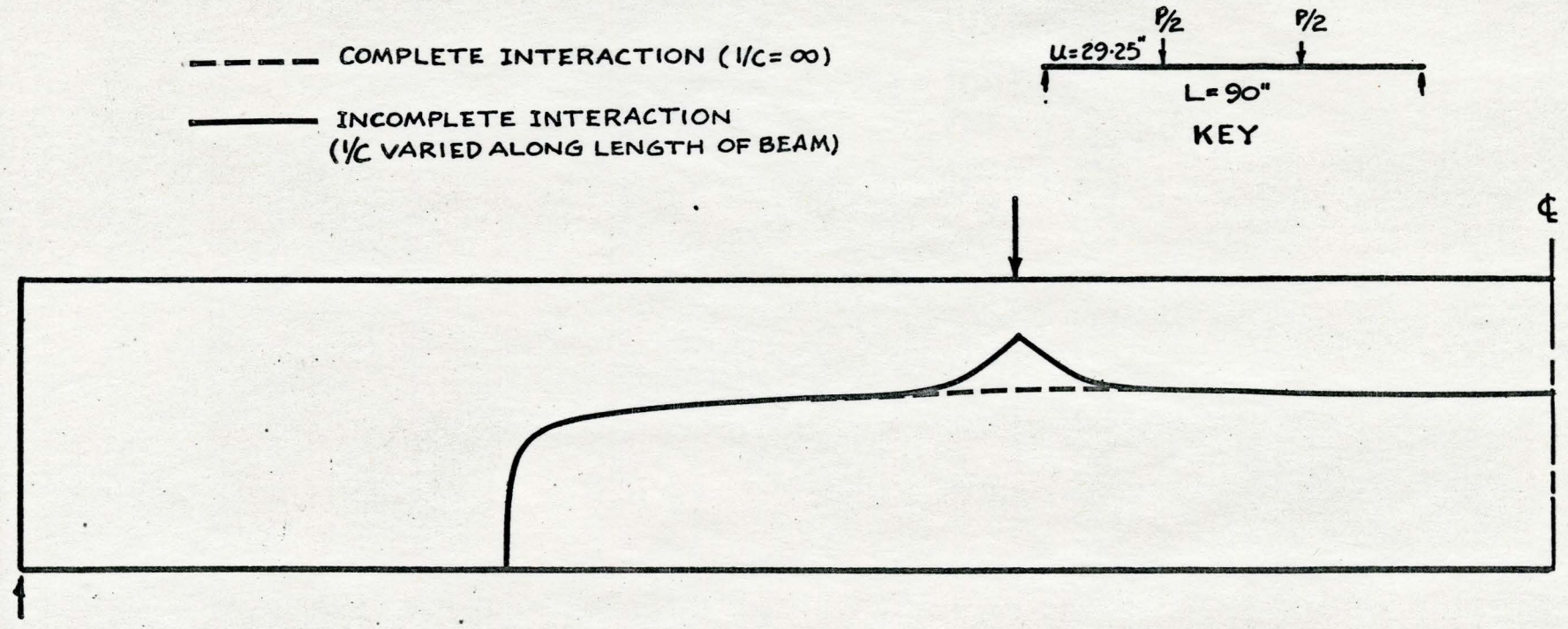

ESTIMATED EXTREMITIES OF POTENTIAL CRACKS OF A REINFORCED CONCRETE BEAM

FIG. 7·7

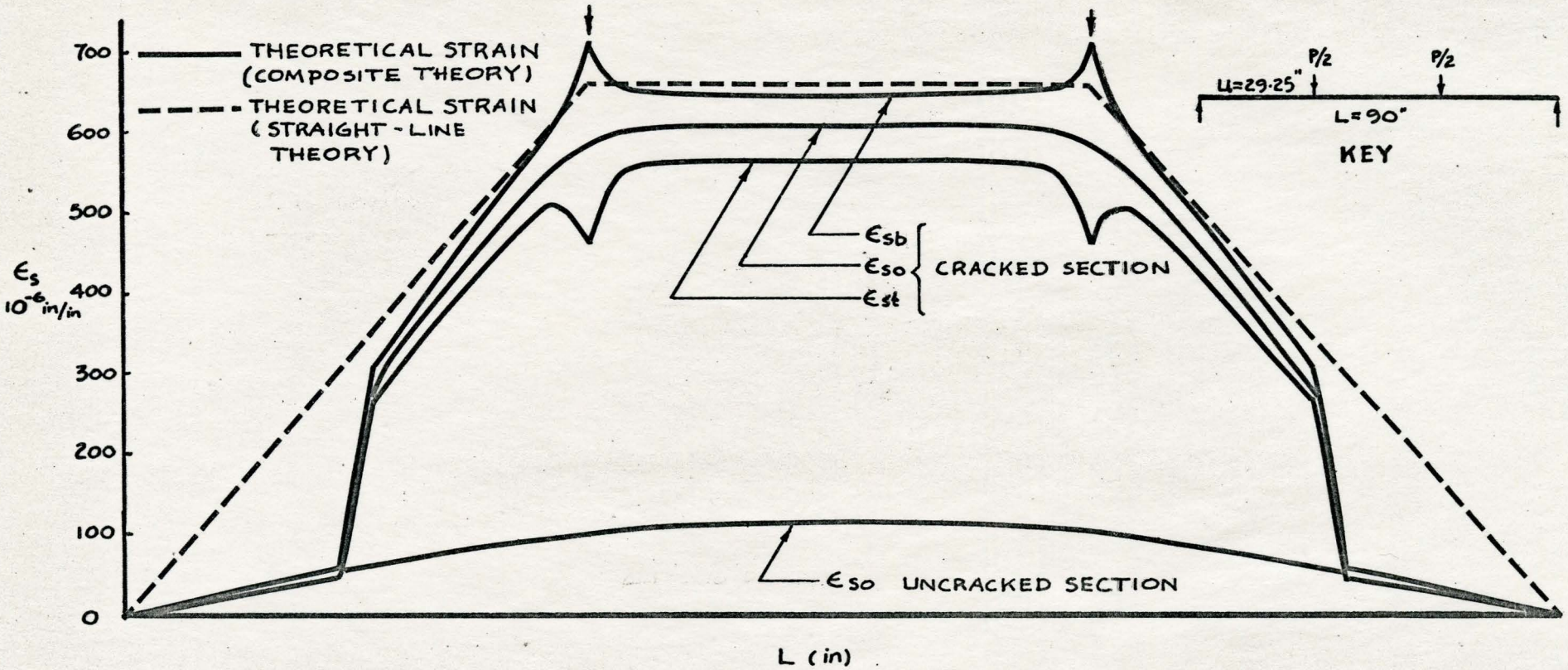

VARIATION OF UPPER, MID-HEIGHT AND LOWER STRAINS ALONG REINFORCEMENT OF REINFORCED CONCRETE BEAM DESIGN LOAD, I/C VARYING ALONG THE BEAM

FIG. 7·8

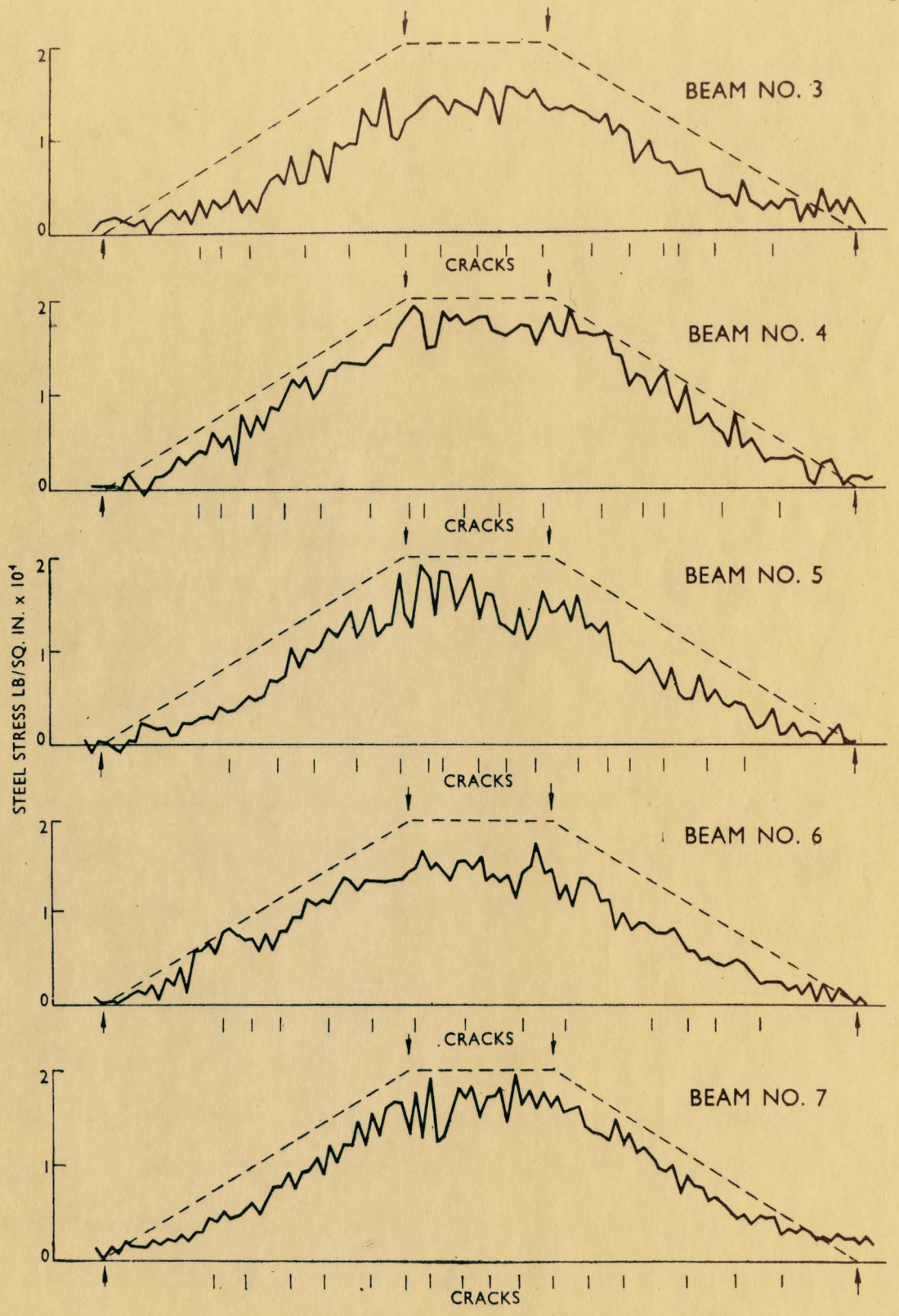

STEEL STRESSES AT DESIGN LOADING IN BEAMS NOS 3, 4, 5, 6, AND 7
Design stress shown by broken line

DUE TO PLOWMAN

FIG. 7·9

in the steel might be as large or even larger in magnitude than that predicted by the straight-line theory. Plowman[2] concluded that the straight-line theory was perhaps conservative from the point of view of design, because his measured strains were lower than that predicted by the straight-line theory. However, as can be seen it is also possible that the strain in the steel, namely the lower fibre strain could be as large or larger than that due to the straight-line theory, particularly in the region of the point loads. Further, it may be seen that a slight shift of location of the stud (a device used in his strain measurements) in an upward direction, might give much lower strain readings. It may be further reasoned that the formation of the zigzag pattern of stress variation along the beam, as observed by Plowman[2], was caused by the cracking process of the beam.

The estimated slip along the reinforcing steel for incomplete interaction, in Figure (7.6c), shows a similar form compared to those measured by Evans and Robinson[23] and Manning[24].

7.5

Phenomenologically, it has been recognized that the diagonal tension crack is initiated from the vertical flexural cracks which form on the tensile surface of the beam. It becomes inclined and curves upwards and towards the nearer concentrated load. With an increase in the applied load the inclined portion of the crack also propagates downward. At a later stage, it has been observed that splitting

of the concrete along the reinforcement in the shear span occurs. In some beams, the failure is caused by initial yielding of the reinforcement which leads to the relative rotation of beam segments adjacent to the inclined crack[6].

It has been pointed out, previously, that the up-shooting portion, shown in the computed crack profiles, may be considered as the incipient path of the inclined crack. Therefore, once the applied load exceeds a certain limit at which cracking begins, the incipient path of the inclined crack begins to form. It may be speculated that increased deformation due to local yielding of the steel reinforcement, caused by break down of interaction, see Figure (7.8), would trigger off the fully matured inclined crack which leads to the so-called diagonal failure. It therefore could be reasoned that the form of the incipient path may determine the pattern and failure mechanism of a reinforced concrete beam.

Chapter VIII

Summary and Suggestions for Further Studies

The problem of the inclined crack in a simply supported reinforced concrete beam which is treated as a composite member, has been investigated analytically. The analysis is made on the basis of complete and incomplete interaction between the composite elements, the concrete and the steel.

On the consideration that the concrete has non-linear stress-strain characteristics, the basic equations which satisfy the conditions of equilibrium and compatibility, for the problem, were derived. Numerical solutions for the estimating of crack profiles were obtained by the trial and error method and were facilitated by the IBM 7040 computer.

Through investigations, it has been found that the development of the non-linear deformation analysis alone could not provide a solution for this problem.

With modification to Newmark[15] solution, the analysis has been able to furnish crack profiles for study of this aspect. It has not been the intention of this analysis to provide the actual crack profiles observed in a reinforced concrete beam. However, from results obtained, it is observed that this analysis does provide, analytically, vivid descriptions of cracking phenomena which occur in test beams.

Therefore, it may be concluded that the main object of this thesis, which is to provide a basis for a more general investigation of the influence of loss of bond and loading condition on the failure mechanism of a reinforced concrete beam, has been fulfilled.

At this stage, many assumptions have been made in the course of study. In order that further study in this problem may be carried on, these assumptions should be verified by experimental data. The writer wishes to make the following suggestions:

1. The theory of composite action should be studied more vigorously on a fundamental base-model studies.
2. To the problem of reinforced concrete beam, data for the slip distribution along the beam, and the bond modulus should be obtained experimentally[25].
3. A study of influence of loss of interaction on the principal stress trajectories of a reinforced concrete beam may lead to a further insight into this problem.
4. An attempt to formulate a solution which includes the elasto-plastic effect of the steel, for this problem, may lead to a better explanation of the phenomena observed in beam tests.

Chapter IX

Conclusions

The conclusions of this study are as follows:

1) The reinforced concrete beam may be considered as a composite beam with incomplete interaction.
2) In spite of the fact that a cracked reinforced concrete beam does not have a distinct interface the conventional theory can still be applied provided a pseudo-interface is assumed.
3) Consideration of a reinforced concrete beam as a composite beam with incomplete interaction emphasizes the significance of bond slip and its variation along the beam.
4) The analysis shows that the cracking pattern is markedly dependent upon the external loading system on the beam.
5) Loss of interaction on bond slip causes a reduction in the average steel strain distribution.
6) Knowing the bond slip characteristics of a beam, or of a particular rod, an envelope for the slip distribution of the beam could be estimated.
7) Further analytical studies may lead to a better understanding of the problem of so-called 'shear failure' of a reinforced concrete beam.

REFERENCES

(1) Robinson, H.: Preliminary investigation of a composite beam with ribbed slab formed by cellular steel decking, 1963.

(2) Plowman, J. M.: Measurement of Stress in Concrete Beam Reinforcement, The Institution of Civil Engineers, June 1963, Proceedings, Vol. 25.

(3) ACI-ASCE Committee 326: Shear and Diagonal Tension, Journal of the ACI, Jan. 1962, Proceedings, V. 59, No. 1.

(4) ACI-ASCE Committee 326: Shear and Diagonal Tension, Journal of the ACI, Feb. 1962, Proceedings, V. 59, No. 2.

(5) Van Den Berg, F. J.: Shear Strength of Reinforced Concrete Beams with Web Reinforcement (Part I and II), Journal of the ACI, Oct. 1962, Proceedings, V. 59, No. 10.

(6) Boris Bresler and Scordelis, A. C.: Shear Strength of Reinforced Concrete Beams, Journal of the ACI, Jan. 1963, Proceedings, V. 60, No. 1.

(7) Mathey, R. G. and Watstein, D.: Shear Strength of Beams without Web Reinforcement Containing Deformed Bars of Different Yield Strengths, Journal of the ACI, Feb. 1963, Proceedings, V. 60, No. 2.

(8) DeCossio, Roger Diag: Shear and Diagonal Tension, Discussion of a Paper by ACI-ASCE Committee 326, Journal of the ACI Sept. 1962, Proceedings V. 59, No. 9.

(9) Taylor, R.: A note on the mechanism of diagonal cracking in reinforced concrete beams without shear reinforcement, Concrete Research, Magazine of 33, Vo. 11, Nov. 1959, Cement and Concrete Association.

(10) Kani, G. N. J.: The Mechanism of So-Called Shear Failure, Trans. Engng. Inst. Canada, April 1963.

(11) Kani, G. N. J.: The Riddle of Shear Failure and its Solution, Journal of the ACI, April 1964, Proceedings, V. 61, No. 4.

(12) Moe, J.: Shear and Diagonal Tension, Discussion of a paper by ACI-ASCE Committee 326, Journal of the ACI, September 1962, Proœedings, V. 59, No. 9.

(13) Rilem,: Symposium of Bond and Crack Formation in Reinforced Concrete, Stockholm, 1957.

(14) Robinson, H.: Discussion of Paper Measurement of Stress in Concrete Beam Reinforcement, The Institution of Civil Engineers, Proceedings, July, 1964, V. 28.

(15) Siess, C. P.: Viest, I. M., Newmark, N. M.: Studies of slab and Beam Highway Bridges: Part III, University of Illinois Engineering experiment Station, Bulletin Series, No. 396.

(16) Bignell, V. F.: Smalley, V. and N. P. Roberts: A New Photoelastic Material for Use in Problems Concerning reinforced Concrete. Concrete Research, Magazine of 45, V. 15, No. 45, Nov. 1963.

(17) Kaplan, M. F.: Strains and Stresses of Concrete at Initial of Cracking and Near Failure, Journal of the ACI, Proceedings, V. 60, No. 7, July 1963.

(18) Viest, I. M., Siess, C. P., Appletou, J. H, Newmark, N. M.: Full-Scale Test of Channel Shear Connectors and Composite T-Beam, University of Illinois, Engineering Experimental Station, Bulletin Series No. 405.

(19) Luis, P. Saenz, Ignacio Martin, and Rafael Tamargo,: Discussion of a Paper by Franco Levi; Work of the European Concrete Committee, Journal of the ACI, Proceedings, V. 58, No. 3, September 1961.

(20) Desayi, P. and S. Krishnan: Equation for the Stress-Strain Curve of Concrete, Journal of ACI, Proceedings, V. 61, No. 3, March 1964.

(21) Phillips, A.: Introduction to Plasticity 1956, The Ronald Press Company, New York.

(22) Butler, R., Kerr, E.: An introduction to Numerical Methods 1962 Sir Isaac Pitman and Sons Ltd. London.

(23) Evans, R. H. and Robinson, G. W.: Bond Stresses in Pre-stressed Concrete from X-Ray Photographs, The Institution of Civil Engineers, Proceedings Pt. 1, 1955, Vo. 4.

(24) Manning, J. T.: Discussion of Paper Measurement of Stress in Concrete Beam Reinforcement, The Institution of Civil Engineers, Proceedings, July 1964, V. 28.

(25) ACI Committee 408: A Guide for Determination of Bond Strength in Beam Specimens, Journal of the ACI, Proceedings, V. 61, No. 2, February 1964.

APPENDIX A

Sample calculations of strain for a reinforced concrete beam with incomplete interaction

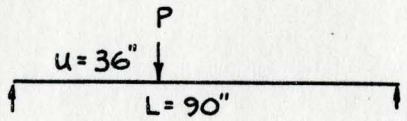

For a section at the location under the design moment.

For an uncracked section of the reinforced concrete beam.

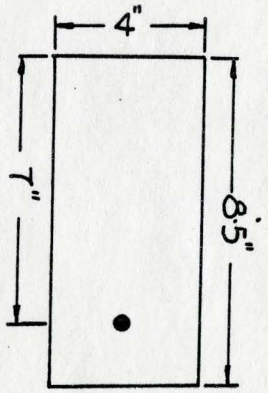

$E_s = 30 \times 10^6$ psi

$E_c = 3.5 \times 10^6$ psi

$A_s = 0.31$ in^2

$A_c = 34.0$ in^2

$z = \frac{8.5}{2} - 1.5$

$= 2.75"$

$\epsilon_{cb} \neq 171.0$ m"/"

$$\frac{1}{\bar{EA}} = \frac{1}{E_s A_s} + \frac{1}{E_c A_c}$$

$$= \frac{1}{30 \times 10^6 \times 0.31} - \frac{1}{3.5 \times 10^6 \times 34.0}$$

$$= 0.116 \times 10^{-6}$$

$\therefore \bar{EA} = 8.62 \times 10^6$

$$\Sigma EI = E_c I_c + E_s I_s \doteq E_c I_c$$

$$= 3.5 \times 10^6 \times \frac{4 \times 8.5^3}{12} = 716 \times 10^6$$

$$\bar{E}\bar{I} = \Sigma EI + \bar{E}\bar{A} \cdot \bar{z}^2$$

$$= 716 \times 10^6 + 8.62 \times 10^6 \times 2.75^2 = 781.2 \times 10^6$$

$$S_c = \frac{y_c}{\Sigma EI}$$

for bottom fibre of concrete

$$y_c = C_c = 4.25"$$

$$S_{cb} = \frac{4.25}{716 \times 10^6} = 0.00594 \times 10^{-6}$$

From equation (3.15), the measure of degree of interaction F/F' for 1/C = 100, at the section located under the point load is equal to 0.93369. Thus, the strain at bottom of concrete fibre is computed from equation (3.24), for design moment (M_t = 36200 lb.in).

$$\epsilon_{cb} = \left[S_{cb} - \frac{F}{F'} \frac{\bar{E}\bar{A}}{\bar{E}\bar{I}} \bar{z} \left(S_{cb} + \frac{1}{E_c A_c} \right) \right] M_t$$

$$= \left[0.00594 \times 10^{-6} - 0.93369 \cdot \frac{8.62 \times 10^6}{781.2 \times 10^6} \times 2.75 \right.$$

$$\left. (0.00594 \times 10^{-6} + 0.0084 \times 10^{-6}) \right] \times 36200$$

$$= 189.38 \times 10^{-6} \text{ in/in}$$

Similarly, ϵ_{ct} , ϵ_{sb} and ϵ_{st} can be calculated, from equations (3·24a) and (3·24b).

Cracking procedures:

$\epsilon_{ct} = -206.62 \times 10^{-6}$ in/in obtained from equation (3·24a).

From equation (3·27), the height of crack is

$$C.H. = \frac{2H(\epsilon_{cb} - \epsilon_p)}{(\epsilon_{ct} + \epsilon_{cb})}$$

for $\epsilon_p = 171.0$ m"/"

$$C.H. = \frac{8.5(189.38 \times 10^{-6} - 171.0 \times 10^{-6})}{(189.38 + 206.62)10^{-6}}$$

$$= 0.39"$$

$$\therefore 2H' = 2H - C.H.$$

$$= 8.5" - .39"$$

$$= 8.11"$$

This process is repeated until $\epsilon_{cb} \leq$ 171.0 micro in/in.

APPENDIX B

Newton-Raphson trial and error method for this problem:

For purposes of illustration this method is presented for this problem, in the case of complete interaction.

From equations (6.1) and (6.2) letting,

$$f(\epsilon_{cb},\alpha) = E_s A_s \epsilon_{cb}\left(\frac{\alpha-1}{\alpha}\right)\left[\left(\frac{\alpha}{\alpha-1}\right)+\frac{B}{2H}-\frac{d}{4H}\right]-\sigma_o A_c\left(\frac{-1-\alpha}{\alpha}\right)\frac{\epsilon_{cb}}{\epsilon_o}$$

$$\left[1-\left(\frac{-1-\alpha}{\alpha}\right)\frac{\epsilon_{cb}}{4\epsilon_o}\right]$$

$$g(\epsilon_{cb},\alpha) = 2b\sigma_o\left[\frac{\epsilon_{cb}H^2}{3\epsilon_o}\left(\frac{\alpha-1}{\alpha}\right)-\frac{\epsilon_{cb}^2H^2}{16\epsilon_o^2}\left(\frac{\alpha-1}{\alpha}\right)^2\right]+\sigma_o A_c z\left(\frac{-1-\alpha}{\alpha}\right)$$

$$\frac{\epsilon_{cb}}{\epsilon_o}\left[1-\left(\frac{-1-\alpha}{\alpha}\right)\frac{\epsilon_{cb}}{4\epsilon_o}\right]-M_t$$

Upon expanding the functions $f(\epsilon_{cb},\alpha)$ and $g(\epsilon_{cb},\alpha)$ in a Taylor series in terms of an arbitrary estimate of the desired solutions of $\bar{\epsilon}_{cb}$ and $\bar{\alpha}$ there results

$$f(\bar{\epsilon}_{cb},\bar{\alpha}) = 0 = f(\epsilon_{cb}^{(o)},\alpha^{(o)})+(\bar{\epsilon}_{cb}-\epsilon_{cb}^{(o)})f_{\epsilon_{cb}}(\epsilon_{cb}^{(o)},\alpha^{(o)})$$

$$+(\bar{\alpha}-\alpha^{(o)})f_{\alpha}(\epsilon_{cb}^{(o)},\alpha^{(o)})+\cdots\cdots$$

$$g(\bar{\epsilon}_{cb},\bar{\alpha}) = 0 = g(\epsilon_{cb}^{(o)},\alpha^{(o)}) - (\bar{\epsilon}_{cb}-\epsilon_{cb}^{(o)})\, g_{\epsilon_{cb}}(\epsilon_{cb}^{(o)},\alpha^{(o)})$$

$$+ (\bar{\alpha}-\alpha^{(o)})\, g_{\alpha}(\epsilon_{cb}^{(o)},\alpha^{(o)}) + \cdots$$

$\epsilon_{cb}^{(o)}$ and $\alpha^{(o)}$ are the initial estimates and $f_{\epsilon_{cb}}$, f_{α}, $g_{\epsilon_{cb}}$ and g_{α} are partial derivaties.

In this case

$$f_{\epsilon_{cb}} = \frac{\partial f}{\partial \epsilon_{cb}} = E_s A_s \left(\frac{\alpha-1}{\alpha}\right)\left[\left(\frac{\alpha}{\alpha-1}\right)+\frac{B}{2H}-\frac{d}{4H}\right] - \sigma_o A_c \left(\frac{-1-\alpha}{\alpha}\right)\frac{1}{\epsilon_o}$$

$$\left[1-\left(\frac{-1-\alpha}{\alpha}\right)\frac{\epsilon_{cb}}{2\epsilon_o}\right]$$

$$f_{\alpha} = \frac{\partial f}{\partial \alpha} = E_s A_s \frac{\epsilon_{cb}}{\alpha^2}\left(\frac{B}{2H}-\frac{d}{4H}\right) - \frac{\sigma_o A_c}{\epsilon_o}\frac{\epsilon_{cb}}{\alpha^2}\left[1-\left(\frac{-1-\alpha}{\alpha}\right)\frac{\epsilon_{cb}}{2\epsilon_o}\right]$$

$$g_{\epsilon_{cb}} = \frac{\partial g}{\partial \epsilon_{cb}} = 2b\sigma_o\left[\frac{H^2}{3\epsilon_o}\left(\frac{\alpha-1}{\alpha}\right)-\frac{1}{8}\frac{\epsilon_{cb}H^2}{\epsilon_o^2}\left(\frac{\alpha-1}{\alpha}\right)^2\right]$$

$$+\left\{\sigma_o A_c\left(\frac{-1-\alpha}{\alpha}\right)\frac{1}{\epsilon_o}\left[1-\left(\frac{-1-\alpha}{\alpha}\right)\frac{\epsilon_{cb}}{2\epsilon_o}\right]\right\} z$$

$$g_{\alpha} = \frac{\partial g}{\partial \alpha} = 2b\sigma_o\left[\frac{H^2\epsilon_{cb}}{3\epsilon_o\alpha^2}-\frac{\epsilon_{cb}^2H^2}{8\epsilon_o^2}\left(\frac{\alpha-1}{\alpha}\right)\frac{1}{\alpha^2}\right]$$

$$+\left\{\frac{\sigma_o A_c}{\alpha^2}\frac{\epsilon_{cb}}{\epsilon_o}\left[1-\left(\frac{-1-\alpha}{\alpha}\right)\frac{\epsilon_{cb}}{2\epsilon_o}\right]\right\} z$$

Calling

$$RR^{(0)} = \bar{\epsilon}_{cb} - \epsilon_{cb}^{(0)}$$

$$BB^{(0)} = \bar{\alpha} - \alpha^{(0)}$$

This gives

$$f(\epsilon_{cb}^{(0)}, \alpha^{(0)}) + RR^{(0)} f_{\epsilon_{cb}}(\epsilon_{cb}^{(0)}, \alpha^{(0)}) + BB^{(0)} f_{\alpha}(\epsilon_{cb}^{(0)}, \alpha^{(0)}) = 0$$

$$g(\epsilon_{cb}^{(0)}, \alpha^{(0)}) + RR^{(0)} g_{\epsilon_{cb}}(\epsilon_{cb}^{(0)}, \alpha^{(0)}) + BB^{(0)} g_{\alpha}(\epsilon_{cb}^{(0)}, \alpha^{(0)}) = 0$$

These two simultaneous equations can be solved for the $RR^{(0)}$ and $BB^{(0)}$ corresponding to $\epsilon_{cb}^{(0)}$ and $\alpha^{(0)}$. Thus the iteration pattern can set up.

By Cramer's rule

$$RR^{(0)} = \frac{f(\epsilon_{cb}^{(0)}, \alpha^{(0)}) \cdot g_{\alpha}(\epsilon_{cb}^{(0)}, \alpha^{(0)}) - g(\epsilon_{cb}^{(0)}, \alpha^{(0)}) \cdot f_{\alpha}(\epsilon_{cb}^{(0)}, \alpha^{(0)})}{g_{\epsilon_{cb}}(\epsilon_{cb}^{(0)}, \alpha^{(0)}) \cdot f_{\alpha}(\epsilon_{cb}^{(0)}, \alpha^{(0)}) - f_{\epsilon_{cb}}(\epsilon_{cb}^{(0)}, \alpha^{(0)}) \cdot g_{\alpha}(\epsilon_{cb}^{(0)}, \alpha^{(0)})}$$

$$BB^{(0)} = \frac{g(\epsilon_{cb}^{(0)}, \alpha^{(0)}) \cdot f_{\epsilon_{cb}}(\epsilon_{cb}^{(0)}, \alpha^{(0)}) \quad g_{\epsilon_{cb}}(\epsilon_{cb}^{(0)}, \alpha^{(0)}) \cdot f(\epsilon_{cb}^{(0)}, \alpha^{(0)})}{g_{\epsilon_{cb}}(\epsilon_{cb}^{(0)}, \alpha^{(0)}) \cdot f_{\alpha}(\epsilon_{cb}^{(0)}, \alpha^{(0)}) \quad f_{\epsilon_{cb}}(\epsilon_{cb}^{(0)}, \alpha^{(0)}) \cdot g_{\alpha}(\epsilon_{cb}^{(0)}, \alpha^{(0)})}$$

Let

$$\epsilon_{cb}^{(1)} = \epsilon_{cb}^{(0)} + RR^{(0)}$$

$$\alpha^{(1)} = \alpha^{(0)} + BB^{(0)}$$

Writing in general form

$$\epsilon_{cb}^{(r+1)} = \epsilon_{cb}^{(r)} + RR^{(r)}$$

$$\alpha^{(r+1)} = \alpha^{(r)} + BB^{(r)}$$

The iteration process is repeated until values of ε_{cb} and α satisfy the simultaneous equations

$$f(\bar{\epsilon}_{cb}, \bar{\alpha}) = 0 \quad , \text{ or}$$

$$< (\epsilon_{(\epsilon_{cb})}, \epsilon_{(\alpha)})$$

$$g(\bar{\epsilon}_{cb}, \bar{\alpha}) = 0 \qquad \text{or}$$

$$< (\epsilon_{(\epsilon_{cb})}, \epsilon_{(\alpha)})$$

$\varepsilon_{(\varepsilon_{cb})}$ and $\varepsilon_{(\alpha)}$ are very small pre-estimated values.

After obtaining $\bar{\epsilon}_{cb}$ and $\bar{\alpha}$ for a particular section, ε_{ct}, ε_{st}, and ε_{sb} can be found by equations in Chapter V. A new section is therefore found. This process is again repeated.

APPENDIX C

General solutions for the non-linear stress-strain characteristics of the concrete, using the Desayi and Krishnan relationship

$$\sigma = \frac{E_c \epsilon}{1 + \left(\frac{\epsilon}{\epsilon_o}\right)^2}$$

$$M_c = 2 E_c b \epsilon_o^2 \left[\frac{2H^2}{\epsilon_{cb}} \left(\frac{\alpha}{\alpha-1}\right) - \frac{4\epsilon_o H^2}{\epsilon_{cb}^2 \left(\frac{\alpha-1}{\alpha}\right)} \tan^{-1}\left\{ \frac{\epsilon_{cb}\left(\frac{\alpha-1}{\alpha}\right)}{2\epsilon_o} \right\} \right]$$

$$F = \frac{E_c \epsilon_o^2 A_c}{\epsilon_o^2 + \left(\frac{-1-\alpha}{\alpha}\right)^2 \frac{\epsilon_{cb}^2}{4}} \left(\frac{-1-\alpha}{\alpha}\right) \frac{\epsilon_{cb}}{2}$$

The equilibrium equation is,

$$M_t = 2 E_c b \epsilon_o^2 \left[\frac{2H^2}{\epsilon_{cb}} \left(\frac{\alpha}{\alpha-1}\right) - \frac{4\epsilon_o H^2}{\epsilon_{cb}^2 \left(\frac{\alpha-1}{\alpha}\right)^2} \tan^{-1}\left\{ \frac{\epsilon_{cb}\left(\frac{\alpha-1}{\alpha}\right)}{2\epsilon_o} \right\} \right.$$

$$\left. + \frac{E_c \epsilon_o^2 A_c}{\epsilon_o^2 + \left(\frac{-1-\alpha}{\alpha}\right) \frac{\epsilon_{cb}^2}{4}} \left(\frac{-1-\alpha}{\alpha}\right) \frac{\epsilon_{cb}}{2} \cdot 2 \right]$$

Difficulties were encountered in obtaining a solution when strain levels were small.

APPENDIX D

Table of Results

(1) Two point loading system - 1/C = 3.125 , linear case

x	M_t	2H'	ε_{ib}	ε_{ct}	ε_{sb}	ε_{st}
(in)	lb-in	in	m in/in	m in/in	m in/in	m in/in
0	0	8.5	0	0	0	0
2.25	2784.6	8.5	14.8	-15.9	8.7	6.5
4.5	5569.2	8.5	29.6	-31.9	17.4	12.9
6.75	8353.8	8.5	44.3	-47.9	26.0	19.3
9.0	11138	8.5	59.2	-63.9	34.6	25.5
11.25	13923	8.5	74.0	-79.8	43.0	31.7
13.5	16708	8.5	88.9	-95.8	51.3	37.7
15.75	19492	3.6	100.0	-211.7	331.8	278.1
18.0	22277	3.4	100.0	-241.1	390.6	327.5
20.25	25062	3.2	100.0	-270.7	447.1	374.7
22.5	27846	3.1	100.0	-300.8	502.4	420.4
24.75	30631	2.9	100.0	-331.7	557.1	465.0
27.0	33415	2.8	100.0	-363.5	611.3	508.7
29.25	36200	2.7	100.0	-396.4	665.3	551.5
31.5	36200	2.8	100.0	-390.7	664.1	553.9
33.75	36200	2.8	100.0	-386.3	663.2	555.8
36.0	36200	2.9	100.0	-382.9	662.5	557.1
38.25	36200	2.9	100.0	-380.5	662.0	558.1
40.5	36200	2.9	100.0	-378.8	661.7	558.9
42.75	36200	2.9	100.0	-377.8	661.5	559.2
45.0	36200	2.9	100.0	-377.5	661.5	559.4

(2) Two point loading system - 1/C varying along the beam, non-linear case.

x (in)	1/C	M_t' (lb-in)	2H' (in)	ε_{cb} m in/in	ε_{ct} m in/in	ε_{sb} m in/in	ε_{st} m in/in
0	200	0	8.5	0	0	0	0
2.25	184.7	2784.6	8.5	14.5	-15.9	10.2	8.0
4.5	169.3	5569.2	8.5	29.0	-31.8	20.5	16.0
6.75	153.9	8353.8	8.5	43.6	-47.9	30.6	24.1
9.0	138.6	11138	8.5	58.3	-64.1	41.2	32.2
11.25	123.2	13923	8.5	73.1	-80.3	51.7	40.4
13.5	107.9	16708	8.5	87.9	-96.6	62.2	48.6
15.75	92.5	19492	4.2	100.0	-195.7	320.0	276.2
18.0	77.2	22277	3.9	100.0	-223.2	381.8	330.0
20.25	61.8	25062	3.7	100.0	-250.4	440.0	380.7
22.5	46.5	27846	3.5	100.0	-278.2	396.5	429.5
24.75	31.1	30631	3.4	100.0	-307.8	552.2	476.7
27.0	15.8	33415	3.2	100.0	-342.1	607.8	521.4
29.25	0.4	36200	1.7	100.0	-597.5	723.2	465.7
31.5	15.8	36200	3.1	100.0	-369.2	661.4	567.9
33.75	31.1	36200	3.2	100.0	-361.8	660.1	570.8
36.0	46.5	36200	3.3	100.0	-357.8	659.7	571.8
38.25	61.8	36200	3.3	100.0	-357.3	659.5	572.2
40.5	77.2	36200	3.3	100.0	-357.3	659.4	572.4
42.75	92.5	36200	3.3	100.0	-357.2	659.4	572.5
45.0	107.9	36200	3.3	100.0	-357.2	659.4	572.5

(3) Two point load system, 1/C varying along the beam - linear case)

x (in)	1/C	M_t	2H'	ε_{cb} 10^{-6}	ε_{ct} 10^{-6}	ε_{sb} 10^{-6}	ε_{so} 10^{-6}	ε_{st} 10^{-6}	γ 10^{-3}	$\varepsilon_{so}(2H)$ 10^{-6}
0	200	0	8.5	0	0	0	0	0	0	0
2.25	184.7	2784.6	8.5	14.4	-15.9	10.2	9.1	8.0	0.02	9.1
4.5	169.3	5569.2	8.5	29.9	-31.7	20.4	18.2	15.9	0.02	18.2
6.75	153.9	8353.8	8.5	43.3	-47.5	30.6	27.3	23.9	0.03	27.3
9.0	138.6	11138	8.5	57.7	-63.4	40.8	36.3	31.9	0.03	36.3
11.25	123.2	13923	8.5	72.1	-79.2	51.0	45.4	39.9	.03	45.4
13.5	107.9	16708	8.5	86.6	-95.1	61.2	54.5	47.8	.04	54.5
15.75	92.5	19492	4.2	100.0	-193.4	317.1	215.2	273.4	.62	63.6
18.0	77.2	22277	3.9	100	-220.3	378.9	353.3	327.6	.94	72.5
20.25	61.8	25062	3.7	100	-246.8	437.2	407.8	378.5	1.4	81.3
22.5	46.5	27846	3.5	100	-273.8	493.7	460.5	427.4	2.0	89.5
24.75	31.1	30631	3.4	100	-302.3	549.3	512.0	474.6	3.1	96.3
27.0	15.8	33415	3.2	100	-335.2	605.0	562.2	519.3	5.9	99.8
29.25	0.4	36200	1.7	100	-575.8	720.6	593.0	465.4	473	34.5
31.5	15.8	36200	3.1	100	-361.0	658.3	612.1	565.9	3.6	108.7
33.75	31.1	36200	3.2	100	-353.8	657.0	612.8	568.6	.94	114.5
36.0	46.5	36200	3.2	100	-351.1	656.5	613.1	569.6	.29	116.7
38.25	61.8	36200	3.3	100	-350.0	656.3	613.2	570.0	.09	117.6
40.5	77.2	36200	3.3	100	-349.5	656.2	613.2	570.2	.03	117.9
42.75	92.5	36200	3.3	100	-349.4	656.2	613.2	570.2	.01	118.1
45.0	107.9	36200	3.3	100	-349.4	656.2	613.2	570.2	0	181.1